DEVELOPMENT OF A NYSTATIN-LOADED MICELLAR SYSTEM FOR ORAL MUCOADHESION

By

NANCY OWUSU AKYERE SARPONG

Submitted in fulfilment of the requirements for the degree of

Magister Scientiae

in the

Faculty of Science

at the

Nelson Mandela University

Supervisor: Prof G Kilian

Co-supervisor: Mr Y Kadernani

Co-supervisor: Prof S Roux

2019

Declaration

I, NANCY SARPONG, Student nr: 212277901, hereby declare that the work on which this dissertation is based is my own work (except where acknowledgements have been made) and that neither the work as a whole, or any part of thereof has been, is being, or is to be submitted for another degree at this or any other university.

NANCY OWUSU AKYERE SARPONG

Signed on this 11 day of January 2019 at the Nelson Mandela University

Dedication

I would like to dedicate this treatise to my family, the Gwimo family, the Masika family and the Sarpong family. Thank you for your prayers, encouragement and sacrifices. Without you, this work would not have been possible. You have proven that it does indeed take a village to raise a child.

Acknowledgements

I wish to extend gratitude to the following people and institutions for contributing towards the success of this treatise.

- My supervisor Prof Kilian, for your constant guidance, support and the long chats.
- My co-supervisors Mr Kadernani and Prof Roux, for their invaluable input and constant support.
- The nanoscience platform and the Department of Science and Technology, for funding the research.
- My colleagues Lana, Jethro, Amy, Yasmin, Yumna, Lauren and Vuyi for your wealth of knowledge and for the constant laughter and jokes.
- Arista and Jean for always being available to teach me new things when I needed them.
- Mama Cynthia and Vuyelwa from the Pharmacy Department, for their encouragement and support and for always helping me find equipment in the lab.
- The staff of the Department of Pharmacy, for their support and motivation.
- Hyacinthe Tonga, for spending late nights at the labs and bringing supper whenever it was necessary.
- Wimana Gwimo for being my lab partner, my typing buddy and my support system.
- Patricia Masika, for the daily check-ups, phone calls, laughter and being my shoulder to cry on.
- My family, for the constant jokes and the support that you have accorded me throughout my academic career.

Summary

Oropharyngeal Candidiasis (OPC) is an opportunistic fungal infection that affects mostly infants and immunocompromised patients. In recent years, the disease has been on the rise due to an increased life span, the HIV pandemic and the increased use of broad spectrum antibiotics. OPC may be treated using a nystatin suspension, which is not as effective as it could be due to the mechanism by which the suspension is applied to the affected tissue. This research aims to improve the effectiveness of nystatin, for the treatment of OPC, by proposing a nystatin loaded micellar system incorporated into a mucoadhesive system for drug delivery. This will ensure that nystatin is gradually released from the film, thus increasing retention time of nystatin at the affected area.

In this study, a mixture design was developed, which was used to determine the most appropriate solvent system for nystatin solubilization. Optimisation of the micelle formulation was achieved by using the central composite rational design (CCRD). The two factors that were taken into consideration were the temperature of the hydration medium (water) and the length of time the micellar solution was exposed to the temperature environment of the rotary evaporator. The responses that were investigated were the mean particle size, mean polydispersity index (PDI), mean zeta potential, change in mean particle size and change in mean PDI. The optimal micelle formulation was characterised for size, stability, morphology and drug encapsulation efficiency. The micelles were found to be spherical and stable with an acceptable size range. However, their drug encapsulation efficiency was low.

The mucoadhesive film was formulated and characterised for physical characteristics, pliability, percentage swelling index and drug release profile. The film was found to be highly pliable and evenly distributed with a smooth surface; no bumps or bubbles were visible. The film was able to swell to up to 550 %. In vitro studies showed that nystatin was gradually released from the film.

Key words: central composite rotational design, mucoadhesive film, oropharyngeal candidiasis, polymeric micelles, response surface methodology

Table of Contents

Page

List of Tables

Page

List Of Figures

Page

List of Abbreviations

°C	Degrees Celsius
µm	Micrograms
µl	Microliter
µg	Micrometer
AFM	Atomic Force Microscopy
ANOVA	Analysis Of Variance
APD	Avalanche Photodiode Detector
BCS	Biopharmaceutics Classification System
CCRD	Central Composite Rotational Design
CI	Confidence Interval
CMC	Critical Micelle Concentration
DLS	Dynamic Light Scattering
DMF	Dimethylformamide
DoE	Design of Experiment
FDC	Franz Diffusion Cells
H_2O_2	Hydrogen Peroxide
HIV/AIDS	Human Immunodeficiency Virus/ Acquired Immune Deficiency Syndrome
HPLC	High Performance Liquide Chromatography
HPMC	Hydroxypropyl Methylcellulose

M	Molar
M3-PALS	Phase Analysis Light Scattering
Mg	Milimeter
Min	Minutes
ml	Mililiter
mPa	Million Pascals
mV	Millivolts
N	Newtons
NDoH	National Department Of Health
NIBS	Non-Invasive Backscatter Optics
Nm	Nanometer
OPC	Oropharyngeal Candidiasis
PDA	Photodiode Array
PDI	Polydispersity Index
PEG	Polyethylene Glycol 400
PSPD	Position Sensitive Photo Detector
PVP	Polyvinylpyrrolidone K-30
PZT	Piezoelectric
RSD	Relative Standard Deviations
RSM	Response Surface Methodology
SD	Standard Deviation

SLN	Solid Lipid Nanoparticles
TEM	Transmission Electron Microscopy
UTS	Ultimate Tensile Strength
UV	Ultra Violet

CHAPTER 1

Introduction

1.1 Background

Oropharyngeal candidiasis (OPC) is known to be one of the most common opportunistic infections affecting humans. It is caused by a *Candida* species known as *Candida albicans* (Darwazeh & Darwazeh, 2014). OPC predominantly affects infants, diabetic patients, patients using broad-spectrum antibiotics and those with a compromised immune system. In South Africa, OPC is treated using a topically applied nystatin suspension (Department of Health, 2013). Due to its mechanism of application, the topical agent is not very effective which results in high instances of recurrence and treatment failure (Garcia-Cuesta *et al.,* 2014). According to Thompson and colleagues (2010), relapse of OPC is more prevalent in patients who were treated using topical agents (Thompson *et al.,* 2010). OPC has received attention due to its increased prevalence which is reflective of the HIV/AIDS pandemic; the increase in invasive medical practices; an increase in the use of broad-spectrum antibiotics and immunosuppressive therapies (D. Williams & Lewis, 2011); as well as an increase in conditions such as diabetes and malnutrition (Patil *et al.,* 2015).

The discovery of a new drug is a time consuming and expensive exercise, but is of utmost importance to develop novel methods that aid in overcoming the limitations associated with everyday drug use (Tiwari *et al.,* 2013). The institution of a minor change to a drug that may not have been effective in its original dosage form, such as a change in the dosage form, may lead to increased efficacy, bioavailability and effectiveness of the drug (Rangasamy & Parthiban, 2010). Nystatin is one such drug that requires a change in dosage form. Although nystatin is used often, it is not as efficacious as it could be due to its dosage form and mechanism of administration (Garcia-Cuesta *et al*., 2014). Nystatin's current dosage form for treatment of OPC is in the form of a suspension, which does not have the ability to adhere to the affected parts of the mucosa. Nystatin is administered orally, using a dropper to accurately take up the recommended dose. The patient uses the dropper to drop the drug near or unto the affected area. Once the drug is in the patient's mouth, they are required to swirl the suspension in their mouth and keep it in their mouth for as long as possible before

it may be either spat out or swallowed (South African Department of Health, 2013). This mechanism of application is difficult to implement in infants and severely ill patients. By changing the dosage form to one that is capable of penetrating into the inflamed tissues and adhering to the mucosa, it may be possible to improve the therapeutic outcome.

A technology that aids in an improved drug delivery system is nanotechnology. According to Singh and Lillard (2009) nanotechnology allows for the synthesis, manipulation, study and characterization of structures and devices that are within the nanometer range, known as nanomaterials or nanoparticles. Advantages associated with nanomaterials include increased solubility of a highly insoluble drug, controlled drug release and the ability of nanomaterials to only accumulate in the inflamed tumour tissue; this occurrence is known as the permeation and retention effect (Singh & Lillard, 2009). It is important for nystatin to have the ability to adhere to the mucosa so as to prevent saliva from washing the drug away. In order for nystatin to be effective it needs to be in contact with the affected area for as long as possible. One way to ensure that nystatin is in constant contact with the mucosa and to minimise the chances of the drug being washed away by saliva is to use a mucoadhesive system (Jin *et al.,* 2018). Mucoadhesion is the adhesion between the mucosal surface and the surface of another material. The advantage of using a mucoadhesive system is that it allows for slow release of the drug and increases the retention time of the drug in the affected area (Donnelly *et al.,* 2011; Sabry, 2018).

1.2 Problem Statement

The problems associated with the use of nystatin oral suspension stem from the dosage form not having the capability to adhere to the mucosa, thus decreasing contact time of the drug with the affected area. This results in the drug not being as effective as it could be (Garcia-Cuesta *et al.,* 2014). Other disadvantages associated with the use of the suspension include a decrease in patient compliance due to the unpleasant taste; and the high frequency of administration, since the suspension needs to be applied four times a day (Thompson *et al.*, 2010). Some nystatin suspension formulations have high levels of sucrose and ethanol which are used to mask the bitter taste of nystatin. The ethanol may cause local irritation and the sucrose may lead to tooth decay and cause unwanted side effects in diabetic patients (Campos

et al., 2012). This study proposes the development of a nystatin-loaded micellar system which will be incorporated into a mucoadhesive film. This allows for longer contact time with the affected area, therefore successfully dealing with the controlled release of the drug to the affected area. The discovery of a new and innovative way to change the dosage form and the mechanism of administration of nystatin oral suspension may make the treatment of OPC easier on patients and caregivers. The ease of care will be experienced as a by-product of the lower dosing frequency and the ease of application of the new innovative film. This may combat the issue of high frequency of treatment failure and recurrence, due to low patient compliance and a poor mechanism of administration (Garcia-Cuesta et al., 2014).

1.3 Aim and Objectives

1.3.1 Aim.

The aim of this study is to develop a buccal mucoadhesive film containing nystatin encapsulated in a polymeric micelle. This is proposed for the treatment of oropharyngeal candidiasis in children and chronically ill patients.

1.3.2 Objectives.

Based on the aim outlined above, the proposed objectives are as follows:

1. Determination of the most appropriate solvent system for solubilizing nystatin using a statistical methodology.
2. Formulation of a polymeric micellar system containing nystatin.
3. Characterisation of the micellar system with respect to particle size and the physical stability, morphology and drug encapsulation efficiency.
4. Formulation of a mucoadhesive film with the incorporated micellar system.
5. Characterisation of the mucoadhesive film with respect to physical characteristics, mechanical strength swelling index and surface pH.

CHAPTER 2

Literature Review

2.1 Oropharangeal Candidiasis (OPC)

2.1.1 Introduction.

OPC can be described as a common opportunistic fungal infection often caused by *Candida albicans* of the *Candida* species (Pankhurst, 2009). In a healthy human, there are small amounts of *Candida* present in the oral cavity, skin and the digestive tract, that form part of the normal microflora. *Candida*, present in small amounts must compete with other microorganisms in the body, including bacteria for nutrition and space. When there is an imbalance in the microflora due to factors such as antibiotic use, chronic illness affecting the immune system, as well as medications that alter hormones in the body, the *Candida* opportunistically becomes a pathogen, thus causing what is known as OPC in the patient (Darwazeh & Darwazeh, 2014; Pietrzak et al., 2018).

The prevalence of OPC varies with the age and strength of immunity of the patient, as well as the medication that the patient may be taking (Akpan & Morgan, 2002). It is agreed upon that immunocompromised patients such as those suffering from cancer and those infected with the HIV/AIDS, diabetic patients, patients who wear dentures, young children and patients using medications such as corticosteroids, antibiotics and contraceptives are at a higher risk of developing OPC (Akpan & Morgan, 2002; Asmarawati *et al.,* 2018; Campinha-Bacote *et al.,* 2002; Pankhurst, 2009; Patil et al., 2015; World Health Organisation, 2014). Garcia-Cuesta and colleagues (2014) found that OPC has been prevalent in the developed countries over the last decade. The authors attribute this to a lengthened life span, extended duration of antibiotic use, the use of dentures, endocrine disorders and dry mouth (Vincent, 2001; Garcia-Cuesta et al., 2014; Williams & Lewis, 2011). OPC has a high frequency of recurrence and treatment failure. This may be attributed to failure by the health care practitioner to identify the underlying condition, thereby putting a patient at risk of OPC, by incorrectly diagnosing the patient, or the patient being prescribed the incorrect antifungal agent for OPC treatment (Darwazeh & Darwazeh, 2014).

2.1.2 The different forms of OPC infections.

Garcia-Cuesta and colleagues (2014) state that OPC may clinically manifest in four different forms, namely: pseudomembranous thrush, erythematous thrush, hyperplastic thrush and *Candida*-associated lesions. Some of the general symptoms associated with OPC include white films in the mouth, altered taste, painful mouth, and a burning sensation on the tongue. These symptoms may result in a general decrease in the quality of life of the patient, as they experience a decline in nutritional intake due to an unwillingness to eat or drink, as well as impaired speech due to the pain associated with the condition (Akpan & Morgan, 2002).

Pseudomembranous thrush is characterized by white plaque found in the throat, on the tongue, gingiva and the buccal mucosa, which on removal results in painful red films where the plaque was. This type of OPC is observed in children, immunocompromised patients as well as patients on corticosteroids. Erythematous thrush is mostly associated with the lengthened use of broad-spectrum antibiotics and is characterized by the presence of smooth red films on the soft and hard palate, buccal mucosa and on the dorsum of the tongue (Patil et al., 2015). Erythematous thrush is seen chronically in HIV/AIDS patients, with this type of OPC often being painful. Hyperplastic thrush is characterized by white plaques which are firmly bound to the buccal mucosa, tongue and palates in a bilateral manner. The plaques, in this case, cannot be removed and this form of OPC is seen most commonly in patients who smoke (D. Williams & Lewis, 2011). The different manifestations of OPC are shown in Figures 2.1 and 2.2.

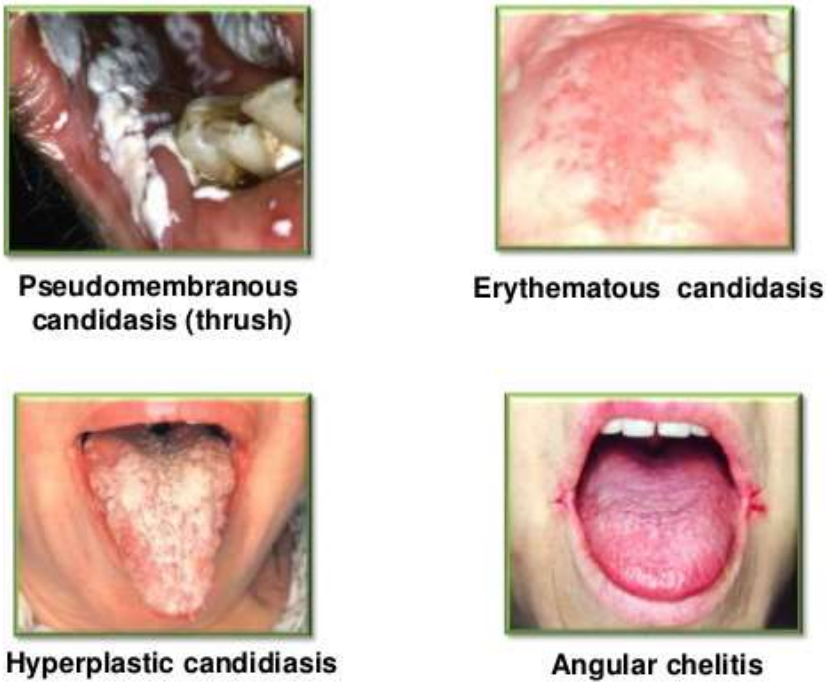

Figure 2. 1: The different manifestation of Oropharyngeal Candidiasis (Shinde, 2016)

2.1.3 Candida associated lesions.

There are many different forms of *Candida-associated* lesions, for example denture stomatitis, linear gingival erythema and angular cheilitis. Denture stomatitis is characterized by the presence of granular or smooth films on the hard palate of the area where the dentures were being worn. This form of thrush is also associated with angular cheilitis and only affects patients who wear dentures (Patil et al., 2015). Linear gingival erythema is associated with HIV/AIDS infected patients. This type of OPC is observed as a linear band of red inflamed tissue, about 2-3 mm long, found on the marginal gingiva. It is caused by *Candida albicans* and/or *Candida dubliniensis*, both of which belong to the *Candida* family (D. Williams & Lewis, 2011). Angular cheilitis mostly affects patients who have been wearing dentures for a long time and those with iron and vitamin B_{12} deficiency. It is characterized by small red and inflamed tears in the corners of the mouth (Akpan & Morgan, 2002). Table 2.1 summarises the different manifestations of OPC while outlining the patients that are most at risk of the different manifestations.

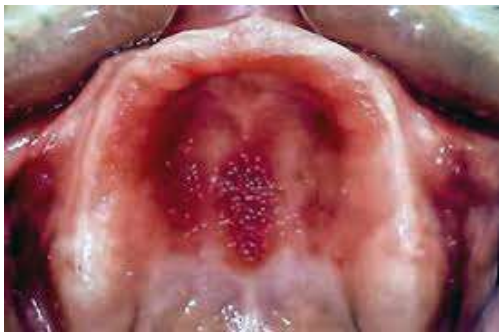

Denture Stomatitis

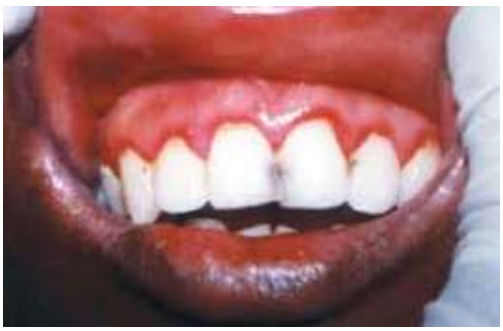

Linear gingival erythema

Figure 2. 2: Clinical manifestations of Candida-associated lesions (Shinde, 2016)

Table 2. 1: The different manifestations of Oropharyngeal Candidiasis

OPC Manifestation type	Characterization	Patients mostly at risk
Pseudomembranous thrush	White plaque in the throat, on the tongue, gingiva and the buccal mucosa.	Children, patients on corticosteroids, contraceptives, diabetic patients and immunocompromised patients.
Erythematous thrush	Painful, smooth red films found on the soft and hard palate, buccal mucosa and on the dorsum of the tongue.	Patients on prolonged treatment of antibiotics and HIV/AIDS patients.
Hyperplastic thrush	White plaque firmly bound to the tongue, buccal mucosa and palates in a bilateral manner.	Smokers.
	Candida Associated lesions	
Denture stomatitis	Presence of granular or smooth films on the hard palate of the area where the dentures were being worn.	Denture wearing patients.
Linear gingival erythema	Presence of red inflamed gums which may be bleeding.	HIV/AIDS infected patients.
Angular cheilitis	Presence of red and inflamed tears in the corners of the mouth.	Denture wearing patients, Geriatric patient, Iron and Vitamin B_{12} deficient patients.

2.1.4 Treatment of OPC.

OPC can be treated successfully using antifungal agents in healthy individuals when it is a primary infection. In patients who experience OPC as a secondary infection, the primary cause needs to be addressed before treatment will be successful. It is of clinical importance to know the lifestyle of the patient so that the it may be accurately diagnosed. This will aid in identification of the underlying cause of the OPC and thus the treatment choice. If the primary cause is not identified, the OPC infection will recur regardless of how well it has been treated (Garcia-Cuesta *et al*., 2014). Once the primary cause has been identified, the correct rectifying action can be taken, be it a lifestyle or drug intervention. OPC is usually treated using local antifungal agents such as nystatin, miconazole and clotrimazole (Rossiter, 2014). Medications that are used for the treatment of oral thrush are available in the form of tablets, liquids, gels and lozenges.

According to Rossiter (2014), there are systemic drugs available for the treatment of OPC such as fluconazole and itraconazole. The systemic drugs may be used in complicated cases of OPC where the patient does not respond to topical treatment. Even though the systemic drugs have been proven to work better than nystatin, they are susceptible to numerous drug interactions, and adverse effects which limits their use in the treatment of topical infections(Lyu *et al.,* 2016).

Although miconazole and nystatin are both local antifungal agents, nystatin is superior to miconazole, because about 17% of *Candida* species have developed resistance to miconazole (Collins, Cookinham, & Smith, 2011). This sometimes results in cross-resistance to other azoles such as fluconazole (Campos *et al*., 2012), while no resistance has been developed by *Candida albicans* to nystatin. Miconazole also has the disadvantage of interacting with other drugs. The major drug interaction to note with topical miconazole use, is that when used simultaneously with warfarin there is a chance of haemorrhaging (Rossiter, 2014). There are no major drug interactions associated with topical use of nystatin. Miconazole is also absorbed by the intestine which promotes hepatotoxicity as a side effect (Garcia-Cuesta *et al*., 2014). Other agents that can be used to treat OPC but are not considered to be antifungal agents include chlorhexidine mouth wash and gentian violet (Rossiter, 2014).

Nystatin is administered orally by instilling 1 ml - 2 ml of the suspension into the mouth every four hours. Nystatin pessaries may be used off-label to be sucked on as a lozenge four times a day (Rossiter, 2014). The problem associated with the first line treatment is its bitter taste and frequency of administration, which decreases patient compliance. The nystatin suspension does not adhere well to the mucous membrane, thereby impairing its efficacy, as most of the drug is washed away by saliva (Garcia-Cuesta *et al.,* 2014).

For more severe cases, fluconazole in a dose of 200 mg is taken orally for 14 days. Fluconazole is an azole antifungal agent and works by preventing lanosterol from being converted into ergosterol which is an essential component of the fungal cell membrane. This results in an increased permeability of the fungal cell leading to a leakage of the cell contents, thereby killing the fungal cell (Katzung *et al.*, 2012). Some side effects associated with fluconazole include nausea, vomiting, abdominal pain and skin rash. Fluconazole interacts with any drug that is metabolized by cytochrome P450 enzymes, as it is a weak inhibitor of the enzyme (Rossiter, 2014). Fluconazole will inhibit their metabolism thus increasing the drug's half-life.

Chlorhexidine is a disinfectant and a broad-spectrum antiseptic agent that may be used in the treatment of OPC and any other superficial gingival infection. For the treatment of OPC, chlorhexidine is used as a mouth wash where the patient would use 15 ml to 30 ml to gargle and spit out every four hours. Some of the side effects associated with chlorhexidine include discoloration of the tongue and surface enamel (Rossiter, 2014).

Gentian violet is an antiseptic dye used for the treatment of fungal infections. In OPC, gentian violet is used by painting it onto the oral mucosa at least three times a day. The problem associated with this treatment is the discoloration of the mouth is not accepted by most patients. Side effects associated with this treatment include ulcerations and irritation of the mucosal membrane caused by the dye, with frequent ingestion potentially resulting in an inflamed oesophagus, larynx and trachea (Rossiter, 2014).

The knowledge of the patient's lifestyle may be beneficial in preventing future OPC infections as lifestyle choices can be changed, and special precautions taken by the

patient. Table 2.2 summarises the treatment options of OPC that are currently available for patients.

Table 2. 2: Treatment options for the successful eradication of oropharyngeal candidiasis

Drug Name and Class	Dosage Form	Dose and directions for use	Side effects
Nystatin (Local antifungal)	Suspension	100 000 IU/ml Instil 1 ml – 2 ml of suspension into the mouth every four hours	Nausea, vomiting, mouth irritation, diarrhoea.
Miconazole (Local Antifungal)	Gel	50 mg – 100 mg Apply 50 mg – 100 mg three to four times a day	Nausea, vomiting, burning sensation at applied area, diarrhoea.
Fluconazole (Systemic Antifungal-for severe cases)	Tablets	200 mg/ day Take 200 mg daily for 14 days	Nausea, vomiting, skin rash, abdominal pain.
Chlorhexidine (Disinfectant, Broad spectrum antiseptic)	Solution	15 ml – 30 ml to gargle and spit out every four hours	Discoloration of tongue and surface enamel.
Gentian Violet (Antiseptic dye, Antifungal)	Solution	Use the brush provided to paint the affected area at least three times a day.	Mouth discolouration, ulceration and irritation of the mucosa, inflamed larynx and trachea.

2.2 Nystatin

2.2.1 Introduction.

Fungi such as the *Candida* species are known to be the causative organisms of numerous opportunistic infections. If these opportunistic infections are not treated correctly, they may lead to a decrease in the quality of life of the patient or in extreme cases, a systemic infection, thereby causing death (Mazu, Bricker, Flores-Rozas, & Ablordeppey, 2016). Opportunistic fungal infections such as OPC may be treated with antifungal agents. Antifungal agents are a pharmacological class of antimicrobials that may be used to successfully treat fungal diseases, including both opportunistic and primary fungal infections. As per the NDoH's essential drugs list of South Africa, the first line treatment of OPC in South Africa is nystatin (South African Department of Health, 2012). Although there are many antifungal agents that may be used to treat OPC, nystatin is the preferred drug. This is because *Candida* species do not develop resistance against it and it can be applied topically to the affected area and does not have any drug interactions (Rossiter, 2014). Nystatin has unique characteristics and exhibits a concentration dependent fungicidal activity and a post-fungal effect. Concentration dependence means that the higher the concentration that enters the cells for elimination, the better. The post-fungal effect means that even after nystatin has been removed from the affected area, it is known to still have antifungal activity (Gunderson, Hoffman, Ernst, Pfaller, & Klepser, 2000). This made nystatin the drug of choice for this study.

2.2.2 Pharmacological actions.

Nystatin is an antimycotic polyene antibiotic, obtained during various fermentation processes using *Streptomyces noursei.* Nystatin is indicated for the treatment of cutaneous or mucocutaneous mycotic infections caused by *Candida* species (Rossiter, 2014). It has been found to have both fungistatic and fungicidal properties against a wide variety of yeasts-like fungi and other organisms such as *Candida parapsilosis, Candida tropicalis, Candida guilliermondi* and *Candida krusei*. However, nystatin does not show any activity against protozoa, viruses or bacteria. Due to the intestine's inability to absorb nystatin, it is a good antifungal agent for the treatment of fungal infections affecting the gastro intestinal tract (Brescansin *et al*., 2013).

Coutinho and colleagues (2004), as well as Katzung and colleagues (2012) have found nystatin to cause cell death by binding to sterols found on the cell membrane of susceptible species, resulting in the leakage of intracellular components due to increased permeability of the cell membrane. Lyu and colleagues (2016) recommend that 1-2 mL of nystatin suspension containing a dose of 100 000 IU per mL should be instilled in the mouth four times a day, for a duration of 1-2 weeks, for successful treatment of non-severe OPC (Rossiter, 2014). For nystatin to work effectively, it needs to be in constant contact with the affected area of the mouth for as long as possible. However, nystatin does not adhere well to the affected area of the mouth as the nystatin suspension does not have good adhesion properties. This allows it to be washed away by saliva during normal processes such as eating and drinking. Therefore, patients should be counselled on taking nystatin after they have eaten or have something to drink. The side effects associated with nystatin use include nausea, vomiting, mouth irritation and diarrhoea (Rossiter, 2014).

2.2.3 Physical properties of nystatin.

Nystatin is available as a yellow to brown powder with a distinctive odour and an unpleasant taste. The powder is both hygroscopic and highly lipophilic with a log P value of 7.08 and a chemical formula of $C_{47}H_{75}NO_{17}$. It has a molecular weight of 926.107 g/mol. It should be stored in an air-tight container in a dark and cool place away from direct sunlight. Nystatin is not soluble in water or alcohol; however, it is completely soluble in dimethyl sulphoxide and dimethylformamide and is slightly soluble in methanol. This is due to its chemical structure, illustrated in Figure 2.3, which contains a large lactone ring with numerous double bonds, which makes nystatin both amphoteric and amphiphilic. This means that nystatin is almost insoluble in aqueous media, which causes solubility challenges when formulating (Campos *et al.,* 2012). Because of its low solubility in aqueous media, nystatin tends to have a low bioavailability (Gajdošová *et al.,* 2016). Incorporating nystatin into a micellar system incorporated into a mucoadhesive film which may allows for increased stability of the drug and it also promotes the drug to be released at a controlled rate at the site of infection. These properties greatly improve nystatin's bioavailability and decreases the dose frequency thus combating the issue of high treatment failure and recurrence of oral thrush (Gelperina, Kisich, Iseman, & Heifets, 2005).

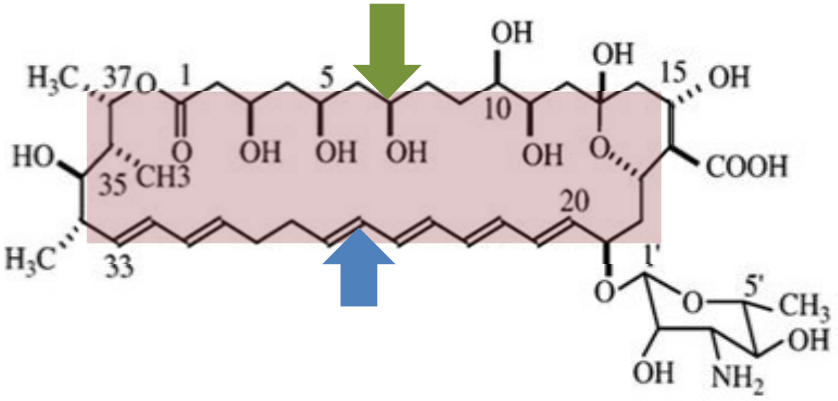

Figure 2. 3: Chemical structure of nystatin (Brescansin, Brescansin, Portilho, & Pessine, 2013).

In Figure 2.3 the pink shaded area represents the large lactone ring, the blue arrow represents the lipophilic area of nystatin as characterised by the numerous double bonds that are present. The green arrow represents the more hydrophilic portion of nystatin, this is characterised by the single bonds and the presence of the hydroxyl (OH) functional group.

2.3 Nanotechnology/ Nanoscience

2.3.1 Introduction.

The most challenging part in drug formulation is finding a drug delivery system which will ensure that the drug is delivered to the part of the body where it is needed without affecting other healthy organs (De Jong & Borm, 2008). A new kind of science which makes delivering drugs to the diseased area easier is nanoscience. Nanoscience has gained significant attention in recent years due to its potential to revolutionise numerous aspects of life such as medicine, chemistry and physics (Park, 2007). According to the National Nanotechnology Initiative (2017), a nanoparticle is defined as a structure with at least one of its dimensions being within the size range of 1 to 100 nm (Safari & Zarnegar, 2014). However, in the context of drug delivery, a nanoparticle can be defined as a structure within the size range of 10 nm to 1000 nm (Jong & Borm, 2008). This is because the nanoparticle may be larger in size than the stipulated dimensions, as it may have drugs incorporated into its matrix or on the surface of the particle (Suri, Fenniri, & Singh, 2007).

The unique size of nanoparticles provides them with new properties that the normal bulk product would not have, thereby making nanoparticles ideal for drug delivery. Some of these unique properties include: their large surface to mass ratio, which allows highly insoluble drugs like nystatin to become more soluble (Jong & Borm, 2008), thereby enhancing the bioavailability of the drug (Mudshinge, Deore, Patil, & Bhalgat, 2011); its small size which allows it to have a longer residence time in the body, thus increasing the half-life of the drug (Alton & Taylor, 2013); and the size of the nanoparticles which allows them to accumulate, using the enhanced permeation and retention effect (Nehoff, Parayath, Domanovitch, Taurin, & Greish, 2014) or active targeting (Mudshinge *et al*., 2011), in inflamed and/or diseased tissue, therefore increasing the efficacy of the drug. Since the drug goes directly to the affected area, lower doses and concentrations of the drug are needed to initiate a therapeutic effect, which decreases the chances of a dose-related toxicity (Mudshinge *et al*., 2011).

Nanoparticles for use in the body may be composed of biodegradable materials such as solid lipids, polymers (natural or synthetic), and metals (Suri *et al*., 2007). Once the nanoparticle containing the drug reaches its site of action, the drug will be released either through degradation, erosion or diffusion (Barakat, Taleb, & Salehi, 2011). For the context of this study, only nanoparticles which may be used to encapsulate drugs such as liposomes, solid lipid nanoparticles (SLN) and polymeric micelles (Wilczewska, Niemirowicz, Markiewicz, & Car, 2012) will be discussed. Polymeric micelles are the nanoparticle of choice due to its suitability for drugs that are poorly soluble in water, such as nystatin (Gaucher, Satturwar, Jones, Furtos, & Leroux, 2010; Taillefer, Jones, Brasseur, van Lier, & Leroux, 2000).

2.3.2 Nanoparticles for drug delivery.

Liposomes are small artificial vesicular sacs composed of one or more phospholipid bilayers surrounding an inner aqueous space. They are synthesized using natural non-toxic phospholipids and cholesterol. Liposomes are ideal for drug delivery systems due to their large size (80-300 nm) and hydrophobic and hydrophilic character (Akbarzadeh et al., 2013). Solid lipid nanoparticles (SLN) are nanoparticles that are composed of solid lipids such as complex glyceride mixtures, highly purified triglycerides or waxes stabilized by various surfactants. Some characteristics associated with SNL include their ability to protect the drugs that have been

incorporated into them from degradation. This is due to their good physical stability (Wilczewska *et al*., 2012). However, the nanoparticle of choice for this research is the polymeric micelle as they have several advantages over the other nanoparticles available for drug delivery. Some of these advantages include their smaller size as compared to other nanoparticulate drug carriers, which allows them to evade the mononuclear phagocyte system (Taillefer *et al*., 2000).

2.3.3 Polymeric micelles.

Micelles are small amphiphilic spherical structures which contain a hydrophilic shell and a hydrophobic core with a size range of about 5-100 nm. Micelles are composed of amphiphiles or surface-active agents known as surfactants (Oerlemans *et al*., 2010). Surfactant micelles had been the popular choice of micelles for many years but due to their high critical micelle concentration (CMC) which causes instability, they are no longer popular. Polymeric micelles, however, have a low CMC, which renders them more stable and tolerable. The low CMC allows polymeric micelles to have a higher drug carrying capacity and a better control release profile (Ahmad *et al.,* 2014).

Polymeric micelles have recently gained attention due to their ability to carry drugs that are poorly soluble in water and their enhanced stability as compared to surfactant micelles. Polymeric micelles are composed of block copolymers (Kedar, Phutane, Shidhaye, & Kadam, 2010). A block copolymer is a polymer which consists of two monomers that cluster together to form repeating units (Helmenstine, 2016) as shown in Figure 2.4. A polymeric micelle's hydrophobic core contains the hydrophobic portion of the block copolymer. The core is where drugs which are poorly soluble in an aqueous media are encapsulated. The outer shell of the polymeric micelles is composed of the hydrophilic portion of the block copolymer which protects the encapsulated drug from the surrounding aqueous environment and also aids in stabilizing the micelle (Kedar *et al*., 2010) as shown in Figure 2.5. For the micelles to be able to encapsulate a drug, the block copolymers that make up the hydrophobic core must be compatible with the drug to be encapsulated (Lu & Park, 2013). Polymers which offer good sustained release are characterised by being physically interactive with the encapsulated drug, thus causing drug retention and a slow release of the drug (Trivedi & Kompella, 2010). The polymers must have a low toxicity and they must be biocompatible.

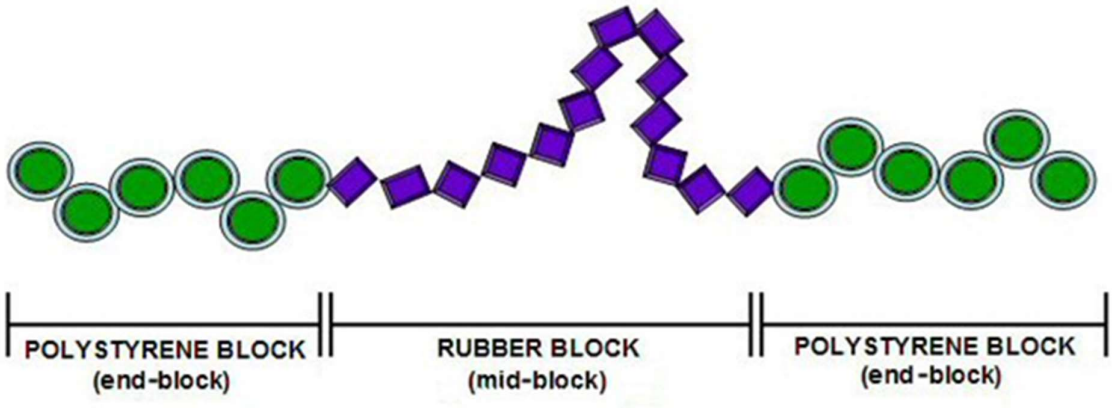

Figure 2. 4: An illustrative drawing of a linear styrenic tri-block copolymer (Eastman Chemical Company, 2017).

2.3.4 Formation of polymeric micelles.

According to Jones and Leroux (1999), two forces drive the spontaneous formation of micelles: attractive and repulsive forces. During self-assembly of polymeric micelles (Xu, Ling, & Zhang, 2013) attractive forces cause the association of molecules while the repulsive forces prevent the uncontrolled growth of the micelles such that they are no longer in the nano range (Jones & Leroux, 1999). Polymeric micelles form spontaneously when amphiphilic block copolymers are exposed to an aqueous solution (Xu *et al.,* 2013), as shown in Figure 2.5. For micelles to spontaneously form in an aqueous medium, the concentration of the block copolymers must increase above a concentration threshold known as the CMC (Jones & Leroux, 1999; Xu *et al*., 2013). Formation of micelles above the CMC is due to the dehydration of the hydrophobic tails, consequently causing a favourable state of entropy (Oerlemans et al., 2010). Once the CMC has been reached, the hydrophobic portions of the block copolymer come together so as to avoid contact with the aqueous environment and the more hydrophilic portion of the block copolymer will come into contact with the aqueous environment. This association of the hydrophobic portions leads to the formation of a micellar core (Jones & Leroux, 1999).

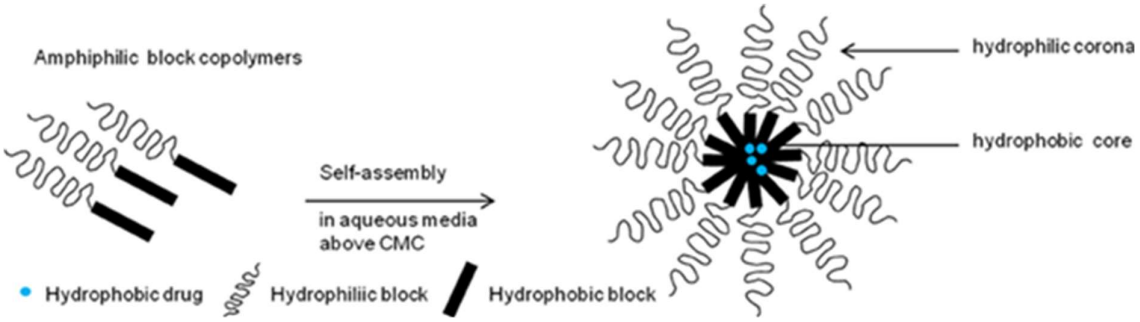

Figure 2. 5: The formation of a drug loaded polymeric micelle in an aqueous solution (Jhaveri & Torchilin, 2014)

2.4 Mucoadhesion

2.4.1 Introduction.

Bioadhesion has been described by several authors as the attachment of two surfaces, held together by interfacial forces for a certain period, with at least one of the materials being biological (Amit, Sharad, & Junaid, 2011; Donnelly et al., 2011; Mansuri, Kesharwani, Jain, Tekade, & Jain, 2016). Mucoadhesion is a type of bioadhesion in which the biological surface is a mucous membrane (Amit et al., 2011). Mucoadhesion, as a drug delivery method, has gained interest in the pharmaceutical industry since the early 1980's. This is because mucoadhesive systems enable intimate contact of the dosage form with the surface of the diseased organ. This increases the retention time of the drug, leading to increased therapeutic efficacy (Mansuri et al., 2016). The use of mucoadhesive systems for drug delivery is recommended for drug molecules that undergo extensive first-pass metabolism, are degraded in an acidic medium and molecules with a high-molecular-weight, such as peptides and oligonucleotides (Donnelly et al., 2011). Mucoadhesive drug delivery systems may be formulated to deliver drugs via the ocular, oral, buccal, sublingual, nasal, enteral, rectal and vaginal routes, for both local and systemic effects (Mahajan, Kaur, Aggarwal, & Harikumar, 2012).

The desired characteristics associated with mucoadhesive systems for drug delivery include their size, taste, release rate of drug from the mucoadhesive system, texture of the mucoadhesive system and ease of use. The size of the mucoadhesive film should be small and flexible to increase patient acceptance. The film must be able to

release the drug at a controlled rate; it should be tasteless and not cause any irritation to the area of the mucosa where it was placed. Appearance-wise, the film must have a smooth surface (Boddupalli, Mohammed, Nath, & Banji, 2010). Some of the advantages associated with the use of mucoadhesive films are: their ability to increase residence time of the drug at the diseased area, which increases the absorption of the drug at the required site, therefore increasing the therapeutic efficacy of the drug. The films are also easy to apply, and treatment may be terminated by simply removing the film (Phanindra, Moorthy, & Muthukumaran, 2013). The drug within the film is released at a slow rate, thereby improving patient compliance, as the patient does not have to apply the film multiple times a day (Kaur & Kaur, 2012). For the proposed drug delivery method to overcome the shortcomings experienced with the nystatin suspension, the drug encapsulated micelles need to be incorporated into a mucoadhesive film, for the oral route of delivery, to provide a local effect in the mouth.

2.4.2 Mucous membrane.

According to Darling and Daley (2005), a mucous membrane is the moist lining that lines the cavities and canals of the body that lead to the external environment such as the eyelids, mouth and nose. The mucous membrane is composed of a mucus layer which accounts for the moist surface of the membrane. Below it is the epithelial layer and below the epithelial layer is the lamina propia, which is made up of connective tissue. Depending on the area where the mucous membrane is found, the epithelial layer may be composed of single or multiple layers. A single layer of epithelial tissue is found in the bronchi, the stomach, small and large intestines. Multi-layered epithelial tissue is found in mucous membranes that line the cornea, oesophagus, mouth and vagina. In the mouth, mucus is secreted onto the epithelial tissue by the salivary glands (Boddupalli *et al*., 2010).

Mucus is composed of inorganic salts, water, lysozyme, immunoglobulins, defensins, growth factors, trefoil, lipids and mucin (high-molecular-weight-glycoproteins). Water accounts for 95% of the weight of mucus, causing it to be extremely hydrated (Williams, Sharafkhaneh, Kim, Dickey, & Evans, 2006). Mucin gives mucus the elastic and viscous gel-like property that it is known for (Bansil & Turner, 2006). The function of mucus is to act as a physical and chemical barrier to pathogens, to lubricate and hydrate the epithelial tissue and to allow for the permeation of nutrients and gasses

(Derrien et al., 2010). Mucin, which is the largest component of mucus besides water, is composed of heavily O-glycosylated molecules which are produced by specialised mucus cells. Mucoadhesion is possible due to the mucin glycoproteins showing hydrophobic, electrostatic and hydrogen bonding interactions which facilitate mucoadhesion (Bansil & Turner, 2016).

2.4.3 Mechanism of mucoadhesion.

The mechanism by which mucoadhesion occurs is divided into two stages, as illustrated in Figure 2.6, namely: the contact stage and the consolidation stage. During the contact stage, contact occurs between the mucous membrane and the mucoadhesive (Kaur, 2012). This intimate contact allows the mucoadhesive to spread and swell over the mucous membrane, resulting in increased surface contact. An increase in surface contact initiates the process of a deep contact of the mucoadhesive with the mucous layer, of the mucous membrane (Boddupalli et al., 2010; Phanindra et al., 2013).

At the contact stage, both attractive and repulsive forces are present. However, for mucoadhesion to take place, the attractive force must be stronger than the repulsive force (Phanindra et al., 2013). In the consolidation stage, moisture is needed to activate and plasticize the mucoadhesive. Moisture allows the molecules and polymer chains within the mucoadhesive to break and link up using weak van der Waals and hydrogen bonds within the mucus (Boddupalli et al., 2010). The consolidation stage may be explained using both the diffusion theory and the dehydration theory.

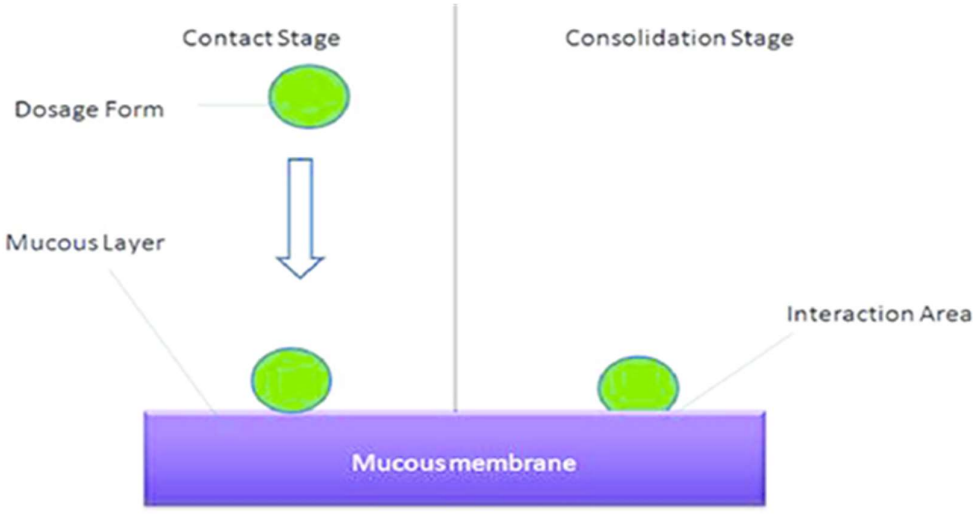

Figure 2. 6: An illustration of the mucoadhesion theory (Jain, Gulati, Kumar, & Nagaich, 2012)

2.4.4 Theories of mucoadhesion.

Mucoadhesion is a complex process that is not well understood. Numerous theories, which explain the mucoadhesive process, have been identified in a bid to help with the understanding of the experimental observations of mucoadhesion (Boddupalli et al., 2010). These theories include: Adsorption theory, diffusion theory, electrostatic theory, fracture theory and the wetting theory. The shortcomings associated with the theories are that they explain a fraction of the interactions that occur during the mucoadhesive bonding (Carvalho, Bruschi, Evangelista, & Gremião, 2010).

2.4.4.1 Adsorption theory.

This theory posits that for mucoadhesion to take place, several surface interactions, namely primary and secondary bonding between the mucous substrate and the adhesive polymer, need to occur after the initial contact of the two surfaces (Boddupalli et al., 2010). These surface interactions are due to interactions of the chemical structures found on the surface of the polymer and the mucus substrate (Donnelly et al., 2011). Primary bonds occur because of chemisorption and lead to strong undesirable bonds such covalent, metallic and ionic bonds. These bonds are undesirable because they are permanent and thus would not allow the patient to easily remove the mucoadhesive film without injuring themselves. The most desirable and

prominent bonds in adsorption theory are the secondary bonds (Amit et al., 2011). These bonds are desirable because they require less energy to break which allows the mucoadhesive film to be removed easily without causing injury. Examples of secondary bonds are van der Waal's forces, hydrogen bonding, and hydrophobic bonding (Donnelly et al., 2011).

2.4.4.2 Diffusion theory.

The diffusion theory proposes that the glycoproteins found in the mucous interact through the interpenetration of the polymeric chains from the mucoadhesive, into the glycoprotein mucin chains. When the interpenetration reaches a sufficient depth within the other matrices, it forms secondary bonds which are semi-permanent. The deeper the interpenetration of mucin and polymer chains, the greater the force of adhesion (Boddupalli *et al.*, 2010). The rate of penetration is dependent on the diffusion coefficient, the nature of the mucoadhesive chains, contact time, flexibility and mobility. For this interaction to occur, the mucoadhesive system must have characteristics that allow for both mechanical interactions and chemical interactions; such as the mucus having a similar chemical structure to the mucoadhesive polymer. The more similar the structures are, the stronger the mucoadhesive bonds. According to Donnelly and colleagues (2011), the necessary depth, for good mucoadhesion to occur, is estimated to be in the range of 0.2–0.5 μm (Donnelly et al., 2011; Amit et al., 2011). The depth of interpenetration (I) may be determined using the equation:

Equation 2.1: determination of depth of interpenetration

$$I = (tD_b)^{½}$$

Equation 2.1: Where t is the contact time and D_b is the diffusion coefficient of the mucoadhesive material in the mucus (Boddupalli et al., 2010)

2.4.4.3 Electrostatic theory.

The electrostatic theory of mucoadhesion postulates that the mucoadhesive material and the mucus membrane both have opposing electrical charges. When the two materials come into contact with each other, this results in electron transfer, which ends up building a double electronic layer at the surface interface. The strength of

the attractive forces in the layer is equal to the strength of the adhesion (Amit et al., 2011; Carvalho et al., 2010; Donnelly et al., 2011).

2.4.4.4 Fracture theory.

The fracture theory of mucoadhesion states that the mechanical strength needed to separate the mucoadhesive material from the surface on which it is attached is equivalent to the adhesion strength. This statement is represented in the following equation:

Equation 2.2: mathematical equation behind the fracture theory

$$\sigma = (E \times \varepsilon/L)^{1/2} \quad (7)$$

Equation 2.2: where σ is the fracture strength, ε fracture energy, E is the young modulus of elasticity, and L is the the critical crack length (Boddupalli et al., 2010; Donnelly et al., 2011).

2.4.4.5 Wetting theory.

The wetting theory is the oldest theory of mucoadhesion. It suggests that the mucoadhesive agent can spread over and penetrate the irregularities found in the mucus membrane, resulting in the adhesive material hardening and creating many adhesive anchors. In order to move freely at the surface, the mucoadhesive material must have the ability to overcome the surface tension. This theory has been shown to apply to low viscosity adhesives and liquid adhesives. The degree of adhesion is measured by the contact angle of the mucoadhesive material over the mucoadhesive surface; the smaller the contact angle the greater the affinity for adhesion (Amit et al., 2011; Carvalho et al., 2010; Mansuri et al., 2016).

2.4.5 Mucoadhesive polymers.

Mucoadhesive materials are usually polymers that consist of hydrophilic groups such as carboxyls amides, hydroxyls and sulphates. The hydrophilic groups attach themselves to the mucus membrane using interfacial forces. The ideal polymer for mucoadhesion must have the following characteristics: the materials and the by-products must be non-toxic and non-absorbable by the human body; the polymer

should not irritate the area that it comes into contact with and it should form a strong noncovalent bond with the mucus membrane. A strong non-covalent bond is ideal as it is strong enough to attach the mucoadhesive in place for as long as is needed but weak enough to be taken out without ripping the mucus membrane. The material should easily allow a drug to be incorporated into it and not hinder the drug's release. It should also adhere quickly to the moistened area it encounters. The polymer must be stable enough not to decompose while it is being stored and it must be affordable (Donnelly et al., 2011).

The polymers used in mucoadhesion can be divided into three categories:

1. Polymers that adhere through nonspecific, noncovalent interactions which are mostly electrostatic in nature.
2. Polymers that have hydrophilic functional groups that form hydrogen bonds with other similar functional groups on the mucus membrane.
3. Polymers that bind only to receptor sites on cells or the mucus surface; this category includes thiolated polymers and lectins (Donnelly et al., 2011).

Factors such as hydrophilicity, cross-linking, swelling, molecular weight, pH and the concentration of the active polymer affect mucoadhesion.

2.4.6 Polymer factors affecting mucoadhesion.

Mucoadhesion could be affected by numerous factors such as: molecular weight, concentration of active polymer, flexibility of polymer chains, cross-linking density and swelling, pH and charge. These are discussed below.

2.4.6.1 Molecular weight.

Polymers with a low-molecular-weight are ideal for interpenetration and polymers that have a high-molecular weight are better suited for entanglements (Donnelly et al., 2011). According to Amit and colleagues (2011), polymers that have a lower molecular weight have an enhanced ability to penetrate the mucus layer, whereas polymers that have a high-molecular-weight struggle to get moist quickly, leading the free groups that are available for interactions not being exposed. This results in the mucoadhesive becoming a loose gel with a high potential of dissolving quickly.

2.4.6.2 Concentration of active polymer.

There is an ideal concentration of polymers to produce the best mucoadhesion. When this concentration has been exceeded, the mucoadhesive strength declines significantly. This is because the coiled molecules become desolvated thus limiting chains that are available for interpenetration (Donnelly et al*.,* 2011).

2.4.6.3 Flexibility of polymer chains.

Amit and colleagues (2011) argue that chain flexibility is important for entanglement and interpenetration. If the mobility of a chain decreases, the number of polymer chains that can penetrate the mucous layer also decrease, resulting in reduced mucoadhesive strength (Saraswathi, Balaji, & Umashankar, 2013).

2.4.6.4 Cross linking density and swelling.

According to Donnelly and colleagues (2011), cross-linking density is inversely proportional to the degree of swelling. If the cross-linking density is low, there will be a higher degree of hydration and flexibility. This results in a large surface area and therefore better mucoadhesion. A polymer with a low cross-linking density is therefore ideal for good swelling (Saraswathi et al., 2013).

2.4.6.5 pH and charge.

The pH found at the interfacial surface of the mucoadhesive and the mucus membrane can affect the adhesion of mucoadhesive polymers with ionisable groups such as those with carboxylic acid end groups. The best adhesion for the polymers is seen at a pH range between 4 and 5, with the strength decreasing as the pH increases above 6. If the local pH is lower than the pk_a, then the polymer will be unionised, which is favourable for mucoadhesion. For good mucoadhesion, mucin reacts better with polymers that are undissociated and anionic than cationic polymers. This is because the anionic polymers freely form hydrogen bonds with mucin (Amit et al., 2011; Donnelly et al*.,* 2011).

2.5 Conclusion

OPC is prevalent in South Africa due to a number of factors such as an increased number of patients suffering from HIV/AIDS, and an increase in the life expectancy of the South African population. According to Statistics South Africa (2015), in 2015, approximately 6.19 million people in South Africa were living with HIV, which had increased by 2.7% from 2014. Life expectancy of a citizen in South Africa was expected to be 72 years for females and 65 years for males in 2015. According to Garcia-Cuesta and colleagues (2014), an increased life span and the poor health of patients contribute greatly to OPC prevalence in developed and developing countries. OPC may be treated using a number of antifungal agents.

In South Africa, nystatin suspension is the first line treatment for OPC infections. Nystatin is superior to other antifungal agents because there is a lack of resistance by the *Candida* species to nystatin, and there is a low chance of the patient experiencing side effects and drug interactions as it is not absorbed in the gut (Campos et al., 2012). Because of these advantages, nystatin has become the treatment of choice for OPC and for this study. Unfortunately, the current nystatin suspension poses some challenges to OPC treatment, as efficacy is hindered by nystatin being easily washed away by saliva; this is because the suspension does not have good adherence to the affected area. To improve the problem of retention time and prevent recurrence of OPC, loading a polymeric micelle with nystatin and incorporating that into a mucoadhesive film may ensure that nystatin is in constant contact with the affected area. The mucoadhesive system may also ensure that the drug is released in a more controlled manner (Gajdošová *et al*., 2016).

CHAPTER 3

Methodology

3.1 Pre-Formulation

3.1.1 Solubilisation of nystatin.

3.1.1.1 Introduction.

It is important for a drug that is intended for clinical use to be water soluble as solubility is directly linked to absorption (Benet, 2013). The Biopharmaceutics Classification System (BCS) is a scientific system that is used to differentiate drugs according to their permeability and solubility as shown in Figure 3.1 (Arrunátegui, Silva-Barcellos, Bellavinha, Ev, & Souza, 2015; Benet, 2013; Ku, 2008). The BCS system divides drugs into four classes; class I, class II, class III and class IV. Drugs that are highly soluble and permeable are placed in class I; drugs with a low solubility and high permeability belong to class II; whereas drugs that have a high solubility and low permeability belong to class III; and drugs with a low solubility and low permeability belong to class IV (Arrunátegui et al., 2015; Benet, 2013; Ku, 2008).

It is advantageous for a drug to have a high solubility as this means that it can be easily solubilised, thus, solubilisation will not hinder the rate of absorption of the drug. Drugs with high permeability are also advantageous as this ensures that the drug can be fully absorbed (Benet, 2013). Nystatin belongs to class IV due to its low solubility and low permeability properties. It is difficult to make formulations using drugs belonging to class IV, because absorption of the drug is a problem (Ghadi & Dand, 2017). In order to improve nystatin absorption in the oral cavity, it is important to find a solvent that can solubilise nystatin. To achieve this, a statistical model was used to show the optimal nystatin solubilisation using dimethylformamide (DMF), methanol and reverse osmosis water.

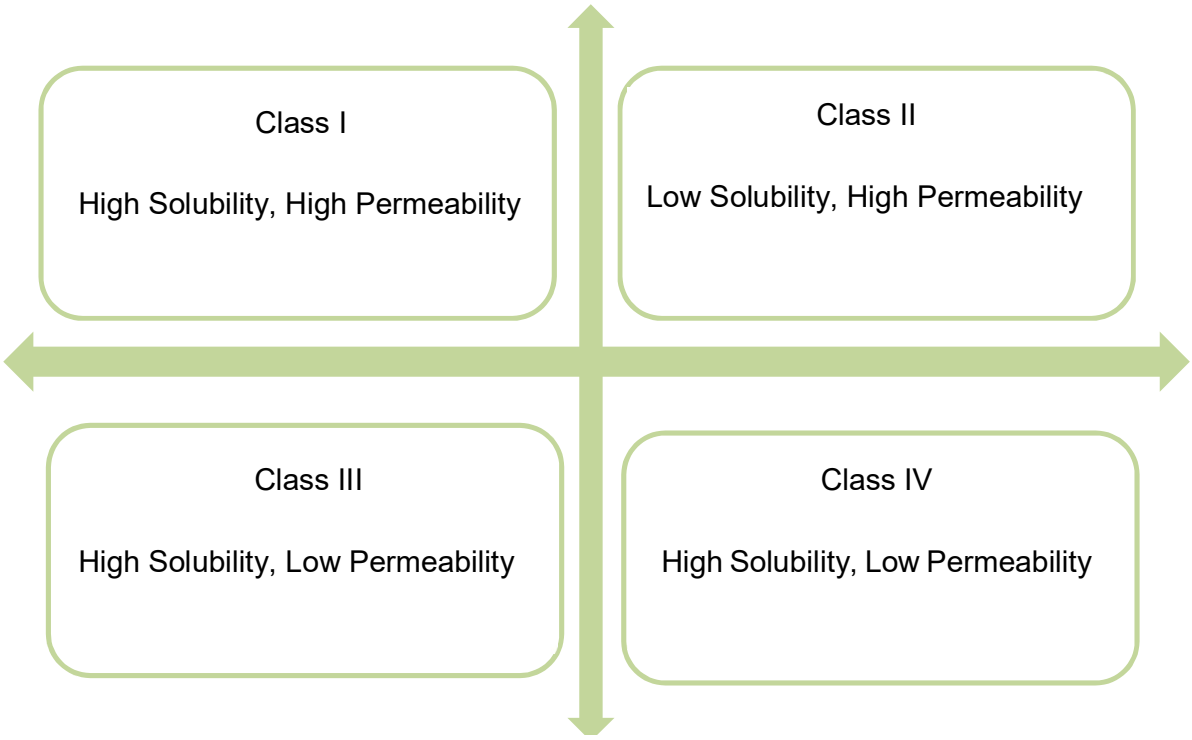

Figure 3. 1: A diagram showing the different BCS classes and what drug properties belong in each class (Milne et al., 2012)

3.1.1.2 Statistical approach to Nystatin solubilisation.

Nystatin solubilisation was tackled statistically using a mixture design, utilising the statistical software Design-Expert version 7.00 (Stat-Ease Inc). A mixture design is a special form of response surface methodology (RSM). This type of design assesses the end product of a mixture based on the different proportions of the solvents added and not based on the amount of the mixture. RSM is a sequential procedure that combines both statistical and numerical techniques to develop, improve and optimize products and processes (Karimi, Abdollahi, Aslan, Noaparast, & Shafaei, 2010; McCarron, Woolfson, & Keating, 1999; Mourabet, El Rhilassi, El Boujaady, Bennani-Ziatni, & Taitai, 2017). The responses obtained in a mixture design are a function of the proportions of the different mixtures that were used. This means that the quality of nystatin solubility will depend on the relative proportion of the different components being investigated.

The experimental design used was a simplex centroid. This design illustrates that the sum of the mixture components is equal to 100% and the experimental space is shown as a triangular plot known as the simplex plot (shown in Figure 3.2). Each side of the triangle represents an axis (x-axis, y-axis and z-axis), each axis is scaled so that when, for example, the x-and y-axis are equal to zero the z-axis will be equal to 100% as shown in Figure 3.2 (Karaman, Yilmaz, & Kayacier, 2011; Weisstein, 2013). A simplex centroid design only shows runs that are the centroid points. This means that for each component that appears in a run in a simplex centroid design, the values may be repeated. This is illustrated in Figure 3.2, where the experimental components of run are shown on the centroid points. As can be observed from point 2 (½, ½, 0), point 4 (0, ½, ½) and point 6 (½ ,0, ½,), the values of the solvents to be mixed are the same but the values are alternated for each solvent. Each of the three points has a 0 value and two values that are non-zero. These points are known as second degree centroids. Point 0 ($^1/_3$, $^1/_3$, $^1/_3$) in Figure 3.3 is known as the third-degree centroids; this point shows that all three points have the same value and no 0 values. Point 1 (1,0,0), point 3 (0,1,0) and point 5 (0, 0, 1) are known as first degree centroids as they have only one non-zero value and two zero values. The three solvents being investigated were DMF, methanol and reverse osmosis water, all with a low value of 0% and a high value of 100%. For a design with 3 solvent components, the highest degree of centroids will be 3. The points discussed above are known as the overall centroid. This design type allows for a reduced number of experiments for the determination of nystatin solubility by using high order polynomial models (Ferreira-Nunes, Gratieri, Gelfuso, & Cunha-Filho, 2017). The model was evaluated using Analysis Of Variance (ANOVA) and a simplex plot, also known as a ternary diagram.

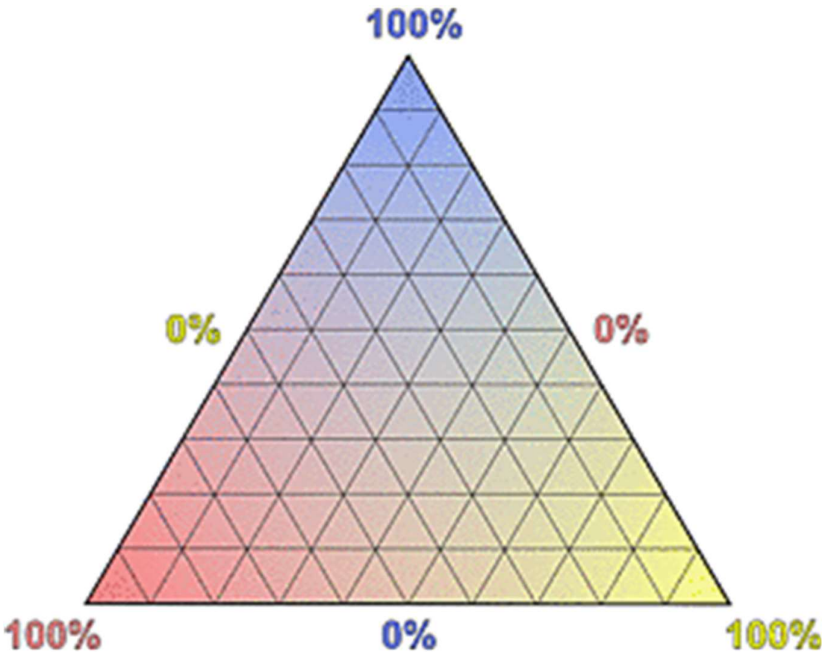

Figure 3. 2: A diagram showing the three axes of a ternary diagram (Akhavan, 2009).

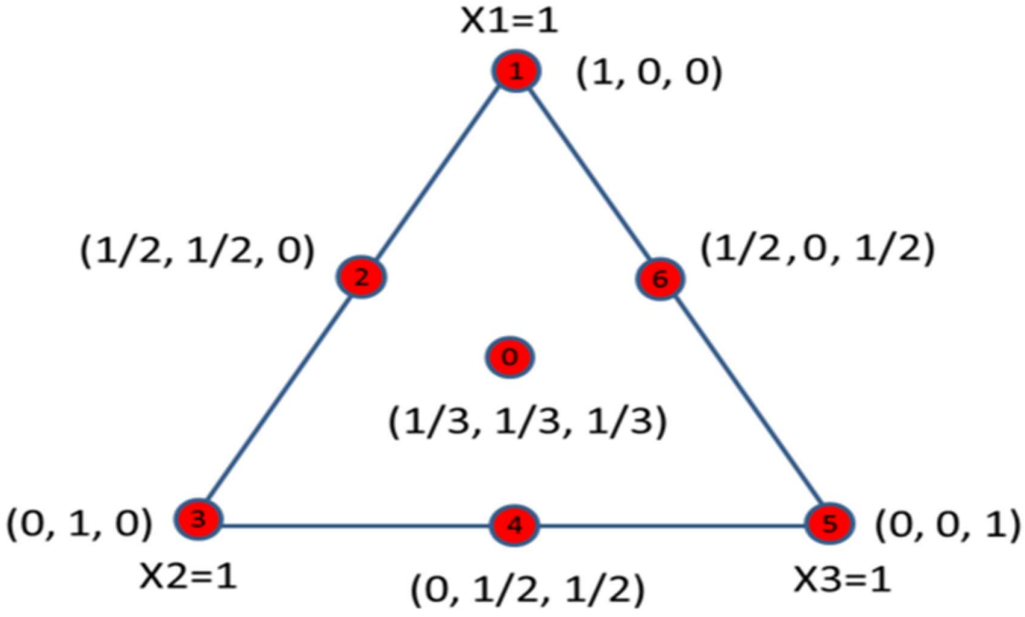

Figure 3. 3: An illustration of the simplex centroid design (Reliability Engineering Resources, 2018)

3.1.1.3 Materials and equipment.

Nystatin, DMF were obtained from Sigma Aldrich, St. Louis, United States of America. Methanol was procured from Merck Laboratory Supplies (Pty) Ltd, Midrand, South Africa and reverse osmosis water was prepared using a Purite Select HP40 GP water purification system (Purite, Thame, United Kingdom) at the Nelson Mandela University, Pharmacy department (Port Elizabeth, South Africa).

3.1.1.4 Procedure.

The following method was adapted from the International British Pharmacopeia (World Health Organisation, 2014). A fixed amount of nystatin powder (22.73 mg) was solubilised using a varied amount of methanol, DMF and distilled water (World Health Organisation, 2014) in a single beaker as shown in Table 3.1. This was done so that the ratios between the three solutions at which nystatin could be solubilised in could be identified. A hundred percent of the solution was 55 ml. In combinations where DMF is present, DMF was added first and a stirring rod was used to solubilise the nystatin in the DMF before other solvents were added. In solutions where only water and methanol were used or only methanol or only water was used, a magnetic stirring rod was placed in the beaker and left to stir for a maximum of 30 minutes at room temperature, then the mixture was assessed to see if all the nystatin had solubilised. The quality of solubilisation was then graded on a scale of 1 to 3; with 3 being well solubilised and 1 meaning that nystatin was not solubilized at all. Table 3.1 shows that some of the experimental runs were replicated. This was to ensure that the experimental design was reproducible and had adequate precision (Vaux, Fidler, & Cumming, 2012).

Table 3. 1: The different ratios at which the solvents were used for the solubilisation of nystatin

Run	Methanol (%)	DMF (%)	Water (%)
1	0	100	0
2	16.667	66.667	16.667
3	50.00	0.00	50.00
4	50.00	50.00	0.00
5	0.00	0.00	100.00
6	100.00	0.00	0.00
7	0.00	0.00	100.00
8	50.000	50.00	0.00
9	100.00	0.00	0.00
10	66.667	16.667	16.667
11	0.00	50.00	50.00
12	16.667	16.667	66.667
13	0.00	100.00	0.00
14	33.333	33.333	33.33

3.1.2 Analytical method development: High Performance Liquide Chromatography (HPLC) method.

3.1.2.1 Introduction.

HPLC is a type of liquid chromatography that uses separation technique to analyse the quality of drugs, proteins, amino acids, nucleic acids, lipids, carbohydrates, vitamins and some biologically active molecules (Coskun, 2016; Siddiqui, AlOthman, & Rahman, 2017; Thammana, 2016). It also allows for the quantification and identification of active compounds and impurities that are present in an analyte, even at low concentrations. Because HPLC is multifaceted, it has become the analytical method of choice for many industries such as the environmental, chemical and pharmaceutical industry (Thammana, 2016). HPLC works by separating components of the analyte, based on the polarity of the analyte and the interaction of the analyte with the adsorbent stationary phase. When the analyte interacts with the stationary phase, the different components of the analyte are separated based on their polarity. This separation affects the retention time of the components of the analyte, thus helping with the identification of the different components of the analyte (Coskun, 2016).

The HPLC system consists of an autosampler, a column (stationary phase), mobile phase reservoir, pumps, detector and an oven, as shown in Figure 3.4. The high-pressured pumping system generates the specific flow of the mobile phase to the stationary phase and then to the detector. The autosampler injects the analyte into the stream of the mobile phase, which carries the analyte injected into the stationary phase and then to the detector. The stationary phase consists of a column that is densely packed with a porous material. The detectors in the system monitor and analyse the eluting substance from the column. A reading is then shown on a processing unit and a display screen in the form of a chromatogram. Examples of detectors include UV spectroscopy, fluorescence, mass spectrometric and electrochemical identifiers (Thammana, 2016).

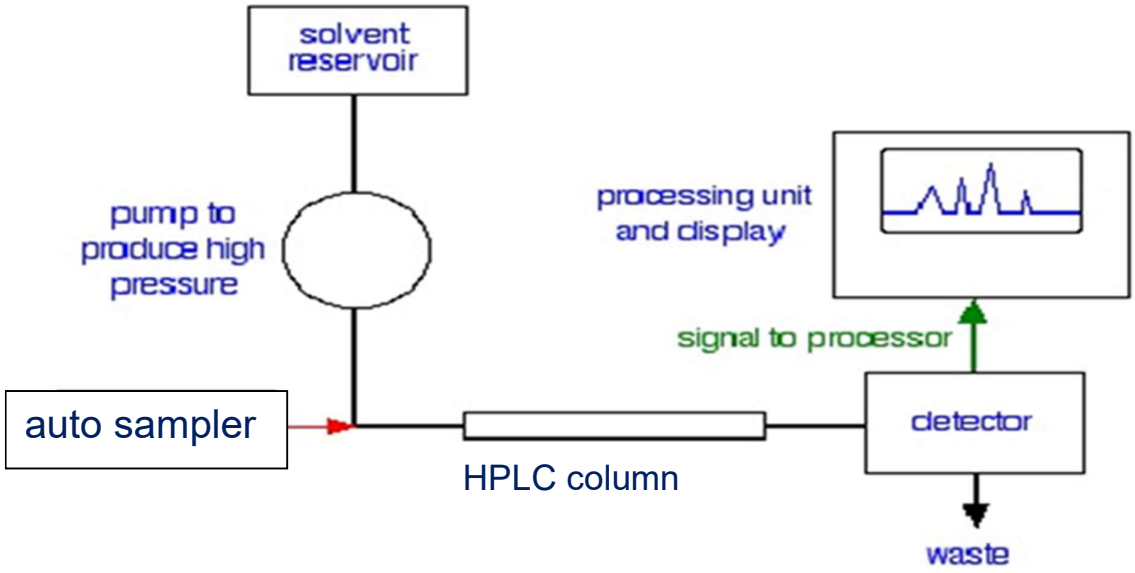

Figure 3. 4: A diagram showing the different parts of the HPLC machine (Clark, 2016)

3.1.2.2 Materials and equipment.

3.1.2.2.1 Materials.

Nystatin was procured from Sigma Aldrich, St. Louis, United States of America, HPLC grade acetonitrile and methanol were obtained from Merck Laboratory Supplies (Pty) Ltd, Midrand, South Africa. Ammonium acetate buffer was prepared using ammonium acetate salt, glacial acetic acid which were all obtained from Merck Laboratory Supplies (Pty) Ltd, Midrand, South Africa and reverse osmosis water was prepared using a Purite Select HP40 GP water purification system (Purite, Thame, United Kingdom) at the Nelson Mandela University, Pharmacy department (Port Elizabeth, South Africa).

3.1.2.2.2 Equipment.

HPLC analysis of nystatin was performed using a Shimadzu LC 20AT System with a SPD M20A Photodiode Array (PDA) detector, a DGU 20A5 degasser, an isocratic pump and a CTO 20A column oven (Shimadzu, Kyoto, Japan). All injections were made through an S/L 20ACHT autosampler with a 100 µL injection loop. A SPD20AV wavelength UV/Vis detector was used to monitor the UV absorbance of samples. The

mobile phase was filtered using a vacuum filter of 0.45 µm pore size, with a Pall GH Polypro membrane (GVS life sciences, Bologna, Italy). The pH of the ammonium acetate buffer for the mobile phase was tested using a pH meter (Crison, Barcelona, Spain). Samples were transferred to 2 ml glass HPLC vials (Thermo Fisher Scientific, Waltham, Massachusetts, United States) using 5 ml syringes (Avacare Health, Rhodesfield, South Africa) and filtered through 0.45 µm syringe filters (GVS life sciences, Bologna, Italy). The stationary phase used was a Supelco C18 column with a particle size of 5 µm (Sigma Aldrich, St. Louis, United States of America).

3.1.2.3 Procedure.

3.1.2.3.1 Mobile phase preparation.

A 0.05 M of ammonium acetate buffer at a pH of 6 was prepared by solubilising ammonium acetate salts (3.85 g) in reverse osmosis water (1000 ml). Glacial acetic acid was added in a dropwise manner to the solution to adjust the pH until the desired pH (pH 6) was reached. The final solution was filtered using vacuum filtration through a cellulose filter with a pore size of 0.45 µm, before it could be used for HPLC. HPLC grade methanol and acetonitrile were used directly from the bottle without filtration. The ammonium acetate buffer was not used for longer than 72 hours, because it would form precipitates which would affect the HPLC instrument and the analysis of the analyte. The mobile phase preparation was based on a method used by Heneedak and colleagues (2012).

3.1.2.3.2 Preparation of stock solution.

The stock solution was prepared by accurately weighing 20 mg of nystatin and solubilising it in 60 ml of methanol; this was considered as 100% concentration. The mixture was left under constant stirring for 30 minutes. 10 ml of the solution was measured using a measuring cylinder into a beaker. 10 ml of the ammonium acetate buffer was measured using a measuring cylinder and added to the beaker containing the methanol-nystatin solution to create a 1:1 solution. The solution was then stirred for a few seconds and then transferred into a syringe. The solution was then filtered through a syringe filter with a pore size of 0.45 µm into an HPLC vial. The vial was closed tightly with a vial cap. The stock solution preparation was based on a method used by Heneedak and colleagues (2012).

3.1.2.3.3 Chromatographic conditions.

The mobile phase for the analysis of nystatin consisted of 30% acetonitrile, 40% 0.05 M ammonium acetate buffer at pH 6 and 30% methanol in an isocratic flow. A C18 column was used at a temperature of 40 °C. The flow rate of the mobile phase was set to 0.8 ml / minute and the wavelength of the detector was set for detection at 250 nm. The injection volume was set to 5 µl.

3.1.2.4 Method development.

3.1.2.4.1 Analytical column of choice.

A C_{18} column [-CH2-(CH2)16-CH3] was chosen as the analytical column due to its availability in the lab and the wide range of literature available detailing its use in quantitative determination of nystatin (Wilson, Stewart, Flournoy, William, & Vancura, 2001; Heneedak et al., 2012). This resulted in fewer difficulties in finding literature on suitable mobile phase conditions for the analytical problem. Therefore, HPLC method development was initiated using Supelco C_{18} column with column dimensions of 150 mm × 4.60 mm, and a 5 µm pore size.

3.1.2.4.2 Choice of mobile phase.

The choice of mobile phase which was a mixture of acetonitrile, ammonium acetate buffer and methanol was based on an analytical method developed by Heneedak and colleagues (2012). The initial mobile phase consisted of 30% acetonitrile, 10% ammonium acetate buffer and 60% methanol. This was adjusted to 30% acetonitrile, 30% ammonium acetate and 40% methanol. This was adjusted because the initial mobile phase had a short retention time of less than 1 minute. The stock solution preparation was as per that explained in section 3.1.2.3.2. The initial temperature and flow rate described by Heneedak and colleagues (2012) was 45 °C and 1ml / min. This was adjusted to 40 °C and 0.8 ml / min, because this also affected the retention time. After all the adjustments were made, the retention time improved from less than a minute to 3.5 minutes. Initially, the UV detector was set to a wavelength of 230 nm; this was adjusted to 250 nm as it yielded the best peak purity.

3.1.2.5 Method validation.

HPLC method validation is a process where the analytical method is investigated for accuracy, precision and reliability. The purpose of validation is to ensure that the results obtained from the analytical method is reproducible, reliable and suitable for its intended purpose (Green, 1996; Paithankar, 2013).

3.1.2.5.1 Linearity.

Linearity of an analytical method demonstrates that when analytes are prepared at a range of different concentrations, the results show that the area under the curve and the peak height is directly proportional to the concentration of the analyte in a linear manner (Green, 1996). Linearity of nystatin was tested by preparing samples with a concentration range between 200% and 25% (200%, 150% 100%, 75%, 50%, 25%). The preparation of the samples is described above in the section on preparation of stock solution. All readings were done in triplicates and the area under the curve was recorded. The area under the curve was used to plot the calibration curve of the area under the curve vs concentration; and a trend line was fitted into the graph. In order for an analytical method to be considered linear, the calibration curve needs to have a regression line with a correlation coefficient greater than or equal to 0.999 and the y value must not be significantly greater than zero. This is true if an assessment value (z value) is between 2 and -2 (ICH Harmonised Tripartite Guideline, 2005). The z value was calculated using the following equation.

Equation 3.1: equation showing the z value used for the assessment of linearity.

$$z\ value = \frac{\text{y intercept}}{50\%\ \text{detector response}} \times 100$$

3.1.2.5.2 Accuracy.

Accuracy of an analytical method is known as the closeness of the measured value to the true value of the sample. The true value of the analyte may either be an accepted reference value or a conventional true value (Green, 1996; *ICH Harmonized Tripartite*

Guideline Q2A, 2005; Bhadra, Das, Roy, Arefeen, & Rouf, 2011). Accuracy of nystatin was determined by preparing samples containing a concentration of 150%, 100% and 50% nystatin. All readings were done in triplicates with three replicate injections. The true values of the analyte, at the various concentrations, was obtained from the linear regression line obtained from the linearity tests and they were compared to the values obtained for accuracy tests. The Relative Standard Deviations (RSD) of the true values were calculated and compared to the RSD values of the samples. This showed if there were any variations within the sample. The acceptance criteria were a percentage recovery of 100% ± 2%. However, lower ranges between 80% to 120% may also be accepted depending on the targeted concentration (Green, 1996).

3.1.2.5.3 Precision.

Precision is known as the measure of the closeness of data obtained from multiple injections of the same homogeneous analyte, at the same analytical conditions. Samples at 100% concentration were prepared using the method mentioned in the section on preparation of stock solution. Five vials containing analytes at a concentration of 100% were injected in triplicates under the same analytical conditions. The mean area under the peaks were calculated along with the RSD. An analytical method is deemed precise when the RSD is less than or equal to 2% (Green, 1996; Bhadra *et al*., 2011).

3.1.2.5.4 Specificity.

Specificity of an analytical method refers to the ability to test an analyte in the presence of other components that may be found in the final product. Specificity must detect, without a doubt, that the peak obtained is indeed the peak of the desired chemical; pure nystatin. Thus, the purity of the peak needs to be checked to ensure that the purity angle is less than the threshold angle. The peak purity is determined by the photo-diode array detector (PDA), which helps in identifying if there are any impurities that are co-eluting with the active ingredient. The PDA detector used in this research was the SPD M20A Photodiode Array, which is an advanced type of UV detector. This detector is able to give three-dimensional information about the analyte. This information allows for an error free assessment of the peak purity, the peak identity and the peak quantitation, all in a single run.

Specificity was measured by preparing an analyte with a concentration of 100% and 50 mg of poly(ethylene glycol) methyl ether-block-poly(lactide-co-glycolide) (PMP) which will be present in the final product. The analytes were prepared according to the method mentioned in the section on the preparation of stock solution. Three analytes were prepared without nystatin and all runs were done in triplicates. For an analytical method to be considered specific, it must have a purity index as close to 1 as possible with no impurities detected (Green MJ, 1996; Bhadra *et al*., 2011). For the samples without nystatin present there should be no peaks around the time that nystatin elutes.

3.2 Polymeric Micelle Formulation

3.2.1 Introduction.

Polymeric micelles are supramolecular structures that are formed due to self-assembly of amphiphilic block polymers. Block polymers are driven to self-assemble as a result of electrostatic interactions, hydrophilic and hydrophobic effects, hydrogen bonding and metal complexations when the polymers are exposed to water (Mourya, Inamdar, Nawale, & Kulthe, 2010). Polymeric micelles have gained attention for drug delivery due to their low toxicity, biocompatibility, enhanced blood circulation time and their ability to solubilize drugs into the micellar core (Xu *et al*., 2013).

3.2.2 Methods and materials.

3.2.2.1 Materials.

DMF, poly(ethylene glycol) methyl ether-block-poly(lactide-co-glycolide) (PMP) and nystatin were obtained from Sigma Aldrich, St. Louis, United States of America. Reverse osmosis water was prepared using a Purite Select HP40 GP water purification system (Purite, Thame, United Kingdom) at the Nelson Mandela University, Pharmacy department (Port Elizabeth, South Africa).

3.2.2.2 Equipment.

Rotary evaporator with a vertical condenser, R-210 was obtained from Buchi, Meierseggstrasse, Switzerland, Snake skin dialysis tubing composed of a 10 K molecular weight cut-off of regenerated-cellulose with a diameter of 35 mm to allow for the exchange of DMF with water was procured from Sigma Aldrich, St. Louis,

United States of America and Zetasizer Nano ZS instrument was procured from Malvern Instruments (Pty) Ltd., Worcestershire, United Kingdom. The atomic force microscopy (AFM) was obtained from Burke South Africa (Pty) Ltd and transmission electron microscopy (TEM) Joel JEM 2100 was obtained from Joel, Tokyo, Japan. A Hermle Z300 universal centrifuge which was obtained from Hermle Labortechnik, Wehingen, Germany was used for drug entrapment efficiency.

3.2.3 Statistical method for micelle optimisation.

The statistical method used for the optimisation of micelle formation was RSM. Optimisation using RSM is done by analysing the effects of many independent variables on the quality characteristics or the performance measure of the sample (Karimi et al., 2010; Mourabet et al., 2017). This method is a convenient technique as it allows for fewer experimental runs to show a mathematical trend rather than exploring the effects of each variable at a time (McCarron et al*.,* 1999; Bai, Saren, & Huo, 2015). RSM aids in investigating the interactive effects of different variables on the sample to be created, and also allows for the researcher to measure the relationship between the controlled input parameters and the obtained response surfaces (Giordano, 2006; Karimi et al., 2010).

The data obtained from RSM is interpreted using multiple regression analysis to define the equation of best fit and using ANOVA to determine how important each factor is (McCarron et al., 1999). One of the main requirements for RSM is the need for a design of experiments (DoE) in order to achieve reliable and adequate data for the measurement of the response of interest (Karimi et al., 2010). DoE is one of the most common statistical techniques used for product optimisation. DoE is described as the combination of planned experiments that show the relationship of set independent variables with independent variables of interest (Oprime, Maria, Pureza, & Conceição De Oliveira, 2015). The experimental design methods which are commonly used for modelling and process analysis are central composite design (CCD), the full factorial and the partial factorial (Karimi et al., 2010). The experimental design used for this research was the central composite rotational design (CCRD). CCRD is useful when building a quadratic model for the response variables. This design consists of a factor which will be varied, with each factor having two levels; usually a high level and a low level. The design also has a set of central points, which are the experimental runs with

values that do not change; these values are the middle point of the high and low levels that had been plotted. These fixed points help to ensure experimental precision. The experiment also has a set of experimental runs which are identical to the central point, except that one factor is the changed factor which will have values both within the lower and higher levels and also outside of these levels (PennState Eberly College of Science, 2018).

3.2.4 Experimental design.

The two factors that were varied were the temperature of the hydration water added to the polymer solution (hydration temperature) and the rotary evaporation time (Kulthe, Choudhari, Inamdar, & Mourya, 2012; Saadat, Amini, Khoshayand, Dinarvand, & Dorkoosh, 2014). Temperature was chosen as one of the critical factors due to micellar formation being temperature dependant (Zhou, Li, Wang, Zhang, & Liu, 2016). According to Zhou and colleagues (2016), environmental factors such as the temperature in which micelle formation takes place can greatly impact the size, shape, stability and drug encapsulation efficiency of the micelles formed. Since change in size and stability were some of the responses that were being evaluated, the two environmental factors which would be investigated were hydration temperature and the length of time at which the micellar solution was exposed to the temperature within the rotary evaporator. An experiment done by Ai and colleagues (2014), showed that hydration temperatures higher than 50 °C resulted in low drug encapsulation efficiency and low stability, therefore, the hydration temperatures investigated in this research were between 30 °C and 45 °C. There had not been any investigations done on the length of time at which the micelles are exposed to the temperature environment of the rotary evaporator, so a time of 60 minutes to 180 minutes was investigated.

This was chosen to aid in evaluating the quantitative relationship between the input variables and the response; which are mean particle size, change in mean particle size, mean polydispersity index (PDI), change in mean PDI, mean zeta potential and change in mean zeta potential. These responses were chosen because they allowed for an evaluation of the physical characteristics of the micelles, and the physical stability of the micelles. The mean PDI was used as a response as it gave an indication of the uniformity of the size of the micelles within the sample solution (Masarudin, Cutts, Evison, Phillips, & Pigram, 2015). Variables were inserted into Design-Expert®.

A run sheet containing all the different experimental runs was constructed and presented in Table 3.2. The central points in this design consisted of a polymeric micelle being formed at a condition where the temperature of the hydration water was 35 °C, and a rotary evaporation time was 135 minutes. The different experimental runs were conducted and using Design-Expert software, they were evaluated for change in size, PDI and zeta potential. The size, PDI and zeta potential of the micelles were evaluated on the day the micelles were formed and 2 weeks after the micelles were formed, in order to help establish the stability of the micelles. Table 4 shows some duplicate experimental runs; this is to ensure that the experimental run is reproducible and that the experimental design has precision (Vaux *et al.,* 2012).

Table 3. 2: Experimental runs for micellar formulation, with the different variables

Run number	Temperature (°C)	Evaporation Time (min)
1	35	135
2	35	135
3	35	135
4	35	198.64
5	35	135
6	40	90
7	30	60
8	27.92	135
9	35	71.36
10	35	71.36
11	40	180
12	35	135
13	30	180

3.2.5 Procedure: micelle formation during optimisation.

For micelle formation, 100 mg of PMP and 10 mg of nystatin were dissolved in 1.5 ml of DMF to form a yellow solution. Reverse osmosis water, 10 ml at a temperature of 30 °C, was added dropwise under stirring to the polymer-DMF-Nystatin solution; this makes the solution slightly cloudy indicating the formation of micelles. The solution was then transferred into a round bottom flask and placed into a rotary evaporator at

60 °C and at a setting 3 on the rotary evaporation equipment. Rotary evaporation occurred under a vacuum to aid the removal of DMF from the solution for a varied amount of time. Once the micelles were formed in the rotary evaporator, the micelles were dialysed, using a dialysis tube which has a diameter of 35 mm, with a 10 K molecular weight cut off of regenerated-cellulose to further remove DMF from the solution. The required amount of the dialysis tube was cut and soaked in I L of distilled water for 15 minutes. Using a rubber band, one end was tied. The micelle solution was poured into the tube from the untied end and tied off using a rubber band. The tube containing the micelle solution was placed in a 1 L beaker containing 1 L of distilled water for four hours. The 1 L water was poured out and replaced with a new batch of 1 L water every two hours. The micelle preparations were based on a literature written by Kulthe and colleagues (2012).

3.2.6 Characterisation of micelles.

Characterisation of micelles is important as the behaviour of the micelles and nanoparticles in general depend on their size, surface area and surface reactivity (Cong et al., 2011). Depending on how the micelles were formed, their characteristics may differ from micelles that were formed using other methods (Kuthle et al., 2012). Physical characterisation of nanoparticles enables the researcher to view properties such as the size of the nanoparticles, surface morphology, the surface charge of the nanoparticles and the percentage drug encapsulation. The chemical characterisation of micelles enables the evaluation of the critical micelle concentration (Mourya et al., 2010).

3.2.6.1 Size and Zeta potential.

The size and zeta potential of the micelles were determined using the Malvern ZS Nano Zatasizer (Malvern Instruments, Worcestershire, United Kingdom). This is an instrument that is widely used for the measurement of size and zeta potential of colloids and nanoparticles. It may also be used for the measurement of electrophoretic mobility of proteins and microrheology of protein and polymer solutions (Kaszuba, Corbett, Watson, & Jones, 2010). The machine was chosen due to its versatility and its ability to measure many aspects of the nanoparticles. It also allows for the detection of aggregates from small or diluted samples and from samples that are highly

concentrated or have a low concentration; thus, a large amount of sample is not needed for assessment (Malvern Panalytical, 2017).

The size of the nanoparticles measured refers to the average particle hydrodynamic diameter of the samples. The hydrodynamic diameter of the micelle is known as a hypothetical hard sphere that is diffused at the same speed as the particle that is being analysed (Malvern Panalytical, 2017). For a polymeric micelle, an average size of 10 nm to 100 nm is acceptable (Kulthe et al., 2012). To ensure that the size distribution of the particles is closely related, the polydispersity index (PDI) is used. The PDI is a number that is calculated from a two-parameter fit to the correlation data. The index indicates how broad the size distribution of the particles is. If the PDI is greater than 0.7, this is an indication that the size distribution of the particles is too wide (Kuthle et al., 2012).

Zeta potential is the measure of the repulsive or attractive charge that molecules or particles have while in a certain medium. Zeta potential comes from the surface charge, the concentration and the types of ions that are present in the solution, and it is one of the important methods used to determine the stability of a sample (Kaszuba et al., 2010). Zeta potential measurements help with the understanding of causes of aggregation, flocculation and dispersion. Samples with a high charge are considered more stable and have a less chance of aggregating and flocculating because the particles have a stronger repulsion for each other, since they have the same charge (Malvern Panalytical, 2017). The stability of a sample may be changed by modifying the ionic concertation, pH, and by using surfactants and polyelectrolytes. A zeta potential of +30 mv or -30 mv is considered stable.

The Malvern ZS nano Zetasizer works by using a variety of techniques. For size analysis, the dynamic light scattering (DLS) technique and Non-Invasive Backscatter optics (NIBS) is used (Malvern Panalytical, 2017). DLS works by measuring the diffusion of erratic and random motions of particles that are suspended in a liquid (known as Brownian motion), and the intensity and random changes in the intensity of the light scattered from the solutes in the suspension. The Malvern ZS nano Zetasizer converts the diffusion of the particles into size range by using the Stokes-Einstein relationship. The Stokes-Einstein relationship is shown in Equation 4 and demonstrates that the rate of diffusion of particles in a suspension at a constant

temperature is inversely proportional to the size of the particle (Aschinger et al., 2012; Stetefeld, McKenna, & Patel, 2016). Particles that are small tend to diffuse faster than particles that are large. The light scatter and the speed of diffusion is measured using a sensitive avalanche photodiode detector (APD). The changes in the intensity of the light scattered are analysed with a digital autocorrelator which generates a correlation function. This results in a curve that shows the size and size distribution of the sample (Aschinger et al., 2012; Stetefeld et al., 2016).

Equation 3.2: The Stokes-Einstein equation

$$D_h = \frac{k_B T}{3\pi\eta D_t}$$

Equation 3.2: The Stokes-Einstein equation showing the relation of size and the diffusion coefficient measured by dynamic light scattering. Where D_h is the hydrodynamic diameter (this is the goal: particle size), D_t is the translational diffusion coefficient (we find this by dynamic light scattering), k_B is Boltzmann's constant (we know this), T is thermodynamic temperature (we control this) and η is dynamic viscosity

Particles and molecules were measured for zeta potential by measuring the velocity with which they move when they are under the influence of an electric field. When an electrical field is applied to particles, particles with a charge tend to move towards the electrodes that applies the electrical field (Malvern Panalytical, 2017; Tucker et al., 2015). The speed at which the particles move is proportional to the electrical field strength and their zeta potential. The velocity of the particles is measured using laser doppler electrophoresis. This works by applying an electric charge to the solution containing the particles or a dispersion of particles. The velocity with which the particles move is measured using the Malvern's patented laser interferometric technique called M3-PALS (Phase analysis Light Scattering). The M3-PALS helps to calculate the zeta potential by calculating the electrophoretic mobility of the particles (Malvern Panalytical, 2017).

3.2.6.1.1 Sample preparation.

The sample of micellar solution was transferred from the dialysis bag into a beaker. The micelles were then filtered using a syringe filter with 0.45 µm pore size into a new beaker and allowed to settle for a few minutes to eliminate any bubbles that may have formed during filtration. The sample of micellar solution was then transferred to a clear, disposable, folded capillary DT5106OC (Malvern Instruments, Worcestershire, United Kingdom) cell for size analysis, PDI and zeta potential analysis. The scatter angle used for the analysis was 173° at a temperature of 25 °C. Water was used as the dispersant with a refractive index of 1.330, the temperature was kept constant at 25 °C. All samples were analysed three times to minimize error.

3.2.6.2 Atomic force microscopy.

Atomic force microscopy (AFM) is a type of high-resolution scanning probe microscope. The AFM is a microscope that is designed for three-dimensional topography of nanoparticles. It uses a probe to measure properties such as friction, height and magnetism of a nanoparticle. AFM was used in this research due to its ability to generate three dimensional images of the sample and the great degree of accuracy of the microscope (Jagtap & Ambre, 2006; Vahabi, Nazemi Salman, & Javanmard, 2013). An AFM system consists of micro-machined cantilever probe which has a sharp tip mounted to a piezoelectric (PZT) actuator and a position sensitive photo detector (PSPD). The PSPD is used for receiving laser beams that are reflected off the top of the cantilever for the detection of cantilever deflection feedback (Vahabi et al., 2013), shown in Figure 3.5.

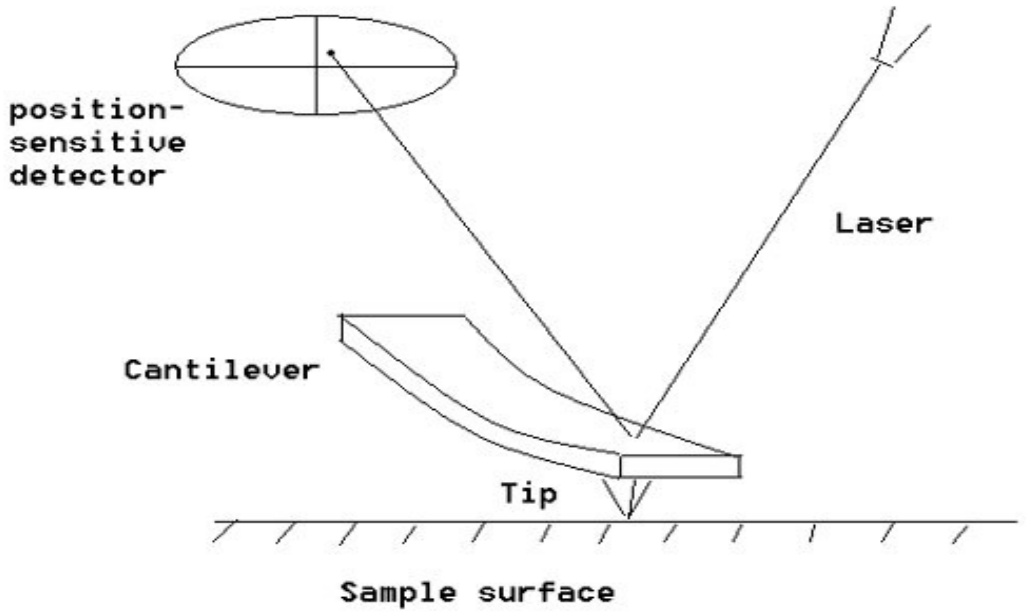

Figure 3. 5: The different constituents of a typical AFM system (Mai, 2017)

The mechanism by which the AFM works is based on the instrument detecting the force that the cantilever tip exerts on the surface of the sample. The AFM uses the cantilever probe and its sharp tip to scan over the surface of the sample. As the tip gets closer to the surface of the sample, attractive forces between the tip and the surface of the sample cause the cantilever to bend towards the surface of the sample. However, when the cantilever tip gets too close to the sample (when the tip and the sample surface touch) repulsive forces are observed between the cantilever tip and the surface of the sample; this force causes the cantilever to bend upwards away from the surface sample (Jagtap & Ambre, 2006; Vahabi et al., 2013). The PSPD detects the bending of the cantilever by detecting the beam that is reflected form the top of the cantilever during bending. Bending of the cantilever will cause a slight change in the way that the laser beam is reflected; the PSPD tracks the changes. When the AFM is scanning an image, it uses the principle explained above. However, a feedback loop enables the PZT actuator to control the cantilever tip in a way that it is always at a constant height or force away from the surface of the sample. In this way, the AFM is able to accurately generate the topography of a sample (Jagtap & Ambre, 2006; Vahabi et al., 2013).

AFM can be used in three different modes namely the contact mode, the non-contact mode and the tapping mode. During contact mode, the sharp tip of the cantilever is in constant contact with the sample and the tip is dragged across the surface of the sample. When the machine is used in non-contact mode, the cantilever tip does not make physical contact with the sample; the tip oscillates about 1 nm to 10 nm away from the sample. In tapping mode, the cantilever tip makes contact with the sample for a very short time; the tip is not in constant contact but rather it taps the sample (Jagtap & Ambre, 2006).

3.2.6.2.1 Sample preparation.

One drop of the micelle solution was placed on a mica disk and left to dry at room temperature for 48 hours, away from any dust. Once dry, the disk was evaluated using AFM (Ruozi, Tosi, Forni, Fresta, & Vandelli, 2005).

3.2.6.3 Transmission electron microscopy.

A transmission electron microscope (TEM) is a high-resolution electron microscope that generates two dimensional images by using electron beams. The microscope shows information such as the morphologic, compositional and crystallographic properties of a nanoparticle (Ma, Shieh, & Qiao, 2006). A TEM microscope has the following compositions: an electron source, thermionic gun, electron beam, electromagnetic lenses, vacuum chamber, two condensers, sample stage, phosphor or fluorescent screen and a computer as shown in Figure 3.6. The microscope produces high resolution black and white images of the sample.

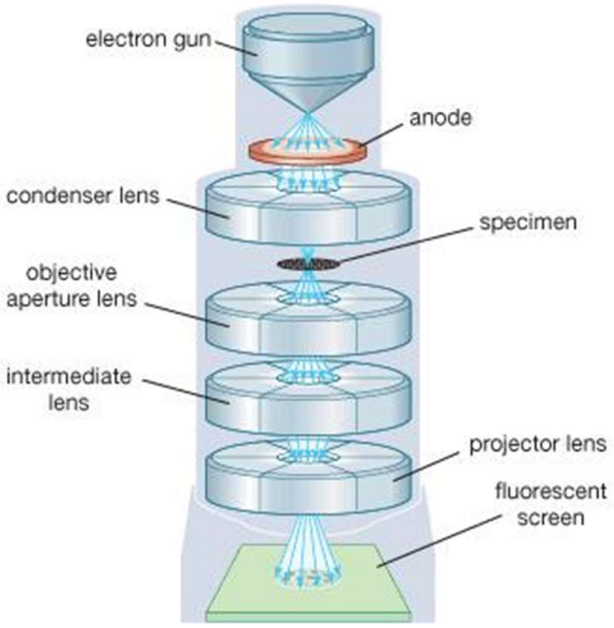

Figure 3. 6: . The constituents of a typical TEM system (Bose, 2017)

The electron gun generates electrons in the form of an electron beam. A beam is emitted that moves through a vacuum present in the microscope. The electron lenses ensure that the electrons emitted are focused into a very thin beam that is directed through to the sample. When the electron interacts with the sample, some electrons are scattered depending on the crystal orientation and the compositional density of the sample. The intensity of the un-scattered electrons generates an image which is seen on the computer screen (Sunoqrot, Alsadi, Tarawneh, & Hamed, 2017; Ma et al., 2006).

3.2.6.3.1 Sample preparation.

A drop of the micelle solution was applied to a carbon coated copper grid and left to dry at room temperature for 48 hours. After the sample was dry, the copper grid was placed in the sample holder and imaged using TEM.

3.3.6.4 Micelle drug encapsulation.

Drug encapsulation efficiency is known as the ratio of the amount of drug remaining in the micelle relative to the amount of drug that was introduced before encapsulation. Drug encapsulation of a micelle is influenced by the method of micelle preparation, the type of copolymer used and the solubility of the drug (Sunoqrot et al., 2017). A method

from Sahu and colleagues (2011), was used to analyse drug encapsulation efficiency of the polymeric micelles. Equation 3.3 was used to determine drug encapsulation efficiency.

Equation 3.3: Equation used to determine % drug encapsulation

$$Drug\ encapsulation(\%) = \left(\frac{Amount\ of\ nystatin\ encapsulated}{Amount\ of\ nystatin\ added\ to\ preperation\ of\ micelles}\right) \times 100$$

3.3.6.4.1 Sample preparation.

The optimal micelles were prepared using the technique mentioned above (3.1.2.3.2). The encapsulated nystatin micelles were separated from the un-encapsulated nystatin by adding a 1:1 ratio of the micelle to 10 mg/ ml of sodium citrate. The micelle sodium citrate mixture was centrifuged for 45 minutes at a rotation of 5000 rotations per minute (Li & Chen, 2017). The supernatant was extracted (5 µl) and added to 5 ml of ammonium acetate buffer and 5ml of methanol and then filtered through a syringe filter. The sample was then transferred to an HPLC vial and analysed using HPLC.

3.3 Mucoadhesive Film Preparation

3.3.1 Introduction.

The use of the oral route for drug delivery remains the best way to deliver drugs. This is because orally administered drugs are widely accepted by both authorities and patients (Lu & Park, 2013). A Mucoadhesive system was chosen for this study because it allows for a more controlled release of nystatin and an increased contact time of nystatin with the affected area (Mansuri et al., 2016). Two mucoadhesive formulations were used for the formation of the mucoadhesive film. The two films were characterised for physical properties such as physical appearance and film pliability. The film with the best results from the characterisation was picked as the film of choice for the study, and it was further characterised for film weight, film thickness, swelling index and drug release studies.

3.3.2 Materials and equipment.

3.3.2.1 Materials.

Hydroxypropyl methylcellulose (HPMC), Sodium Carboxymethylecellulose (SCMC) Polyvinylpyrrolidone K-30 (PVP) and Polyethylene glycol 400 (PEG) were procured from Merck Laboratory Supplies (Pty) Ltd, Midrand, South Africa, reverse osmosis water was prepared using a Purite Select HP40 GP water purification system (Purite, Thame, United Kingdom) at the Nelson Mandela University, Pharmacy department (Port Elizabeth, South Africa).

3.3.2.3 Equipment.

The equipment and apparatus used for testing the film are as follows: Jenway 3510 pH meter obtained from Jenway, Staffordshire, United Kingdom. Franz diffusion cell procured from Sigma Aldrich St. Louis, United States of America, HPLC equipment Shimadzu LC 20AT obtained from Shimadzu, Kyoto, Japan and a micrometer screw gauge procured from Thermo Fisher Scientific, Massachusetts, United States).

3.3.3 Procedure: preparation of films.

Mucoadhesive forming polymers were utilized to prepare mucoadhesive films using the solvent casting method used by Saxena and colleagues (2011). The HPMC film was prepared using 10 ml of reverse osmosis water heated to 90 ºC in a glass beaker. 300 mg of HPMC was weighed and added to the heated water. Once added, the polymeric solution was stirred using a magnetic stirrer until the solution became clear. 6 mg of PVP was weighed and added to the polymeric solution and stirred until the mixture became homogenous. The micelles that were previously formed containing 10 mg of nystatin were added to the mixture, then 0.12 ml of PEG was measured and added and stirred until the polymeric solution became homogenous. The polymeric solution was then poured into a petri dish and placed in an incubator at 37 ºC for 4 hours.

The Sodium Carboxymethylecellulose (SCMC) film was prepared using 10 ml of reverse osmosis water which was heated to 90 °C using the same method as above. 400 mg of SCMC was weighed and added to the heated water. The polymer mixture

was stirred until it was clear, then 4 mg of PVP was weighed and added to the polymer mixture. 0.16 ml of PEG was measured and added to the polymer mixture and stirred until the mixture was homogeneous. The nystatin micelles were added to the polymer solution as explained in the HPMC method. The polymer solution was then poured into a petri dish and placed in an incubator at 37 ºC for 4 hours.

After the films were left to dry, they were characterised. Table 3.3 tabulates the different excipients used for each film.

Table 3. 3: The different excipients used for solvent casting method of the mucoadhesive films.

Excipient	HPMC Film	SCMC Film
Polymer	(HPMC) 300 mg	(SCMC) 400 mg
PVP	6 mg	4 mg
PEG	0.12 ml	0. 16 ml
Reverse osmosis water (at 90 °C)	10 ml	10 ml

3.3.4 Film characterisation.

The mucoadhesive film was characterised for physical characteristics such as the surface smoothness and physical appearance, folding endurance, surface pH, and the swelling index of the film. The film was also characterized for drug release kinetics using a Franz diffusion cell (FDC) and tensile strength.

3.3.4.1 Surface smoothness and physical appearance.

The surface smoothness test includes observing the films for any visible imperfections such as surface texture, clarity, colour and plasticity. It is important for the film to have a smooth and uniformed surface and texture as this is preferred by patients.

3.3.4.2 Film weight and thickness.

Film weight and thickness was explored in order to have a way of assessing whether the drug content in the film was cast uniformly or not. An increase in variation of weight and thickness of the film is indicative that drug distribution within the film is not uniform (Sabry, 2018).

3.3.4.2.1 Sample preparation.

The weight of the film was evaluated by weighing three films on a digital balancing scale and taking the mean weight as the weight of the film. The evaluation of film thickness was done by taking three films and measuring them for thickness using a micrometre screw gauge at three different places on the film. The mean value of the thickness of the films was used as the thickness of the film (Semalty, Semalty, & Kumar, 2008; Sabry, 2018).

3.3.4.3 Folding endurance.

The folding endurance of the film is done to illustrate the flexibility of the film. This flexibility shows that the film can be applied without it (the film) breaking (Karki et al., 2016; Sabry, 2018).

3.3.4.3.1 Sample preparation.

The folding endurance of the films were determined by repeatedly folding the film at the same point until the film was broken. All folding tests were done in triplicates and the mean was taken as the final value for the folding endurance of the film. The folding endurance of the film is done to illustrate the flexibility of the films (Semalty et al., 2008).

3.3.4.4 Surface pH determination.

It is important to assess the surface pH of the film, because a drastic change in pH which is significantly higher or lower than the physiological pH of the mouth (approximately 6.7 to 7.6) may cause the patient to experience tooth decay and irritation to the mucosa (Shaik *et al*., 2011). A change in pH also influences the degree of hydration of the polymer chains, which affects the drug permeation and mucoadhesion of the film (Semalty et al., 2008, Sabry, 2018).

3.3.4.4.1 Sample preparation.

The surface pH of the films was determined by cutting a small square (4 cm x 4 cm) of the film and exposing the film to 10 ml of distilled water at room temperature for 60 min. The pH of the distilled water was first measured and recorded before the film was introduced to the water. After the 60 minutes time had been reached, the pH of the distilled water containing the film was measured using a pH meter (Semalty et al., 2008).

3.3.4.5 Swelling index.

Hydration of the mucoadhesive film forming polymers allows them to expand and spread over the mucosa, thus starting the process of bioadhesion by initiating the interpenetration process between the mucin and the polymer chains. When the polymer swells, it exposes the bioadhesive sites on the film so that they are able to form non-covalent bonds such as electrostatic interactions and hydrogen bonds which are necessary to complete the process of bioadhesion between the polymer and the mucin networks (Semalty et al., 2008; Boddupalli, 2010; Muzib & Kumari, 2011; Sabry, 2018).

3.3.4.5.1 Sample preparation.

The swelling Index tests were performed by cutting the films into a small square (2 cm x 2 cm). The cut film was then placed on a microscope glass slide which was pre-weighed in order to determine the weight of the film itself. The glass slide containing the film was then weighed, where the difference between the two weights was the weight of the film. The glass slide was then placed into a petri dish containing 20 ml of a 0.1 M phosphate buffer solution which had a pH of 6.9 at a temperature of 37 ºC. The petri dish was then placed in an incubator at 37 ºC to maintain the temperature. The use of the phosphate buffer and the temperature was to mimic the conditions of the human mouth. The glass slide was removed from the petri dish every 15 minutes, then dried using filter paper and weighed to determine weight gain and weight loss of the film. The calculation used to determine the percentage of swelling is shown in Equation 6 (Semalty, Semalty, & Nautiyal, 2010; Sabry, 2018).

Equation 3.4: Showing the % swelling calculation (Semalty, 2010).

$$Percentage\ Swelling\ (\%) = \frac{weight\ of\ wet\ film - weight\ of\ innitial\ dry\ film}{weight\ of\ innitial\ dry\ film} \times 100$$

3.3.4.6 Mechanical and physical properties.

The mechanical properties of a film may be important as it gives information about the flexibility and strength of the film. A film with good mechanical properties is easily removed from the plate that it was cast on and easily rolled up. A film that is too flexible may become too elongated during cutting which may change the drug distribution within the film. This leads to the drug not being distributed uniformly within the film (Ikram, Gilhotra, & Gilhotra, 2015). The mechanical property that was tested on this film was the tensile strength. Tensile strength is the measure of the capacity of a material to withstand loads that tend to elongate the material and cause it to break (Satishbabu & Srinivasan, 2008). The tensile tests were done on six small discs of the film that were randomly punched out. The mucoadhesive film was gradually pulled by the load at a speed of 250 mm per minute. This allowed for the measurement of the ultimate tensile strength (UTS), which is a measurement of the maximum stress that the material is capable of withstanding before it breaks, as well as the thickness and width of the mucoadhesive film after the load was applied. Films were analysed for tensile strength using an MF longtravel extensometer at Aberdare Cables (Port Elizabeth)

3.3.4.7 Drug release profile.

It is essential to evaluate the drug release kinetics of the film because it is the rate limiting step in the absorption process. According to Morales and McConville (2011) the rate at which a drug is released from the polymer matrix of a film is dependent on the morphology and the physicochemical properties of the film. Drug release from a film is also influenced by the pH and temperature of the given environment. By varying the temperature and the pH of the environment for drug release studies, the diffusion of the drug from the film may be increased or decreased. It is believed that a drug is

released from a film once the film has eroded. For this to take place, the film needs to come into contact with biological fluids, in this case a phosphate buffer, which will cause the film to swell. Once the film swells, the polymer chains present in the film will relax thus releasing the drug from the polymer matrix.

For the purpose of this research a franz diffusion cell (FDC) was used to assess the drug release kinetics of the film, as shown in Figure 3.7. An FDC is a type of *in vitro* permeation assay that is used to assess the diffusion of drugs from a dosage form. An FDC is made up of two compartments, namely the donor cell and the acceptor cell. The two compartments are separated by a semipermeable membrane that mimics the buccal mucosa. The donor cell is where the film to be tested is applied. This cell is placed on top of the semipermeable membrane. Below the membrane is where the acceptor cell is found. The acceptor cell was filled with a phosphate buffer with a pH of 6.9 at a constant temperature of 37 °C. This was the chamber that the samples for testing were taken from at regular intervals. The samples were taken from the acceptor cell for six hours. During the first hour, a sample was taken every 20 minutes and after that, a sample was taken every hour for the next 5 hours. Once a sample was taken from a acceptor cell, the same amount (as of sample taken out) was replaced with a phosphate buffer to maintain the quantity of the phosphate buffer within the acceptor cell.

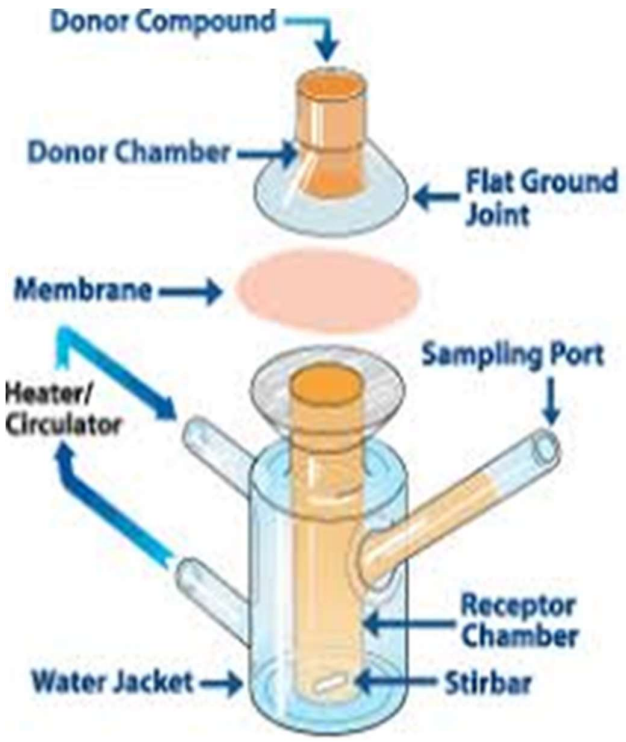

Figure 3. 7: A graphical representation of a FDC (PermeGear, 2017)

3.3.4.7.1 Sample preparation.

500 µl of sample was taken from the sampling port of the FDC acceptor cell and placed into a beaker. 5 ml of methanol and 5 ml of ammonium acetate buffer were added to the beaker and stirred. The solution was then filtered through a syringe filter and placed into an HPLC vial for testing.

3.3.4.7.2 Sample analysis.

The percentage release of the drug from the mucoadhesive film was calculated by calculating how much drug was present in a 2 cm x 2 cm film. Using the linear calibration curve's equation, the area under the peak that corresponds to the total drug in the 2 cm x 2 cm film was taken as the total peak area. The peak area obtained from the samples was used to calculate the percentage release using equation 3.5 below. The cumulative percentage release was calculated using an equation proposed by Chandrasekaran and colleagues stated below in Equation 3.6.

Equation 3.5: Percentage drug release from film

$$Percentage\ drug\ release\ (\%) = \frac{Peak\ area\ from\ sample}{Total\ peak\ area} \times 100$$

Equation 3.6: Cumulative drug release calculation

$$Cumulative\ percentage\ release\ (\%) = \left(\frac{Volume\ of\ Sample\ withdrwan\ (ml)}{Bath\ volume} \times P\ (t-1) + Pt\right) \times 100$$

Equation 3.6*: the cumulative drug release calculation where Bath volume is the total volume of the acceptor cell (15 ml), P (t-1) is the percentage release previous to time 't' and Pt is the percentage release at the current time 't' (Chandrasekaran et al., 2011).*

3.4 Statistical Analysis

3.4.1 Statistical analysis: solubilisation of nystatin.

Design-Expert software 7.00 was used to generate a table with the experimental runs to be performed (Table 3.1). The results were interpreted using a statistical software (Design-Expert software 7.0) and plotted on a ternary diagram also known as a simplex plot. The influence of the mixture components on the solubility of nystatin was determined statistically using analysis of variance (ANOVA).

3.4.2 Statistical analysis: analytical method.

All HPLC measurements were conducted in triplicates. All statistical analysis was conducted using Microsoft Excel® 2010 (Microsoft Corporation). The statistical analysis of the results involved calculating the mean values, the standard deviation (SD) and the relative standard deviations (RSD). Linearity was determined using linear regression analysis, with a correlation coefficient (R^2) of greater than or equal to 0.999 being an indication of acceptable linearity.

3.4.3 Statistical analysis: polymeric micelle formulation.

Design-Expert software 7.00 was used to generate a table with the experimental runs to be performed (Table 3.2). The results were interpreted using a statistical software (Design-Expert software 7.0). The data was analysed using ANOVA analysis. A probability (p) value was calculated to show significance within the 95% confidence interval. If $p < 0.05$, this was defined as being significant. All other experiments were conducted in triplicates.

3.4.4 Statistical analysis: mucoadhesive film.

All tests were performed in triplicates. Data was captured using Microsoft Excel and descriptive statistics such as the mean, standard deviation and relative standard deviation calculated accordingly. Graphical representation of data was facilitated using Microsoft Excel.

3.5 Ethical Considerations

No ethical clearance was needed for this study as there was no use of any human or animal samples in the study. This study was funded by the South African Department of Science and Technology. It should be noted that no conflict of interest existed during the course of the study.

CHAPTER 4

Results and Discussions

Pre-Formulations

4.1 Nystatin Solubilisation

The experimental runs were conducted and analysed for their responses. The response being evaluated was the quality of nystatin solubilisation which was represented using a grading system on a scale of 0 to 3. Grading 0 represents the experimental runs that did not solubilize at all, and even after being kept for three months at room temperature and at 4 °C fridge temperature, they still did not solubilize. Grading 1 represented experiments that took more than 10 minutes to solubilize nystatin initially but remained soluble, both at room temperature and at 4 °C fridge temperature after three months. Grading 2 meant that the mixture of the three solvents solubilized nystatin well initially, but after being kept at room temperature and at 4 °C fridge temperature for three months, only the experiments at room temperature remained without precipitation. Grading 3 meant that the mixture of the three solvents solubilized nystatin well and nystatin remained solubilized after being kept at room temperature and at 4 °C fridge temperature for three months.

Table 4. 1: The mixture components and the response to the mixture components using the grading system.

Run	Methanol (%)	DMF (%)	Water (%)	Response of solubility (Grading)
1	0	100	0	3
2	16.667	66.667	16.667	3
3	50.00	0.00	50.00	0
4	50.00	50.00	0.00	3
5	0.00	0.00	100.00	0
6	100.00	0.00	0.00	0
7	0.00	0.00	100.00	0
8	50.000	50.00	0.00	3
9	100.00	0.00	0.00	0
10	66.667	16.667	16.667	1
11	0.00	50.00	50.00	3
12	16.667	16.667	66.667	1
13	0.00	100.00	0.00	3
14	33.333	33.333	33.33	1

Keys to grading

0 – Does not solubilize nystatin

1 – Takes more than 10 minutes to solubilize

2 – Dissolves only at room temperature

3 – Dissolves at both room temperature and at 4 °C

4.1.1 ANOVA analysis of nystatin dissolution.

The ANOVA analysis was used to assess how well the chosen model (quadratic model) fits the response variables using the F-value and the p-value. The F-value and p-value in an ANOVA analysis give an indication of the significance of the data. A small p-value of less than 0.05 and a large F-value indicate that that the model is significant (Varanda, Portugal, Ribeiro, Silva, & Silva, 2017). In the ANOVA analysis presented in Table 4.2, it can be seen that the model, linear mixture components, AB, BC and ABC are significant model terms; with A being DMF, B being methanol and C being water. This is illustrated with a high F-value and low p-value of less than 0.05. These results mean that the model could be used to evaluate the design space.

Table 4. 2: ANOVA data for nystatin solubilisation.

Terms Investigated	F-Value	p-value	Significance
Model	164.47	0.0001	Significant
Linear Mixture	*403.92*	*0.0001*	Significant
AB	*120.21*	*0.0001*	Significant
AC	*0.063*	*0.8087*	Non-significant
BC	*77.24*	*0.0001*	Significant
ABC	*38.92*	*0.0004*	Significant

Keys

- A = DMF

- B = methanol

- C = water

4.1.2 Diagnostics plot.

Diagnostic plots are used to assess how the data fits the model. The diagnostic tools used in this experiment were the normal plot of residuals plot, and the predicted versus actual plot.

4.1.2.1 Normal plot of residuals.

The normal plot of residuals is a graphical technique used to evaluate whether a data set is normally distributed. This is done by identifying outliers and validating the normality of the experimental errors. The data set to be investigated is plotted against a theoretical normal distribution (shown as the diagonal line). In the ideal normal plot of residuals, the data set points would follow a straight line along the diagonal line; however some moderate scatter is expected. Data set points that are not appproximately linear, and show an s-shaped curve demonstrate a non-normality in distribution (State-Ease, 2018).

The normal plot of residual for nystatin dissolution is illustrated in Figure 4.1. Figure 4.1 does not show an S-shaped curve and the data points are set close to the diagonal line. This shows a normal distribution of residuals.

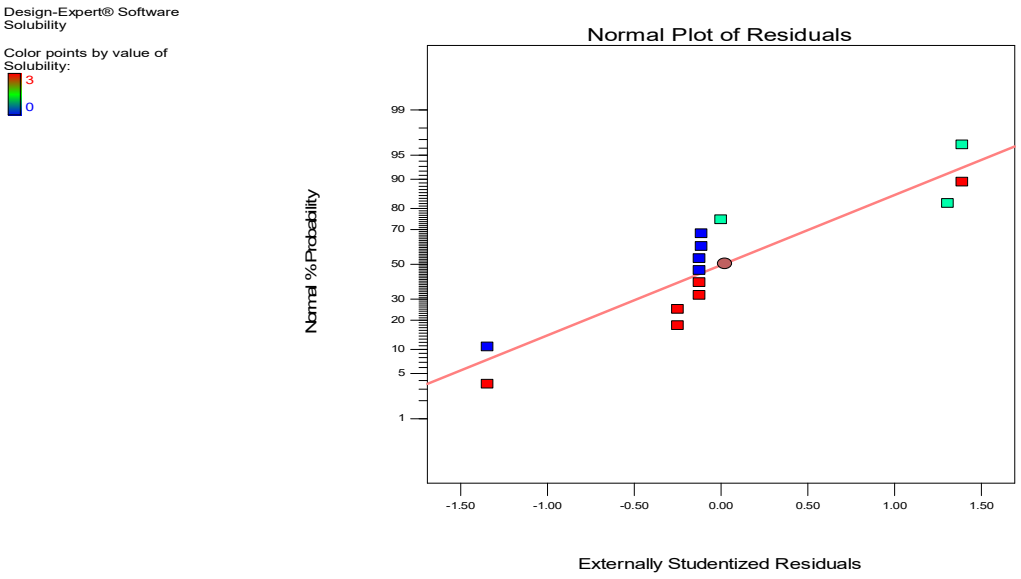

Figure 4. 1: Normal plot of residuals for nystatin dissolutio

4.1.2.2 Predicted versus actual.

The predicted vs actual plot is a graph of the predicted response values versus the actual response values obtained. This graphical technique is used to identify data sets that may not be easily predicted by the statistical model. For the data set to be

considered to have a good fit, it needs to be closely fitted onto the diagonal line. The diagonal line represents the predicted data set. Points that are further away from the diagonal line indicate that those data sets are outliers (Stat-Ease Inc, 2018). A plot of predicted vs Actual for nystatin dissolution is illustrated in Figure 4.2. The data sets are found closely fitted around the solid diagonal line. This indicates that the data set for nystatin dissolution fits the model design well.

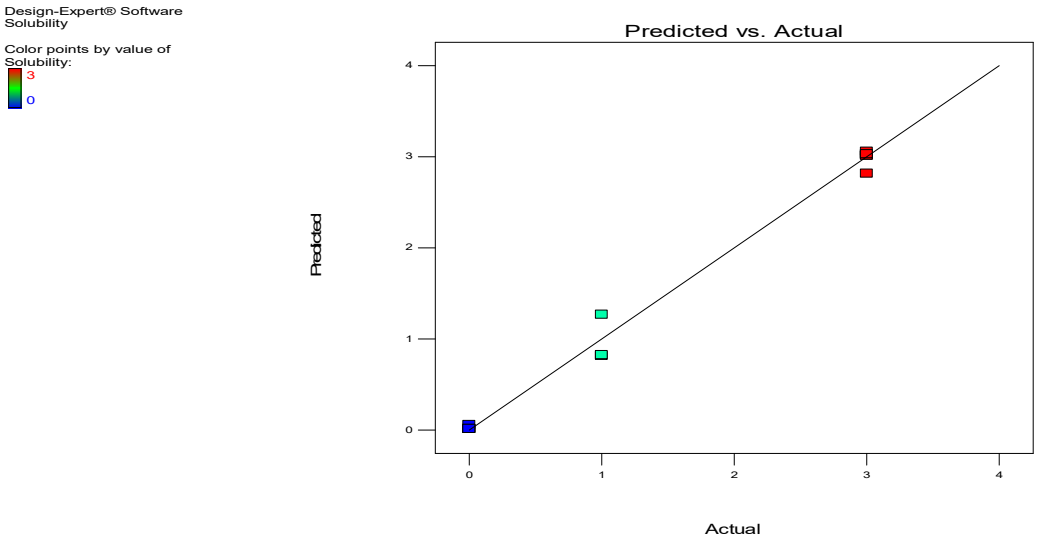

Figure 4. 2: Predicted vs actual Plot

4.1.3 Response surface plots.

To better illustrate the results obtained from the grading of nystatin solubilisation, a visual three-dimensional response surface plot is shown in Figure 4.3. The red areas represent areas that would solubilise nystatin to a grading of three; the yellow areas show a grading of 2; the green areas show a grading of 1; and the blue areas show a grading of 0. The plot shows that DMF is essential for nystatin solubilisation, when les DMF is added to the mixture, nystatin solubility decreases. This is shown visually, where the areas away from point B lose their red shading and change colour. It was observed that nystatin was only soluble in the presence of DMF. This was evident from the plot as Point B was coloured in red. In experimental runs where DMF was not included as a solvent, nystatin did not solubilise. This was interpreted from the plot, as

point A and C had a deep blue colour showing that water and methanol alone could not solubilise nystatin.

4.2 Analytical Method Development

4.2.1 Linearity.

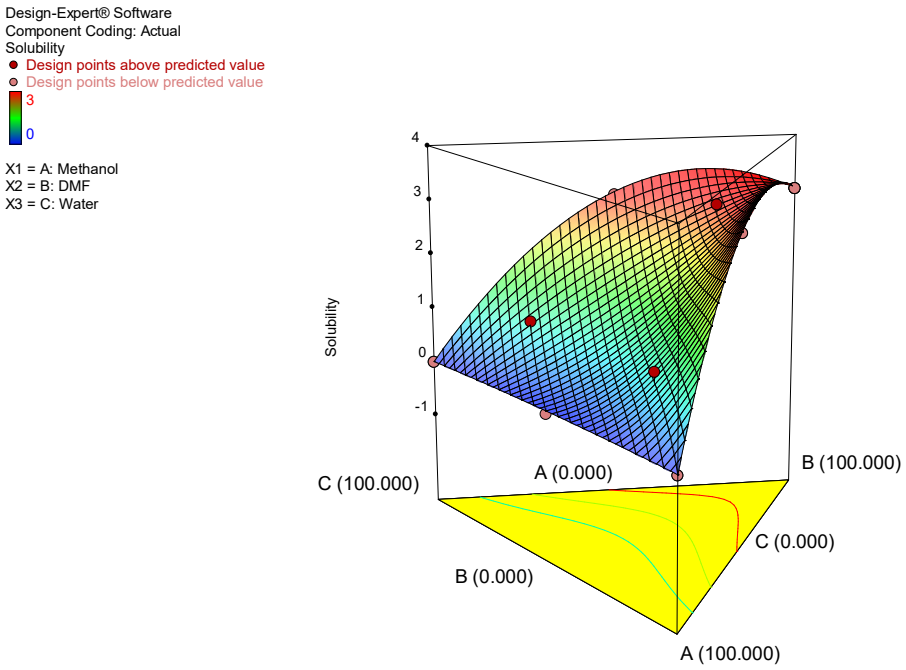

Figure 4. 3: Three-dimensional graphical representation of nystatin solubility

The method was tested for linearity using six different concentrations (200 %, 150 %, 100 %, 75 %, 50 %, 25 %). A calibration curve was created using Microsoft excel to plot a graph (illustrated in Figure 4.4) of the area under the curve versus nystatin concentration using Table 4.3. The plot was used to determine the correlation coefficient (R^2). According to Green (1996), the acceptable range for R^2 is greater than or equal to 0.999. The R^2 for this method was found to be 0.997. Although this value does not equal 0.999, it is still acceptable. This was based on an experiment conducted by Hussien (2014), where the R^2 was found to be 0.997 and was considered acceptable. The author believed that an R^2 of 0.997 is able to show correlation between the area under the peak and the concentration of the samples.

The linear regression equation for the concentration range of 25% to 200% resulted in y = 332763x – 55715. This equation was used to calculate the z value (Equation 3.1). This resulted in a z value of -0.168, which is between the range of -2 and 2 and is therefore acceptable. The %RSD calculated for the different concentrations were all below or equal to 1.91%. The results from the data show that the analytical method is indeed linear.

Table 4. 3: Calibration data used for the analysis of the analytical method used for the pre-formulation studies of nystatin

Concentration (%)	Mean peak area (n=3)	% RSD
25 %	41881,67	1,91 %
50 %	97763,45	0,39 %
75 %	184706,42	1,84 %
100 %	275096,36	1,03 %
150 %	458492,55	0,15 %
200 %	604343,92	1,30 %

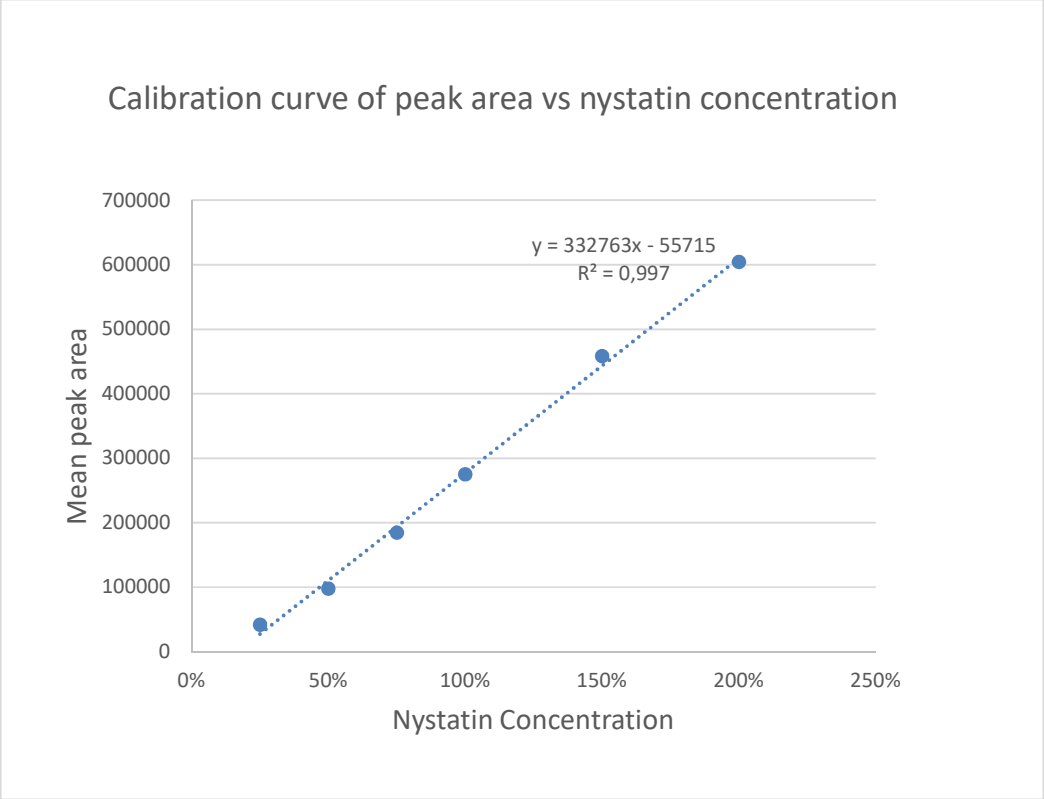

Figure 4. 4: A calibration curve showing mean peak area vs nystatin concentration. y = 332763x – 55715; R2 = 0.997.

Z value calculation

Z value = (-55715 / 33 220 585) x 100

Z value = -0.168

4.2.2 Accuracy.

Table 4.4 shows the concentrations that were investigated and their percentage recovery. Accuracy of the analytical method was acceptable because all the concentrations tested gave a percentage recovery of between 98 % and 102 % range.

Table 4. 4: Accuracy data for the pre-formulation studies of nystatin

	Theoretical value	Measured mean area under peak (n=3)	% Recovery
25 %	41881	41912,00	100 %
100 %	275096,4	271516,92	99 %
150 %	458492,5	468777,55	102 %

4.2.3 Precision.

Table 4.5 represents the data obtained from the precision validation. The precision for the analytical method was within the accepted range, as the %RSD of all the samples taken from each vial was lower than 2.

Table 4. 5: Precision data for the pre-formulation studies of nystatin

Vial number	mean peak area (n=3)	SD	RSD (%)
1	357311	6024,59	1,69 %
2	354005,7	6591,09	1,86 %
3	358715,7	905,242	0,25 %
4	361094	6784,385	1,88 %
5	368152,7	1017,633	0,28%

4.2.4 Specificity.

The purity index of the contaminated sample showed that there were no impurities detected as can be seen in figure 4.5. This shows that the method is specific for the detection of nystatin. Figure 4.6 illustrates an analyte that contains nystatin and Figure 4.7 shows an analyte that had no addition of nystatin. As can be seen from Figure 4.7, there was no peak at time 3.25 minutes as would be expected if nystatin was present. This was interpreted to mean that the solvents that nystatin was solubilised in and the mobile phase were not the peak that was seen at time of 3.25 minutes as nystatin.

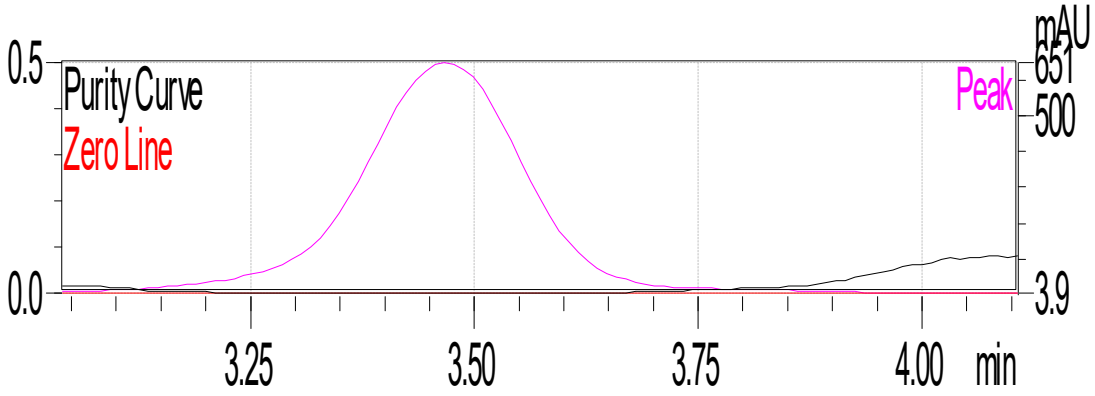

Figure 4. 5: A diagram showing the purity curve of nystatin in the presence of poly(ethylene glycol) methyl ether-block-poly(lactide-co-glycolide)

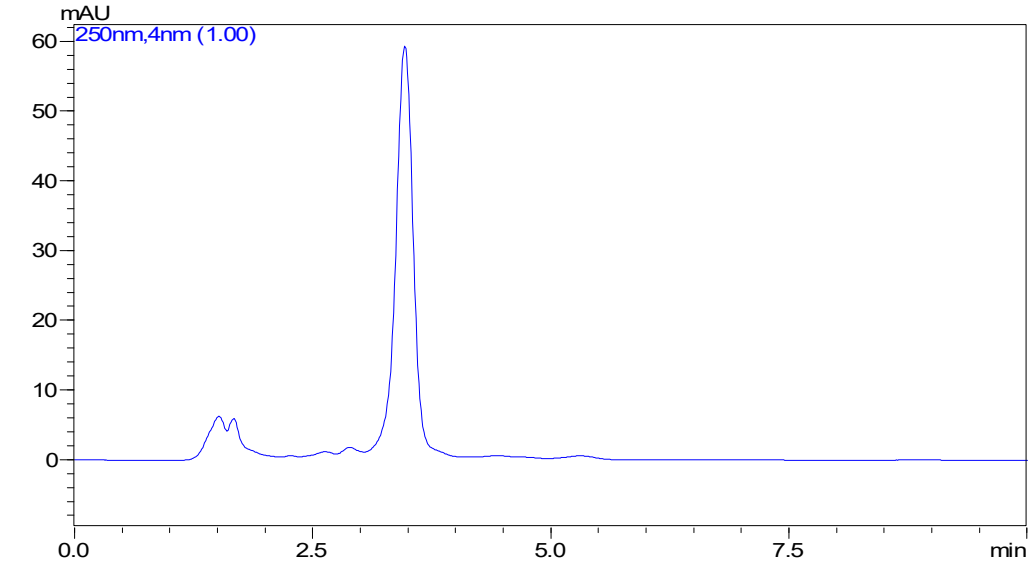

Figure 4. 6: A chromatogram showing a peak for nystatin reading in the presence of poly(ethylene glycol) methyl ether-block-poly(lactide-co-glycolide)

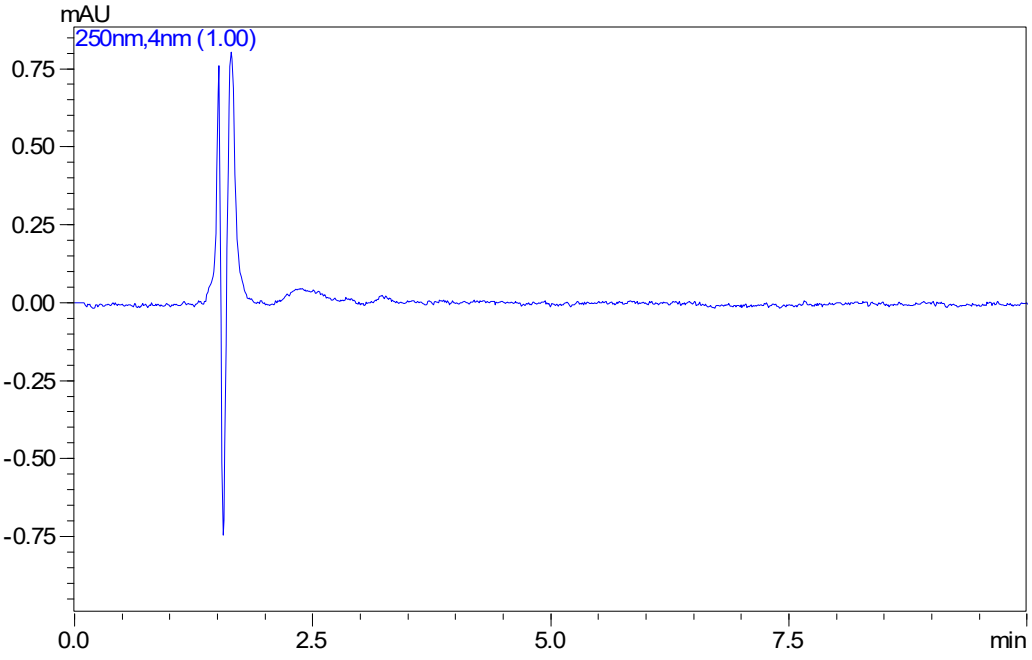

Figure 4. 7: A chromatogram showing the results of an analyte without nystatin present

4.3 Polymeric Micelles Formation and Characterisation

4.3.1 Statistical analysis of data.

Each experimental run was conducted in the laboratory and analysed for five responses. The responses that were being evaluated were mean particle size, mean PDI, mean zeta potential, change in mean particle size and change in mean PDI which were evaluated two weeks after the micelles were initially formed. The design model which best suited the responses was the quadratic design. The model was evaluated using ANOVA analysis and diagnosed using the normal plots of residuals. The responses were then further illustrated using three-dimensional response surface plots.

4.3.1.1 Statistical Evaluation of mean particle size.

4.3.1.1.1 ANOVA analysis of mean particle size.

The ANOVA analysis for mean particle size is shown in Table 4.6. Table 4.6 illustrates that the model and the terms B, A^2, B^2 are significant model terms. This is evidenced by a large F-value and a low p-value of less than 0.05; with model term A being the temperature of the hydration medium and B being the rotary evaporation time. Term A was shown to be non-significant as was evidenced by the p-value greater than 0.05. The results indicate that the temperature of the hydration water added alone did not influence the mean particle size and the model could be used to evaluate the design space.

Table 4. 6: ANOVA analysis of mean particle size

Terms Investigated	**F-Value**	**p-value**	**Significance**
Model	5.09	0.0248	Significant
A-Temperature	*2.58*	*0.1472*	Non-significant
B-Rotary evaporation time	*5.81*	*0.0425*	Significant
A^2	*5.42*	*0.0482*	Significant
B^2	*8.06*	*0.0218*	Significant

4.3.1.1.2 Statistical diagnosis of mean particle size.

The quadratic model was evaluated to assess if the data set was quadratic when using a normal plot of residuals. The data points on the normal plot of residuals should be approximately linear following the diagonal trend line. A non-linear pattern, such as an s-shaped curve implies that there is non-normality in the error term. Figure 4.8 is the normal plot of residual of mean particle size. As can be seen in figure 4.8, there is an s-shaped curvature present (circled in red). This means that there is a non-normality in the error term. This implies that the experimental data do not behave as predicted by the statistical model.

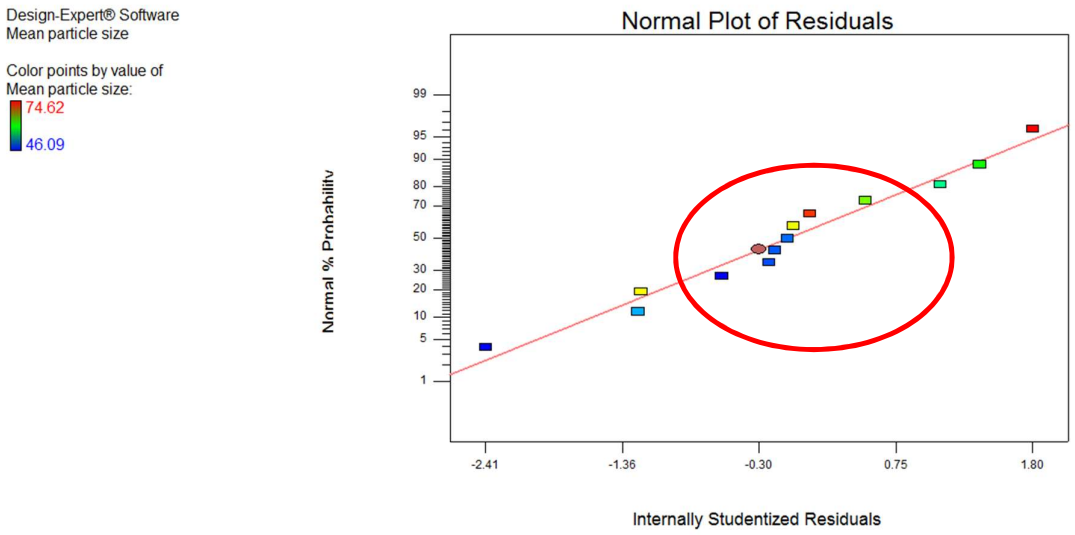

Figure 4. 8: The normal plot of residual of mean particle size. The red circle shows the s-shaped curvature.

4.3.1.1.3 Response surface plot analysis of mean particle size.

A three-dimensional response surface plot was used to aid in visualizing the relationship between the factors and the response. Figure 4.9 represents the relationship between the two factors and the mean particle size. The areas that are shaded in blue indicate that at short rotary evaporation time and at temperatures between 32.5 ºC to 40 ºC, the micelles had a mean particle size of 46.09. The figure also shows that the longer the micelles are exposed to the conditions of the rotary evaporator, the larger the mean particle size becomes irrespective of the hydration temperature. This is shown as the areas of the response surface plot that are shaded in red.

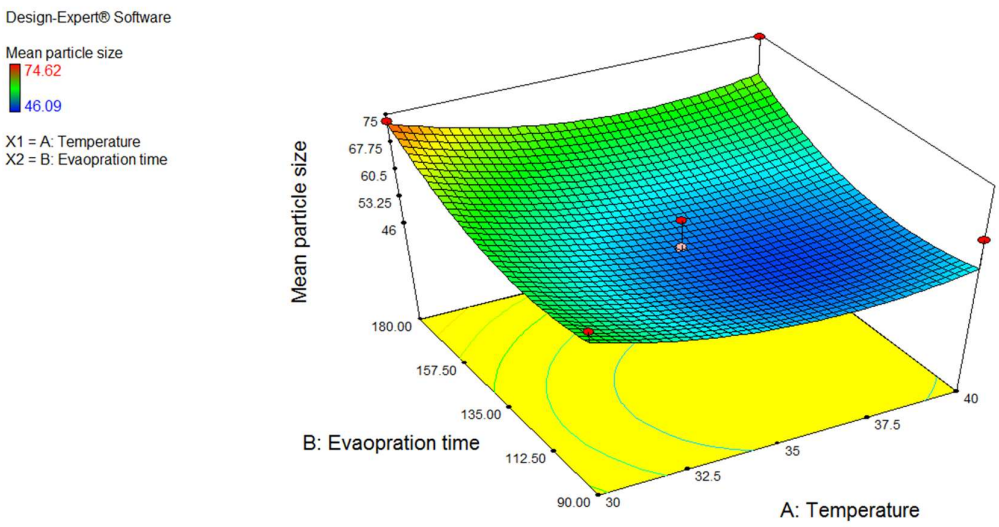

Figure 4. 9: Response surface plot of mean particle size

4.3.1.2 Statistical Analysis of mean PDI.

4.3.1.2.1 ANOVA analysis of mean PDI.

The ANOVA analysis of the mean PDI is shown in Table 4.7. The model and terms B, AB, A^2 were not significant. This was due to the terms having a large p-value of greater than 0.05. Term B^2 was significant as it had a p-value of less than 0.05. This shows that only model term B^2 was significant; with model term A being the temperature of the hydration medium and B being the rotary evaporation time.

Table 4. 7: ANOVA analysis of mean PDI

Terms Investigated	F-Value	p-value	Significance
Model	3.14	0.1026	Non-significant
B-Rotatory evaporation time	*1.04*	*0.3482*	Non-significant
AB	*1.26*	*0.3043*	Non-significant
A^2	*3.14*	*0.1269*	Non-significant
B^2	*10.90*	*0.0164*	Significant

4.3.1.2.2 Statistical diagnosis of mean PDI.

Figure 4.10 shows the normal plot residuals of mean PDI. There is no s-shaped curvature present and the data sets are close to the linear line. This means that the data set has a normal distribution.

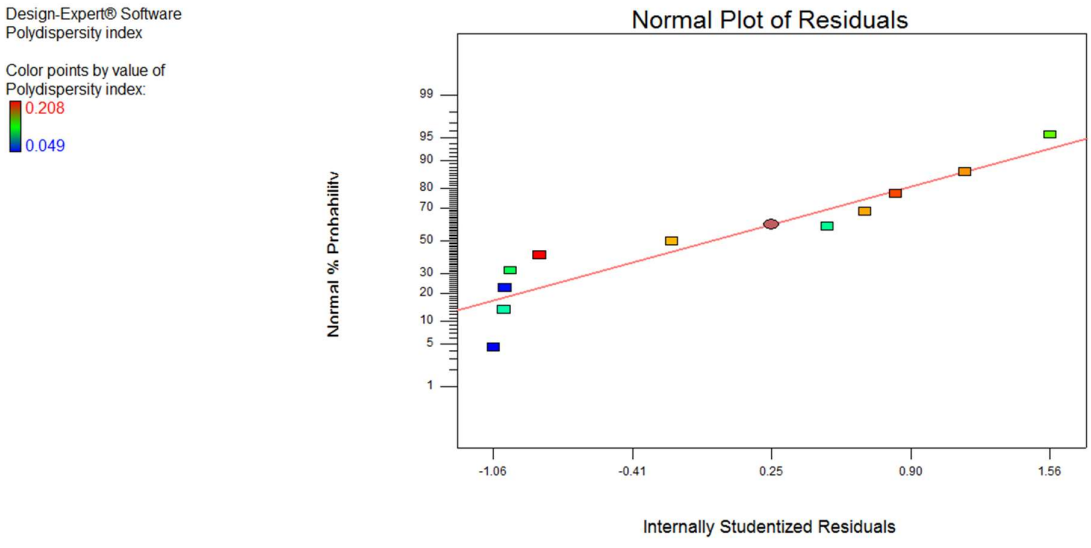

Figure 4. 10: The Normal plot of residuals of mean PDI.

4.3.1.2.3 Response surface plot analysis of mean PDI.

Figure 4.11 represents the response surface plot showing a relationship between the two factors and the mean PDI. The response surface plot shows that when the polymer solution was exposed to low hydration temperature (30 ºC) and a shorter time (90 min) within the rotary evaporation environment, the mean PDI was higher at approximately 0.208. This is indicated by the red shaded areas. According to Figure 4.11 the mean PDI was lower when exposed to hydration temperatures of between 32 ºC and 37 ºC and at a rotary evaporation time of between 112.50 minutes and 157.50 minutes. The results indicate that rotary evaporation time had an effect on the PDI of the micellar system.

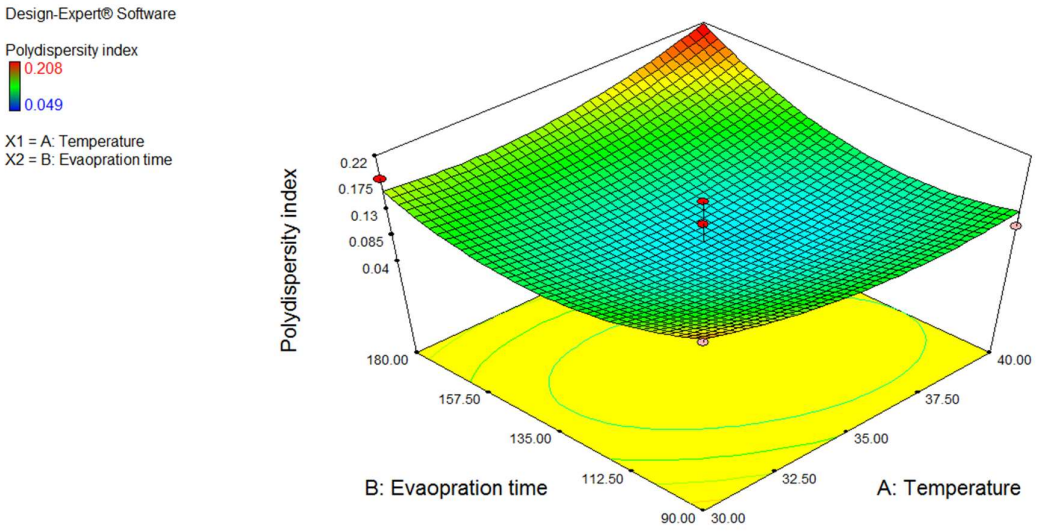

Figure 4. 11: Response surface plot of mean PDI

4.3.1.3 Statistical Analysis of mean zeta potential.

4.3.1.3.1 ANOVA analysis of mean Zeta potential.

The ANOVA analysis of the mean zeta potential is shown in Table 4.8. The model and term B^2 were shown to be significant. This is due to their large F-value and their small p-value; that is less than 0.0500. This means that the other model terms, such as temperature of hydration medium added and rotary evaporation time, did not have a significant effect on the zeta potential of the micelles.

Table 4. 8: ANOVA analysis of mean zeta potential

Terms Investigated	F-Value	p-value	Significance
Model	4.53	0.0397	Significant
A-Temperature	*0.91*	*0.3619*	Non-significant
B^2	*8.15*	*0.0171*	Significant

4.3.1.3.2 Statistical diagnosis of mean zeta potential.

Figure 4.12 represents the normal plot of residual of the mean zeta potential. There are no s-shaped curvatures seen on the plot and all the data points are close to the linear line. This means that the data set has a normal distribution.

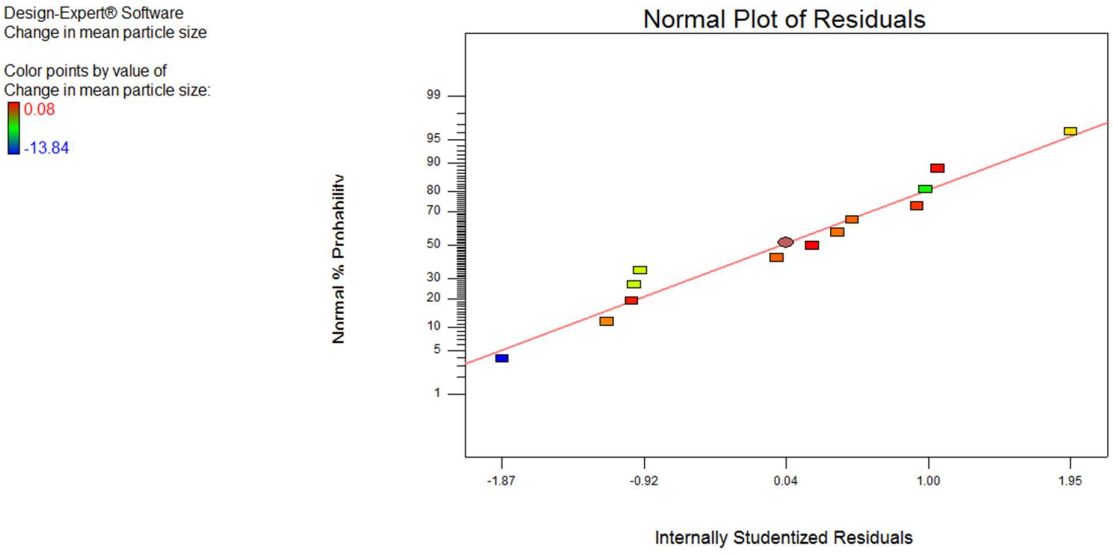

Figure 4. 12: Normal plot of residuals of the mean zeta potential

4.3.1.3.3 Response surface plot analysis of mean zeta potential.

Figure 4.13 represents the relationship between the two factors and the mean zeta potential. According to the surface response diagram indicating hydration temperature did not have an impact in changing the mean zeta potential. However, the length of time at which the micelles were exposed to the rotary evaporator, had an impact on

the change in mean zeta potential. The mean zeta potentials were mostly negative as shown by a large area being shaded in blue. A negative zeta potential indicates that the micelles had a negative charge.

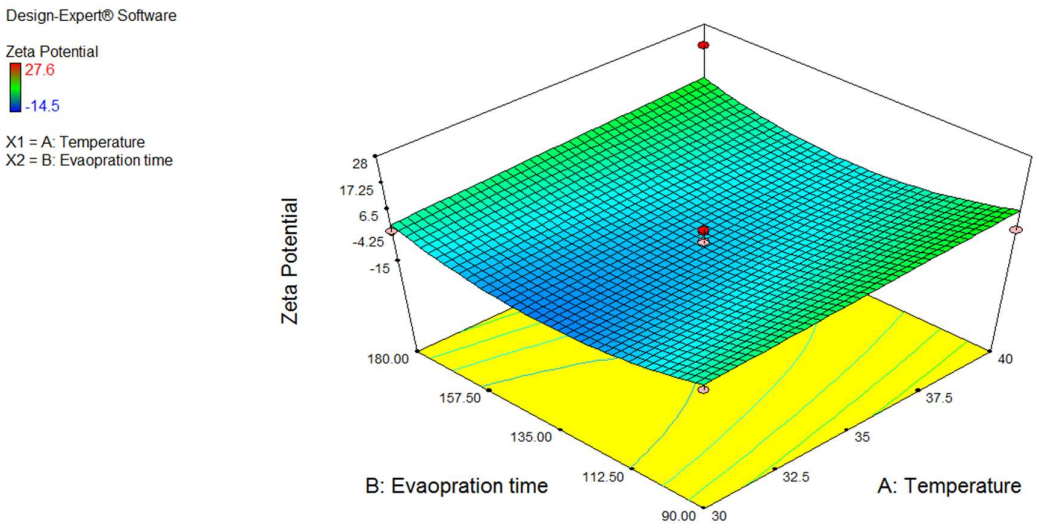

Figure 4. 13: Response surface plot of mean zeta potential

4.3.1.4 Statistical analysis of change in mean particle size.

4.3.1.4.1 ANOVA analysis of change in mean particle size.

The ANOVA analysis of the change in mean particle size is shown in Table 4.9. The model and the terms B and B^2 were found to be significant because they had a large F-value and a low p-value of lower than 0.0500. This means that the temperature of water added did not have a significant effect on the change in size; with model term A being the temperature of the hydration medium and B being the rotary evaporation time.

Table 4. 9: ANOVA analysis of Change in mean particle size

Terms Investigated	F-Value	p-value	Significance
Model	5.78	0.0199	Significant
A-Temperature	5.089	0.9826	Non-significant
B-Evaporation time	*18.29*	*0.0037*	Significant
AB	*1.13*	*0.3225*	Non-significant
A^2	*1.49*	*0.2619*	Non-significant
B^2	*6.97*	*0.0334*	Significant

4.3.1.4.2 Statistical diagnosis of change in mean particle size.

Figure 4.14 represents the normal plot of residual of change in mean particle size. There were no s-shaped curvatures seen on any of the plots and all the data points were close to the linear line. This means that the data set has a normal distribution.

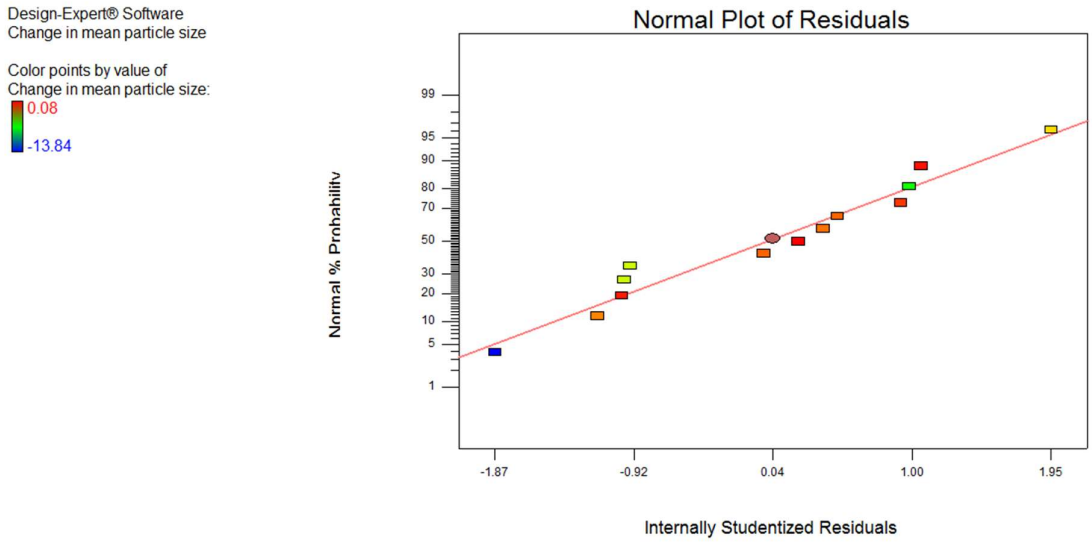

Figure 4. 14: Normal plot of residuals of change in mean particle size

4.3.1.4.3 Response surface plot analysis of change in mean particle size.

Figure 4.15 illustrates the relationship of the two factors and the change in mean particle size. As shown in Figure 4.15 the change in particle size was mostly small, this is shown by most of the area on the response surface plot being shaded in red. The red shading indicates that the change in mean particle size was 0.08. This shows that there was not much difference in the size of the micelles after it had been kept for two weeks. This indicates that the micelles are stable. This indicates that the micelles were stable enough not to aggregate together

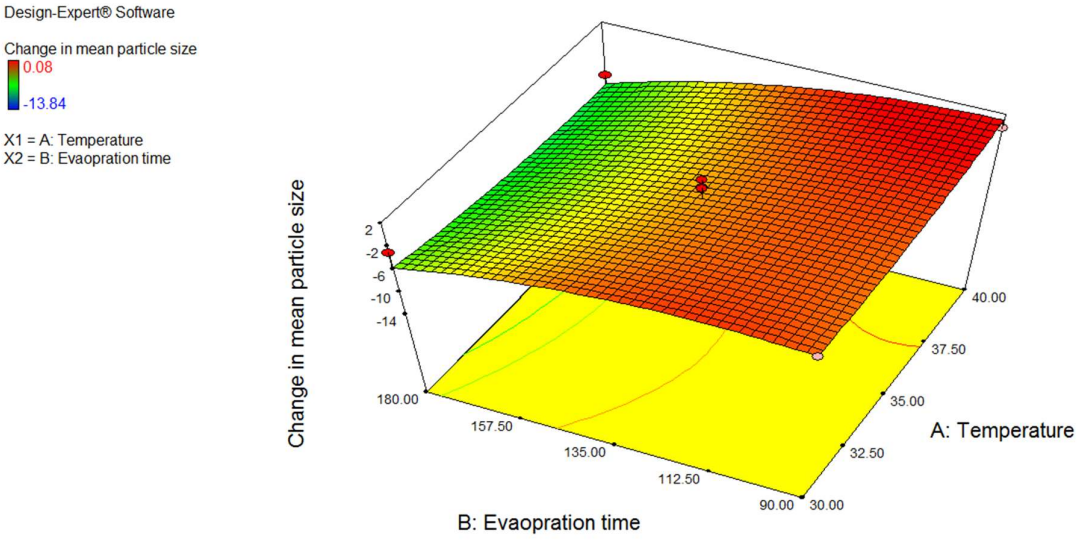

Figure 4. 15: Response surface plot of change in mean particle size

4.3.1.5 Statistical analysis of change in mean PDI.

4.3.1.5.1 ANOVA analysis of change in mean PDI.

The ANOVA analysis of the mean change in PDI is shown in Table 4.10. The model and all terms investigated were not significant. This was evident from all of them having a high p-level above 0.0500. This means that none of the model terms had a significant effect on the change in PDI.

Table 4. 10: ANOVA analysis of change in mean PDI

Terms Investigated	F-Value	p-value	Significance
Model	1.60	0.2905	Non-significant
A-Temperature	0.44	0.5336	Non-significant
B-Evaporation time	*3.22*	*0.1227*	Non-significant
AB	*0.66*	*0.4476*	Non-significant
A^2	*0.91*	*0.3777*	Non-significant
B^2	*2.01*	*0.2001*	Non-significant

4.3.1.5.2 Statistical diagnosis of change in mean PDI.

Figure 4.16 represents the normal residual plot of change in mean PDI. No s-shaped curvatures were identified on the plot. All the data points are close to the linear line meaning that the data set has a normal distribution.

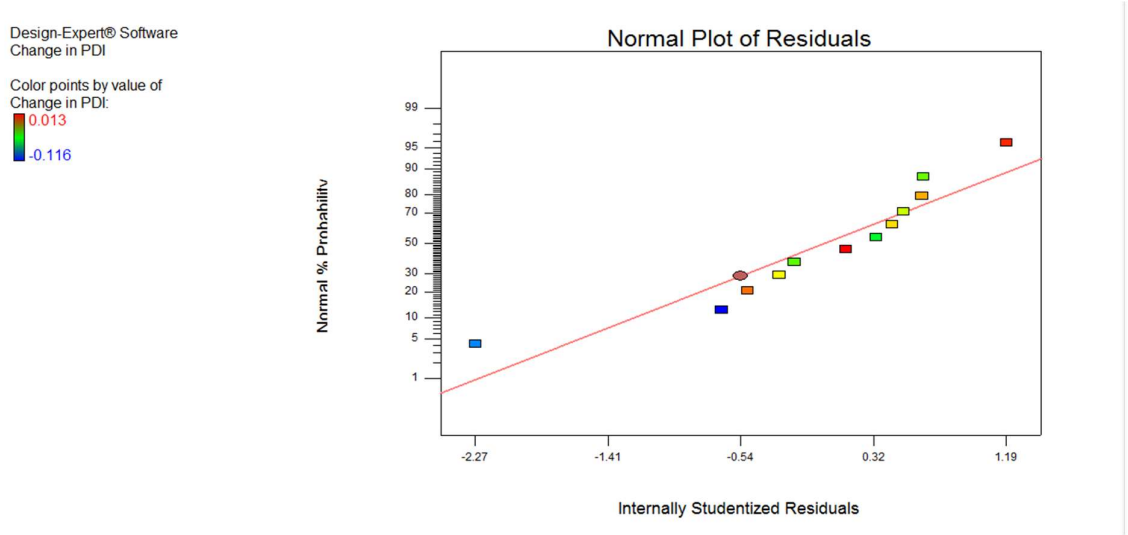

Figure 4. 16: The normal plot of residuals of change in mean PDI.

4.3.1.5.3 Response surface plot analysis of change in mean PDI.

Figure 4.17 illustrates the relationship between the two factors and change in mean PDI. The three-dimensional response surface plot shows that the change in mean PDI was well distributed. The change ranged from 0.013 to -0.116. The mean change in PDI leaned closer to the 0.013 value. This is indicated by having most of the plot area being shaded in red, yellow and green. This means that the change in mean PDI was very small and that even after the micelle solution was kept for two weeks, it was still well distributed within the solution.

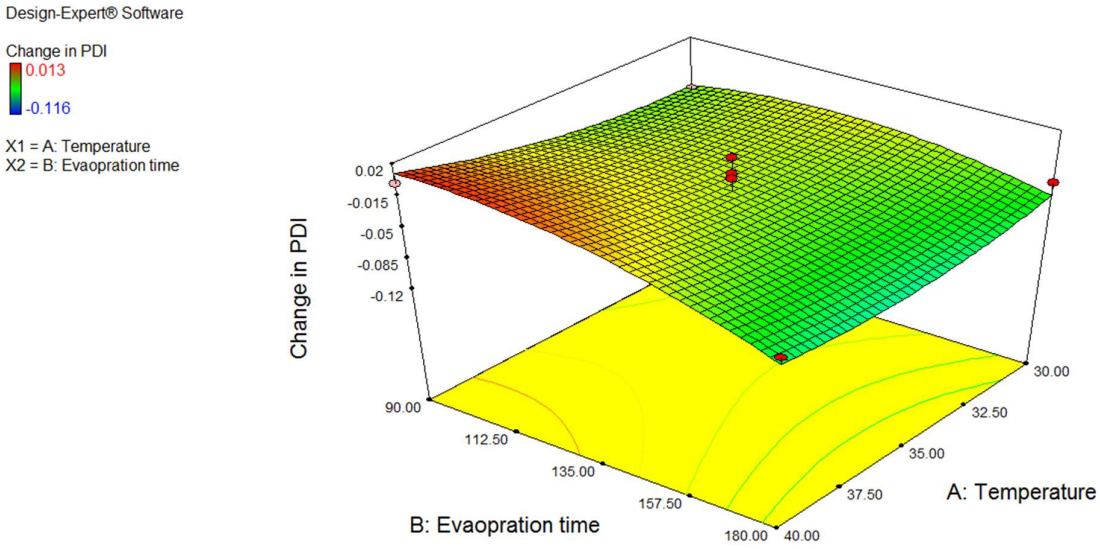

Figure 4. 17: Response surface plot of change in mean PDI

4.3.1.5 Point prediction of optimal values

Point prediction uses the information obtained from the model fit analysis to predict what the responses would be for the optimal micelles (Stat-Ease Inc, 2018). It was observed from the statistical data that the longer the rotary evaporation time, the larger the mean particle size of the micelles. Temperature of hydration water added did not seem to have any effect on the size, PDI or zeta potential of the micelles. This means that other factors such as the solvent composition should have also been taken into consideration while forming the micelles. Once the optimal response was established, the operating conditions were used to form the optimal micelles. These were done in

triplicates, and the mean responses were taken and compared to the predicted responses. The optimal operating conditions were a rotary evaporation time of 180 minutes and a temperature of water of 30 °C. Design Expert does not only give a predicted value; but low and high values at a 95 % confidence interval (CI) in which the expected response values of the runs may be in.

There were significant inconsistencies seen with the experimental results which may have caused the failure of the predicted model to fit the experimental results. This can be seen in Table 4.11 where the responses for mean particle size and mean PDI fall within the predicted range. The response for change in mean PDI did not fall within the predicted range; it is off by a very low value of 0.002. The mean zeta potential and the change in mean particle size did not fit in range of the predicted values. This is also evident in the p-values that did not seem to fit well. A common problem associated with the production of nanoparticles, that may have also contributed to the inconsistencies, is maintaining a batch-to-batch reproducibility of the micelles. This may have been overcome by adding more experimental runs.

Table 4. 11: The predicted response versus the actual response of the optimal micelles

Response	Prediction	95% low (CI)	95% high (CI)	Actual
Mean particle size	58.5712	51.41	65.73	63.26
Mean PDI	0.15	0.091	0.21	0.164
Mean Zeta potential	1.296	-1.82	7.41	-8
Change in mean particle size	-6.5688	-9.06	-4.07	-0.715
Change in mean PDI	-0.059	-0.10	-0.016	0.018

4.3.2 Micelle characterization.

4.3.2.1 Size and zeta potential.

Figure 4.18 shows the hydrodynamic size distribution of the micelles within the micelle solution. The results were obtained from doing triplicate runs of the micelle solution using the Malvern ZS nano Zetasizer. The mean hydrodynamic size of the polymeric micelles was found to be 78.98 nm. This is within the acceptable size range. According to Wang and colleagues (2005), micelles should be no larger than 100 nm thus 78.98 nm is still within the size range of micelles (Wang, Mongayt, & Torchilin, 2005). The mean PDI, which indicates the extent of size distribution of the micelles within a solution, was found to be at 0,266. This indicates that there was a moderate distribution of the particle size and that the solution was moderately homogeneous (Alonso & Csaba, 2012).

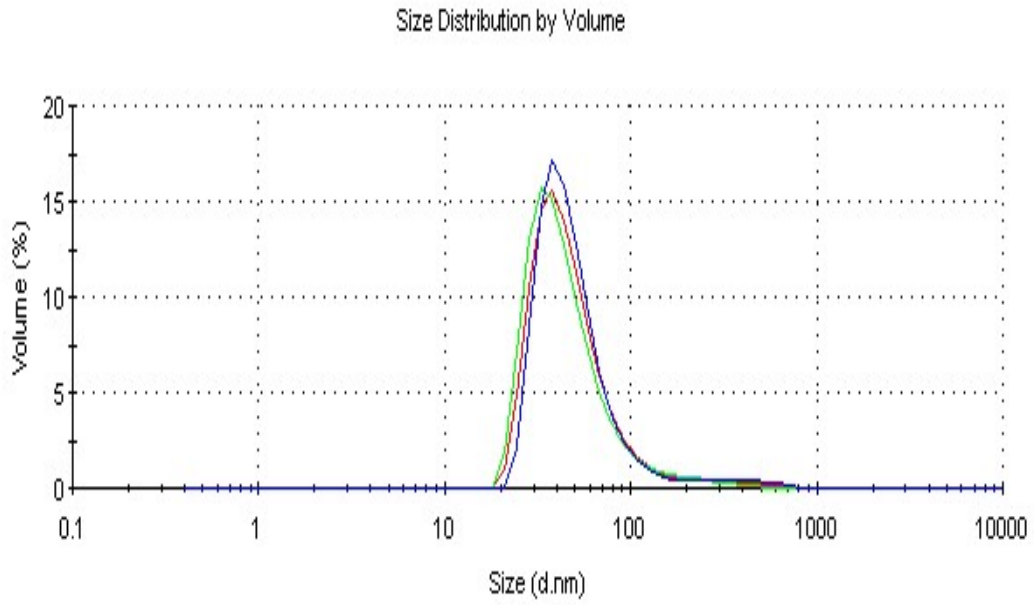

Figure 4. 18: The hydrodynamic size distribution plot of the polymeric micelles

Figure 4.19 illustrates the phase plot of the zeta potential of the polymeric micelle solution. The mean zeta potential of the micelles was found to be -9.1 mV. This indicated that the micelle solution had a weak negative charge. A small negative charge indicates that the micelle solution has a weak repulsive force which prevents them from aggregating. Although -9.1 mV is considered as a zeta potential that is associated with an unstable micellar solution, this is not the case. The zeta potential

was low because the polymer used in micelle formation did not have a high charge, therefore the micellar solution would also not have a high charge. This means that the micellar solution was stable with no aggregation of the micelles seen even after 2 weeks of being kept at -4 °C.

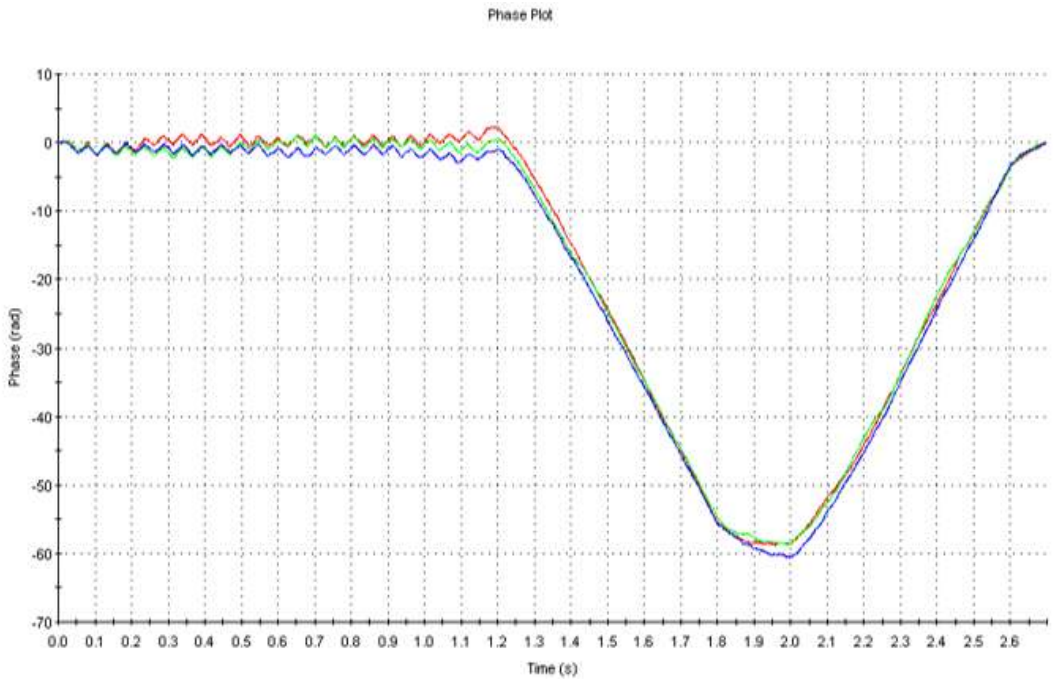

Figure 4. 19: Phase plot of the zeta potential of the polymeric micelles

4.3.2.2 Atomic force microscopy.

Figure 4.20 shows the three-dimensional image of the micelles with the lighter parts being the most elevated parts of the micelles. Figure 4.21 shows the two-dimensional image of the micelles with the measurement of one of the micelles. The lighter parts of the image indicates the presence of a micelle (the white oval shapes). The AFM determined that the micelles had a spherical shape with a diameter ranging from 68.4 nm to 98.6 nm and a hydrodynamic size of 78.98, just as predicted by literature.

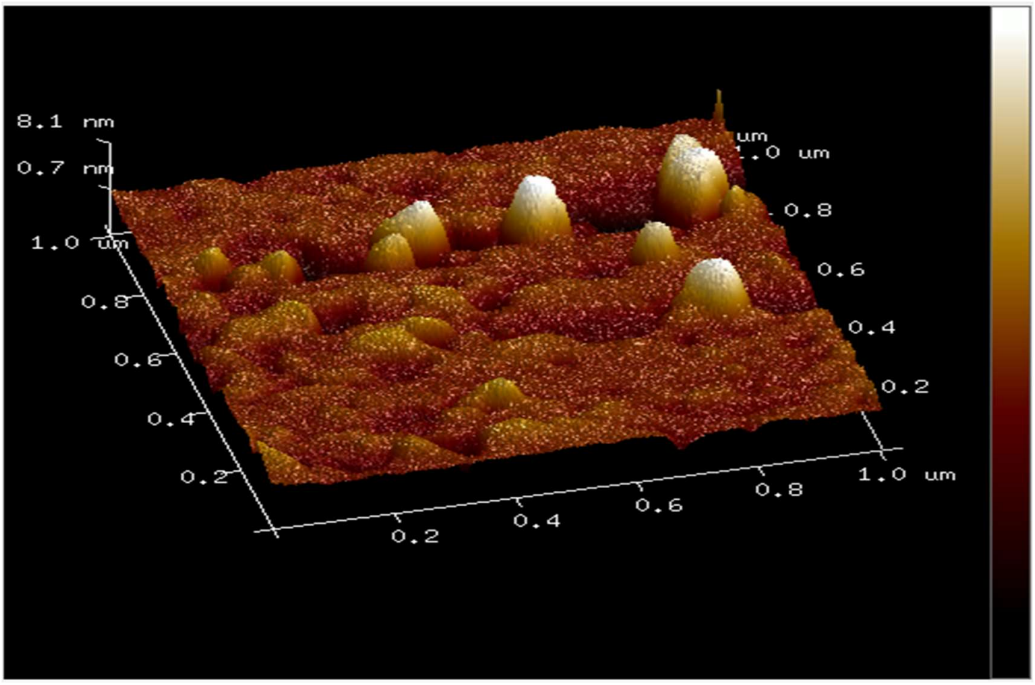

Figure 4. 20: Three-dimensional view polymeric micelle using AFM imaging

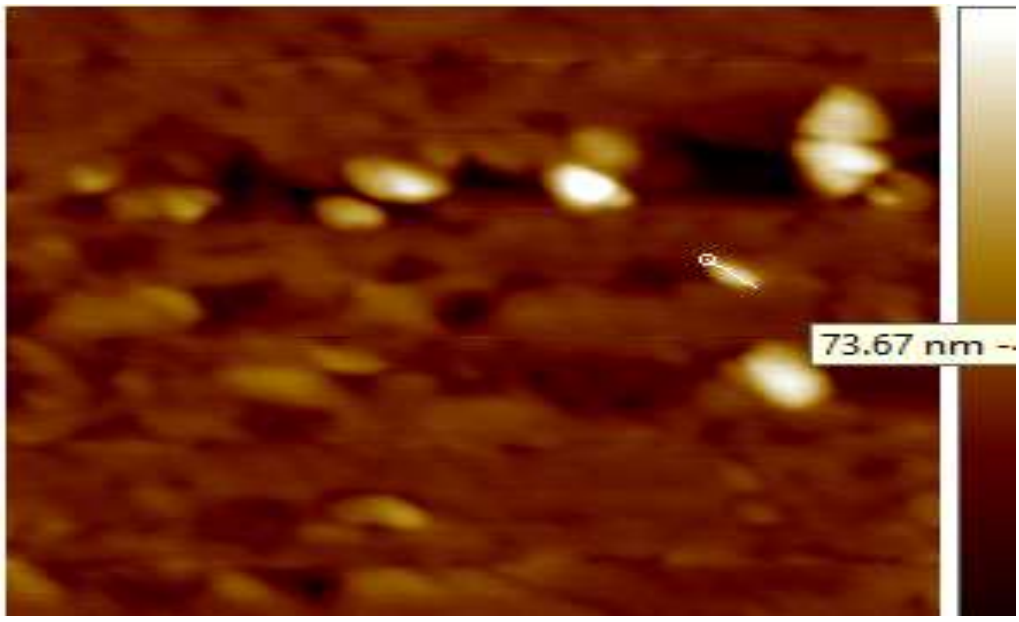

Figure 4. 21: Two-dimensional image of polymeric micelle

4.3.2.3 Transmission electron microscopy.

The TEM image seen in Figure 4.22 confirms what was seen in the AFM. The TEM images show that the polymeric micelles are spherical in shape, and the size of the micelles ranged from 60 nm to 105 nm. This shows that the size is still within the nanometer range and that there is a narrow size distribution of the micelles.

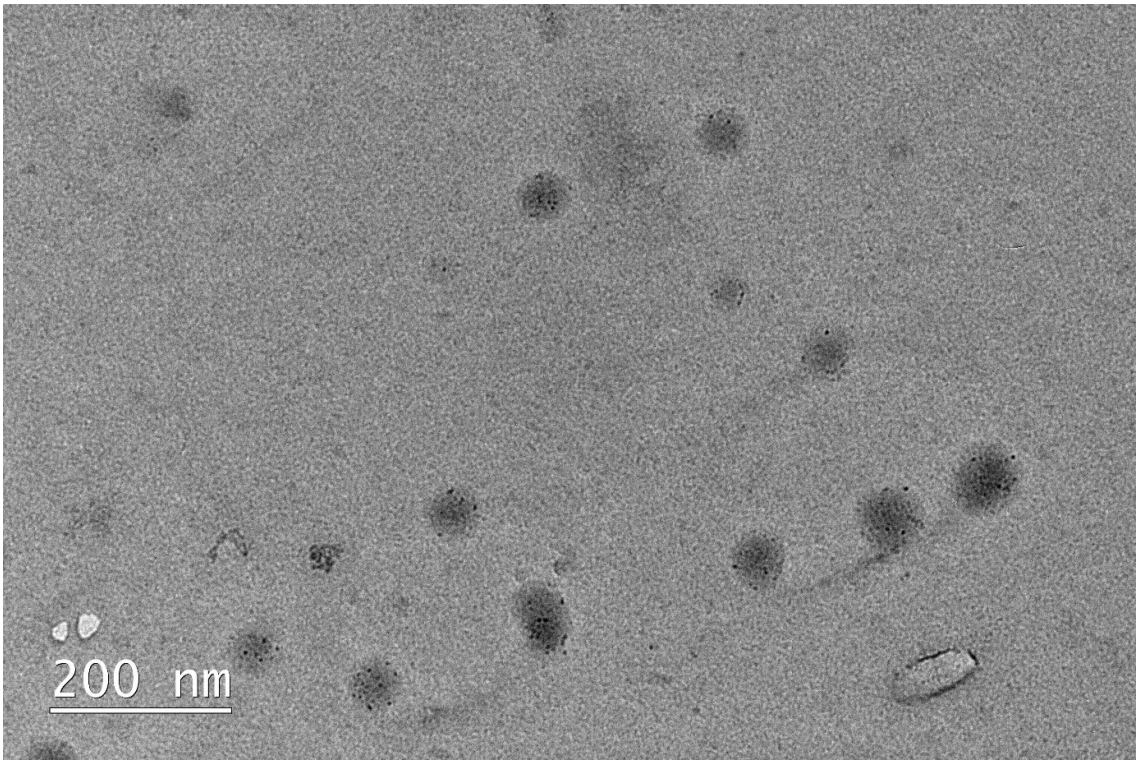

Figure 4. 22: TEM images showing nystatin encapsulated micelles

4.3.2.4 Micelle drug encapsulation.

The initial amount of drug introduced for micelle encapsulation was 10 mg. Using the calibration curve from the HPLC linearity validation, the amount of drug encapsulated within the micelles was quantified to be 3.6 mg. This resulted in the drug encapsulation efficiency being 36%. This means that nystatin was not encapsulated effectively, because less than 50% of the drug was encapsulated. This could be due to the amount of block co-polymer that was used for micelle formation being of small quantity. Drug encapsulation may be improved by increasing the amount of polymer solubilized for micelle formation. Figure 4.23 is a TEM image that shows the micelles encapsulating nystatin. The red circle shows the micelles, and the red arrow is pointing to the

encapsulated nystatin. The blue arrow is showing the free nystatin that was not encapsulated (the free floating small black dots).

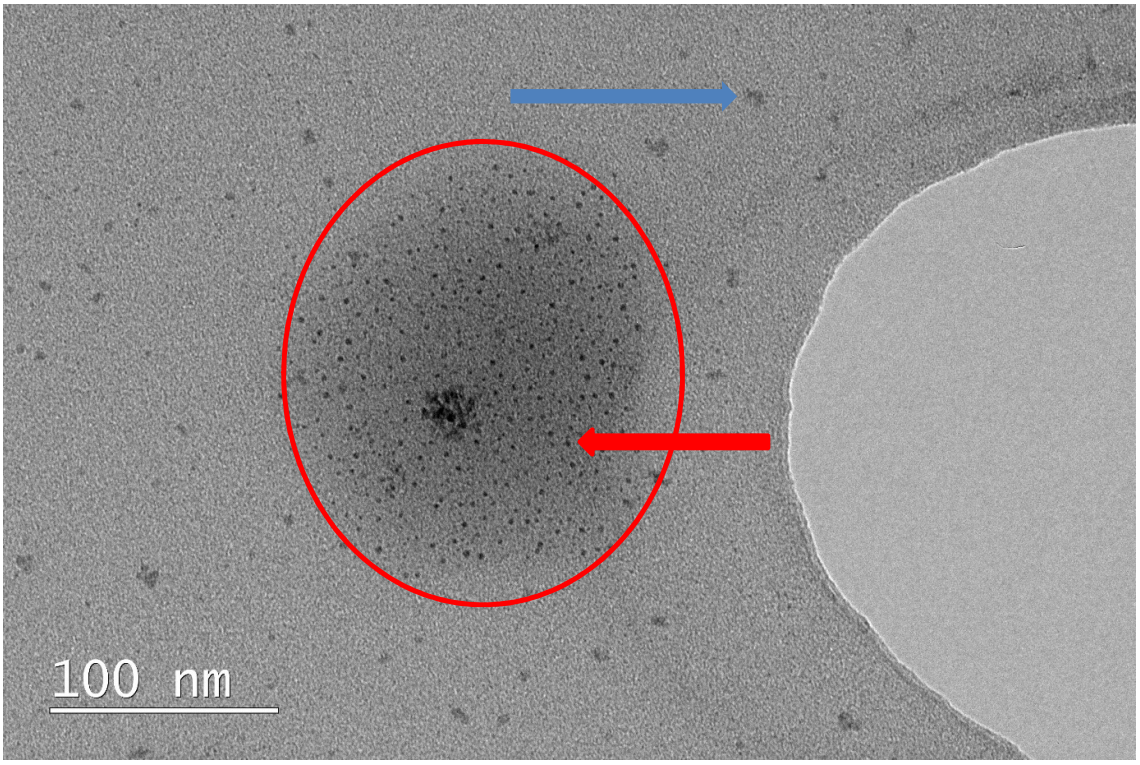

Figure 4. 23: TEM image showing drug micelle encapsulation of nystatin

4.4 Mucoadhesive Film Characterisation

4.4.1 Film characterization.

4.4.1.1 Surface smoothness and physical appearance.

The surface smoothness of the films was evaluated visually and through touch, to see if there were any inconsistencies or bumps. The HPMC film appeared clear and colorless. It was also smooth to the touch, with no visible bumps or bubbles on the surface. This shows that the film has a good physical appearance. Such characteristics are highly patient acceptable (Boddupalli et al., 2010). Figure 4.24 shows physical appearance of the HPMC film. The SCMC film was smooth to the touch with no visible bumps or bubbles on the surface. However, the film had a cloudy white colour which may not be patient acceptable as patients do not prefer products that may discolour their tongue (Rossiter, 2012).

Figure 4. 24: HPMC mucoadhesive film

4.4.1.2 Folding endurance.

Film pliability was tested using the folding test. The HPMC films were folded at the same place over 300 times, and this was taken as the end point. The film did not show any signs of breaking or damage. This means that the film is highly pliable and will not break while being handled. The SCMC films were folded at the same place and broke after being folded 10 times. This means that the film was not pliable and breaks easily; this is illustrated in Figure 4.25 where the film could not be lifted out of the petri dish that it was cast in without breaking. A film that demonstrates low pliability is not preferred by patients, because it may break while it is being handled by a patient. Due to the SCMC film breaking easily, the HPMC film was taken as the superior film and no further characterization was conducted on the SCMC film.

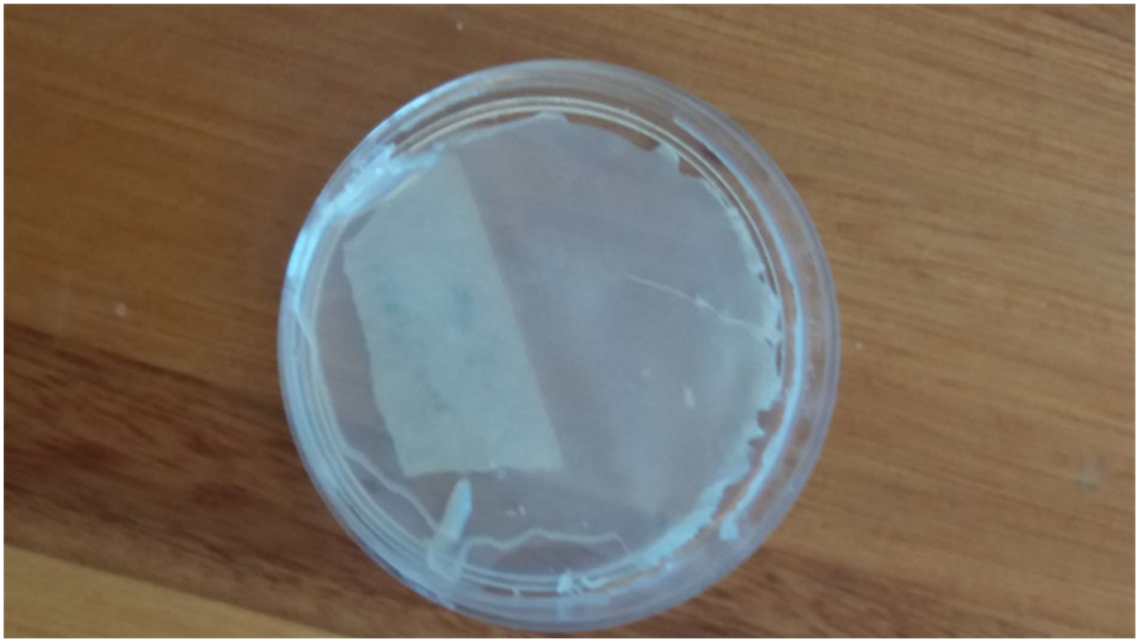

Figure 4. 25: The Sodium Carboxymethylcellulose film with a cloudy white colour

The film was found to have low pliability as is evident from the film tearing while being lifted out of the petri dish.

4.4.1.3 Film weight and thickness.

The mean HPMC film weight was 483,37 mg and the average film thickness was 0.087 µm. The film thickness was consistent throughout the three films tested, with a relative standard deviation of 6.6%. The consistent film thickness and weight shows that the drug within the film is evenly distributed, as there are no areas of the film that are significantly thicker than others. This meant that there are no areas of the film with a higher drug concentration than the other areas.

4.4.1.4 Surface pH determination.

The mean surface pH for HPMC film was determined to be 7.29, which is within the pH range of the mouth. This means that the film will not cause irritation to the mucosa while it is being applied for treatment.

4.4.1.5 Swelling Index.

The HPMC film was able to swell to a maximum of 550%. This was noted after 30 minutes of exposing the film to a phosphate buffer at a temperature of 37 °C. This means that the film can easily spread over the mucosa for adhesion. This is illustrated graphically in Figure 4.26. The non-linear regression line was added using Microsoft Excel and had an equation of y = 3.0383ln(x) + 0.2264 with a R^2 value of 0.97.

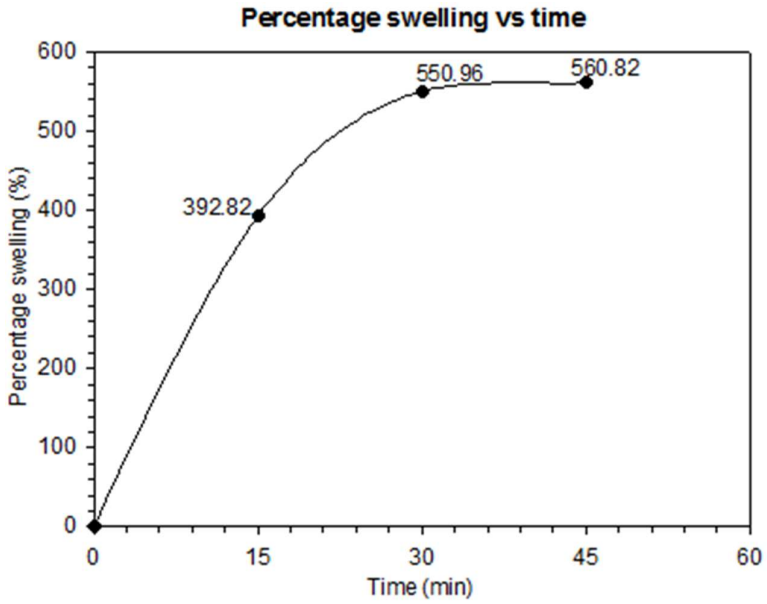

Figure 4. 26: Percentage swelling vs time graph, showing the percentage swelling of the film at specific times

The non-linear equation for the graph is y = 3.0383ln(x) + 0.2264 with a R2 value of 0.97.

4.4.1.6 Mechanical and physical properties.

Mechanical testing was repeated six times. The force that was used to break the HPMC films was determined by measuring the weight of the load that caused the breakage (Satishbabu & Srinivasan, 2008). The mean ultimate tensile strength (UTS) of the samples was 16.5 MPa, with a RSD of 24 %. The mean maximum load applied to cause a fracture was 5,098 N with a RSD of 22.7 %. The mean thickness after the load was applied was 0,082 mm with a RSD of 10 % and the mean width after the load was applied was 3,817 mm with an RSD of 7.2 %. These results are presented in table

4.12. The results show that the film has a high tensile strength with a low chance of elongation. This is evident when the width of the film, after a load has been applied, is compared to the width of the film before the load was applied and it (the width) is almost unchanged. This means that the film has good mechanical properties. A good mucoadhesive film should be strong and flexible. The film in this research meets thiscriteria (Bahri-Najafi, Tavakoli, Senemar, & Peikanpour, 2014).

Table 4. 12: Mechanical test results

Name	UTS (MPa)	Load @ MAX (N)	Thickness (mm)	Width (mm)
Test Run 1	15,9	4,917	0,080	3,870
Test Run 2	16,4	5,289	0,080	4,020
Test Run 3	10,0	3,225	0,080	4,040
Test Run 4	15,2	4,721	0,090	3,440
Test Run 5	20,3	5,737	0,070	4,030
Test Run 6	21,3	6,702	0,090	3,500
Mean	16,5	5,098	0,082	3,817

4.4.1.7 Drug release profile.

In-vitro release studies were conducted using the FDC. The results are presented in Figure 4.27. Figure 4.27 illustrates that most of the drug is released from the HPMC film within the first 60 minutes after the film has been exposed to the FDC system. Although most of the drug is released within the first 60 minutes, this is not of concern as nystatin exhibits a post-fungal effect; thus nystatin will be showing antifungal activity even after the hour when most of the drug has been released (Gunderson *et al.,* 2000*)*. The film is also not intended to be in the mouth for a long period of time (greater than 4 hours), as this would interfere with normal oral functions such as eating and drinking. It is therefore an advantage that most of the drug is released in the first hour. In order

to prevent have better drug release control perhaps a different mucoadhesive polymer should be used instead of the polymer investigated. The drug might have been released quickly due to the polymer which may not have been compatible with nystatin

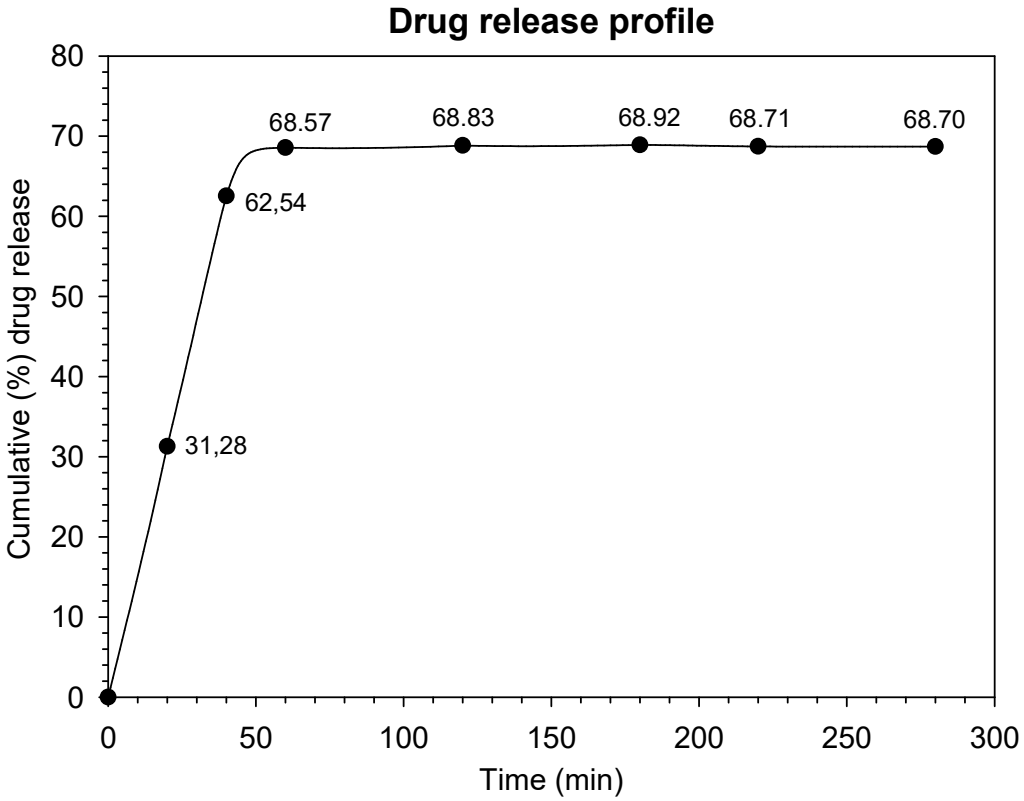

Figure 4. 27: Drug release rate from mucoadhesive film

CHAPTER 5

Conclusion and Recommendation

5.1 Conclusion and Recommendations for Further Studies

5.1.1 Conclusion.

This study aimed to improve drug delivery of nystatin for the treatment of oral thrush, by developing a nystatin loaded micellar system to be incorporated into a mucoadhesive film for drug delivery. This was achieved by using the statistical software Design Expert to create a mixture design (the simplex lattice design), to allow for an appropriate solvent system for the solubilization of nystatin to be established. The model selected by the statistical software for the solubilisation system of nystatin proved to be effective and nystatin was successfully solubilised. According to the statistics software, nystatin may be solubilised using a mixture of methanol, water and DMF. It was observed that the presence of DMF was necessary for nystatin solubilisation.

Design Expert was also used for the statistical optimization of the nystatin encapsulated polymeric micelles using the CCRD design. The design recommended for the polymeric micelles was a challenge, because not all the responses were accurately predicted by the statistical model. This may have been due to batch to batch inconsistencies associated with nanoparticle synthesis and formation.

Once the micelles were formed, they were characterised for size, stability, morphology and drug encapsulation efficiency. Characterisation for size showed that the micelles were all within an acceptable size range. They were moderately distributed within the micelle solution. The micelles were also found to be stable, despite their zeta potential being low. This was evidenced by the small change in size, after the micelles had been kept at 4 ºC for two weeks. Morphology of the micelles was investigated using AFM and TEM. Both instruments illustrated that the micelles were spherical in shape and all were within the appropriate size range. The drug encapsulation efficiency of the micelles was low; only encapsulating 36% of nystatin. This may have been due to the amount of polymer used for encapsulation being too little.

The nystatin encapsulated micelles were incorporated into a mucoadhesive film which was cast using the solvent casting method. Two films, with two different polymers (HPMC and SCMC) were investigated. The two films were characterised for physical appearance and pliability. The HPMC film was found to be superior and was characterised for film weight and thickness, mechanical properties, swelling index and drug release profile. The HPMC film had a patient acceptable physical appearance and feel. The film was found to be pliable, and it had a consistent thickness and weight. The mechanical properties of the film were acceptable, as it exhibited strength and flexibility. The swelling index test was done to investigate how well the film could spread over the mucosa. The film was found to swell 550% of its initial weight, indicating that it can easily spread over the mucosa. Drug release profile was investigated using the Franz diffusion cells. 62.5% of the drug was released within 60 minutes. This shows that the drug has a controlled release.

The aim of this research was to develop a buccal mucoadhesive film containing nystatin encapsulated in a polymeric micelle. This is proposed for the treatment of oropharyngeal candidiasis in children and chronically ill patients. The proposed buccal mucoadhesive film is a major need because (1) there is an increase in OPC infections in recent years and (2) the mechanism of application of the current OPC treatment (nystatin suspension) is not patient friendly, as it needs to be applied often because the suspension does not adhere to the affected area. Based on the major findings of this study, a nystatin loaded micellar system was successfully developed and incorporated into a mucoadhesive film.

These are the first steps in the journey to creating novel delivery systems for the treatment of common diseases, and there are still many challenges to overcome before this novel product can appear in the market. The first problem that must still be addressed stems from batch to batch variability of the micelles, because this contributes to an unknown amount of drug being encapsulated in each micelle, and size variation of each micelle. Secondly, the effectiveness of the nystatin film is still unknown, as this was not tested in this study. This leaves room for future studies of this nature; to investigate if the dose used and the drug release rate is sufficient to effectively kill OPC causing microorganisms. Another important aspect that should be investigated with regards to the effectiveness of nystatin is the minimal time the film

should be in contact with the affected area, and the minimal concentration to be entrapped in the micelle to effectively kill the oropharyngeal causing microorganisms. This is because nystatin is a concentration dependant antifungal agent and not a time dependant antifungal agent. It is crucial that attention is also given to the affordability of this novel system, which aims to make the treatment of OPC easier, as OPC is a condition more common in immune compromised patients who may already be struggling with medical costs. Studies on cost effective ways of developing novel drug delivery systems, that have proven to work, should be conducted. The development of more effective delivery systems such as that proposed in this study, will (1) encourage patient compliance, (2) decrease recurrence of OPC and (3) will make it easier for caregivers to administer OPC treatment to patients thus improving the treatment outcomes.

5.1.2 Recommendation.

Some of the challenges encountered in this study was batch to batch variability and drug entrapment efficiency. This problem may perhaps be solved by using a larger quantity of polymer when forming the micelles. The researcher recommends clinical testing to be conducted, to determine the effectiveness of the film and its antifungal properties. More physical testing should be conducted on the film, to determine the storage conditions of the film.

References

Ahmad, Z., Shah, A., Siddiq, M., & Kraatz, H.-B. (2014). Polymeric micelles as drug delivery vehicles. *Royal Society of Chemistry Advanced.*, *4*(33), 17028–17038. http://doi.org/10.1039/C3RA47370H

Ai, X., Zhong, L., Niu, H., & He, Z. (2014). Thin-film hydration preparation method and stability test of DOX-loaded disulfide-linked polyethylene glycol 5000-lysine-di-tocopherol succinate nanomicelles. *Asian Journal of Pharmaceutical Sciences*, *9*(5), 244–250. http://doi.org/10.1016/J.AJPS.2014.06.006

Akbarzadeh, A., Rezaei-Sadabady, R., Davaran, S., Joo, S. W., Zarghami, N., Hanifehpour, Y., … Nejati-Koshki, K. (2013). Liposome: classification, preparation, and applications. *Nanoscale Research Letters*, *8*(1), 102. http://doi.org/10.1186/1556-276X-8-102

Akhavan, A. . (2009). The Quartz Page: Appendix - Ternary Diagrams. Retrieved September 1, 2018, from http://www.quartzpage.de/app_td.html

Akpan, A., & Morgan, R. (2002). Oral candidiasis. *Postgraduate Medical Journal*, *78*(922), 455–9. http://doi.org/10.1136/PMJ.78.922.455

Alonso, M. J., & Csaba, N. S. (Eds.). (2012). *Nanostructured Biomaterials for Overcoming Biological Barriers*. *Nanostructured Biomaterials for Overcoming Biological Barriers*. Cambridge: Royal Society of Chemistry. http://doi.org/10.1039/9781849735292

Amit, A., Sharad, S., & Mohammed Junaid, K. (2011). Theories and Factors Affecting Mucoadhesive Drug Delivery Systems: A Review. *International Journal of Research in Ayurveda & Pharmacy*, *2*(4), 1155–1161. Retrieved from www.ijrap.net

Aschinger, A., Winter -Dusty, J., Fortov, V. E., Khrapak, A. G., Khrapak, S. A., & Org Winter, J. ¨. (2012). Dynamic light scattering study of transitions in three-dimensional complex plasmas. *New Journal of Physics*, *14*(36pp), 93036. http://doi.org/10.1088/1367-2630/14/9/093036

Asmarawati, T. P., Putranti, A., Rachman, B. E., Hadi, U., & Nasronudin. (2018). Opportunistic infection manifestation of HIV-AIDS patients in Airlangga university hospital Surabaya. *IOP Conference Series: Earth and Environmental Science*, *125*(1), 012061. http://doi.org/10.1088/1755-1315/125/1/012061

Aulton, M.E., & Taylor, K.M.G. (2013) *Aulton's pharmaceutics: The design and manufacture of medicines* (4th ed.). London: Elsevier Health Sciences UK.

Bahri-Najafi, R., Tavakoli, N., Senemar, M., & Peikanpour, M. (2014). Preparation and pharmaceutical evaluation of glibenclamide slow release mucoadhesive buccal film. *Research in Pharmaceutical Sciences*, *9*(3), 213–23. Retrieved from http://www.ncbi.nlm.nih.gov/pubmed/25657792

Bai, Y., Saren, G., & Huo, W. (2015). Response surface methodology (RSM) in evaluation of the vitamin C concentrations in microwave treated milk. *Journal of Food Science and Technology*, *52*(7), 4647–4651. http://doi.org/10.1007/s13197-014-1505-5

Bansil, R., & Turner, B. S. (2006). Mucin structure, aggregation, physiological functions and biomedical applications. *Current Opinion in Colloid & Interface Science*, *11*(2–3), 164–170. http://doi.org/10.1016/J.COCIS.2005.11.001

Barakat, N. S., Taleb, D. A. Bin, & Salehi, A. S. Al. (2011). Target Nanoparticles: An Appealing Drug Delivery Platform. *Journal of Nanomedicine & Nanotechnology*, *s4*(009). http://doi.org/10.4172/2157-7439.S4-009

Barbosa Arrunátegui, L., Márcia Silva-Barcellos, N., Rezende Bellavinha, K., da Silveira Ev, L., & de Souza, J. (2015). Biopharmaceutics classification system: importance and inclusion in biowaiver guidance. *Brazilian Journal of Pharmaceutical Sciences*, *51*(1), 143–154. http://doi.org/10.1590/S1984-82502015000100015

Benet, L. Z. (2013). The role of BCS (biopharmaceutics classification system) and BDDCS (biopharmaceutics drug disposition classification system) in drug development. *Journal of Pharmaceutical Sciences*, *102*(1), 34–42. http://doi.org/10.1002/jps.23359

Bhadra, S., Das, S. C., Roy, S., Arefeen, S., & Rouf, A. S. S. (2011). Development and Validation of RP-HPLC Method for Quantitative Estimation of Vinpocetine in Pure and Pharmaceutical Dosage Forms. *Chromatography Research International*, *2011*, 1–7. http://doi.org/10.4061/2011/801656

Boddupalli, B. M., Mohammed, Z. N. ., Nath, R. A., & Banji, D. (2010). Mucoadhesive drug delivery system: An overview. *Journal of Advanced Pharmaceutical Technology & Research*, *1*(4), 381–7. http://doi.org/10.4103/0110-5558.76436

Bose, A. (2017). *Transmission Electron Microscopy (TEM)*. Retrieved from: http://www.pharmainfo.net/book/emerging-trends-nanotechnology-pharmacy-physicochemical-characterization-nanoparticles accessed on 01 June 2018

Brescansin, E., Brescansin, E. G., Portilho, M., & Pessine, F. B. T. (2013). Physical and chemical analysis of commercial nystatin. *Acta Scientiarum. Health Sciences*, *35*(2), 215–221. http://doi.org/10.4025/actascihealthsci.v35i2.12769

Campinha-Bacote, J., Transcultural, F., & Associates, C. A. R. E. (2002). The Process of Cultural Competence in the Delivery of Healthcare Services: A Model of Care. *Journal of Transcultural Nursing*, *13*(3), 181–184. Retrieved from http://journals.sagepub.com/doi/pdf/10.1177/10459602013003003

Campos, F. F., Calpena Campmany, A. C., Delgado, G. R., Serrano, O. L., & Naveros, B. C. (2012). Development and Characterization of a Novel Nystatin-Loaded Nanoemulsion for the Buccal Treatment of Candidosis: Ultrastructural Effects and Release Studies. *Journal of Pharmaceutical Sciences*, *101*(10), 3739–3752. http://doi.org/10.1002/jps.23249

Carvalho, F. C., Bruschi, M. L., Evangelista, R. C., & Gremião, M. P. D. (2010). Mucoadhesive drug delivery systems. *Brazilian Journal of Pharmaceutical Sciences*, *46*(1), 1–17. http://doi.org/10.1590/S1984-82502010000100002

Clark, J. (2016). Carrying out HPLC. Retrieved September 2, 2018, from https://www.chemguide.co.uk/analysis/chromatography/hplc.html

Collins, C. D., Cookinham, S., & Smith, J. (2011). Management of oropharyngeal candidiasis with localized oral miconazole therapy: efficacy, safety, and patient

acceptability. *Patient Preference and Adherence*, *5*, 369–74. http://doi.org/10.2147/PPA.S14047

Cong, Y., Pang, C., Dai, L., Banta, G. T., Selck, H., & Forbes, V. E. (2011). Importance of characterizing nanoparticles before conducting toxicity tests. *Integrated Environmental Assessment and Management*, *7*(3), 502–503. http://doi.org/10.1002/ieam.204

Coskun, O. (2016). Separation techniques: Chromatography. *Northern Clinics of Istanbul*, *3*(2), 156–160. http://doi.org/10.14744/nci.2016.32757

Coutinho, A., Silva, L., Fedorov, A., & Prieto, M. (2004). Cholesterol and ergosterol influence nystatin surface aggregation: relation to pore formation. *Biophysical Journal*, *87*(5), 3264–76. http://doi.org/10.1529/biophysj.104.044883

Darling, M. R., & Daley, T. (2005). Blistering mucocutaneous diseases of the oral mucosa--a review: part 1. Mucous membrane pemphigoid. *Journal (Canadian Dental Association)*, *71*(11), 851–4. Retrieved from http://www.ncbi.nlm.nih.gov/pubmed/16480600

Darwazeh, A. M. G., & Darwazeh, T. A. (2014). What Makes Oral Candidiasis Recurrent Infection? A Clinical View. *Journal of Mycology*, *2014*, 1–5. http://doi.org/10.1155/2014/758394

De Jong, W. H., & Borm, P. J. A. (2008). Drug delivery and nanoparticles:applications and hazards. *International Journal of Nanomedicine*, *3*(2), 133–49. Retrieved from http://www.ncbi.nlm.nih.gov/pubmed/18686775

Derrien, M., van Passel, M. W. J., van de Bovenkamp, J. H. B., Schipper, R., de Vos, W., & Dekker, J. (2010). Mucin-bacterial interactions in the human oral cavity and digestive tract. *Gut Microbes*, *1*(4), 254–268. http://doi.org/10.4161/gmic.1.4.12778

Donnelly, R., Shaikh, R., Raj Singh, T., Garland, M., & Woolfson, Ad. (2011). Mucoadhesive drug delivery systems. *Journal of Pharmacy and Bioallied Sciences*, *3*(1), 89. http://doi.org/10.4103/0975-7406.76478

Eastman Chemical Company. (2017). Eastman Tackifier Center - Understanding Block Copolymer. Retrieved August 31, 2018, from https://www.eastman.com/Markets/Tackifier_Center/Pages/Block_Copolymer.aspx

Epstein, J. B., & Polsky, B. (1998). Oropharyngeal candidiasis: a review of its clinical spectrum and current therapies. *Clinical Therapeutics*, *20*(1), 40–57. Retrieved from http://www.ncbi.nlm.nih.gov/pubmed/9522103

Ferreira-Nunes, R., Gratieri, T., Gelfuso, G. M., & Cunha-Filho, M. (2017). Mixture design applied in compatibility studies of catechin and lipid compounds. *Journal of Pharmaceutical and Biomedical Analysis*, *149*, 612–617. http://doi.org/10.1016/j.jpba.2017.11.069

Gajdošováa, M., Vetchýa, D., Doležela, P., Gajdzioka, J., Landováa, H., Muselíka, J., Zemana, J., Knotekb, A., Hauptmanb, K., & Jeklb, V. (2016). Evaluation of mucoadhesive oral films containing nystatin. *Journal of Applied Biomedicine*, 14(4), 247-256. http://doi: 10.1016/j.jab.2016.05.002

Garcia-Cuesta, C., Sarrion-Pérez, M.-G., & Bagán, J. V. (2014). Current treatment of oral candidiasis: A literature review. *Journal of Clinical and Experimental Dentistry*, *6*(5), e576-82. http://doi.org/10.4317/jced.51798

Gaucher, G., Satturwar, P., Jones, M.-C., Furtos, A., & Leroux, J.-C. (2010). Polymeric micelles for oral drug delivery. *European Journal of Pharmaceutics and Biopharmaceutics*, *76*(2), 147–158. http://doi.org/10.1016/j.ejpb.2010.06.007

Gelperina, S., Kisich, K., Iseman, M. D., & Heifets, L. (2005). The potential advantages of nanoparticle drug delivery systems in chemotherapy of tuberculosis. *American Journal of Respiratory and Critical Care Medicine*, *172*(12), 1487–90. http://doi.org/10.1164/rccm.200504-613PP

Ghadi, R., & Dand, N. (2017). BCS class IV drugs: Highly notorious candidates for formulation development. *Journal of Controlled Release*, *248*, 71–95. http://doi.org/10.1016/j.jconrel.2017.01.014

Giordano, G. (2006). A New Dimension in the Factorial Techniques: the Response

Surface - PDF Free Download. *Statistica Applicata*, *18*(2), 359–373. Retrieved from https://tiptiktak.com/a-new-dimension-in-the-factorial-techniques-the-response-surface.html

Green, J. M. (1996). Peer Reviewed: A Practical Guide to Analytical Method Validation. *Analytical Chemistry*, *68*(9), 305A–309A. http://doi.org/10.1021/ac961912f

Gunderson, S. M., Hoffman, H., Ernst, E. J., Pfaller, M. A., & Klepser, M. E. (2000). In vitro pharmacodynamic characteristics of nystatin including time-kill and postantifungal effect. *Antimicrobial Agents and Chemotherapy*, *44*(10), 2887–90. Retrieved from http://www.ncbi.nlm.nih.gov/pubmed/10991881

Helmenstine, A. M. (2016). What Is a Block Copolymer? Chemistry Definition. Retrieved August 31, 2018, from https://www.thoughtco.com/definition-of-block-copolymer-604834

Heneedak, H. M., Salama, I., Mostafa, S., & El-Sadek, M. (2012). HPLC and Chemometric Methods for the Simultaneous Determination of Miconazole Nitrate and Nystatin. *Journal of Chromatographic Science*, *50*(10), 855–861. http://doi.org/10.1093/chromsci/bms127

Hussien, E. M. (2014). HPLC method validation for modernization of the tetracycline hydrochloride capsule USP monograph. *Bulletin of Faculty of Pharmacy, Cairo University*, *52*(2), 239–244. http://doi.org/10.1016/J.BFOPCU.2014.08.002

ICH Harmonised Tripartite Guideline. (2005). Validation of Analytical Procedures: Text and Methodology Q2(R1). In *International Conference on Harmonisation of Technical Requirements For Registration of Pharmaceuticals for Human Use*. Retrieved from https://www.ich.org/fileadmin/Public_Web_Site/ICH_Products/Guidelines/Quality/Q2_R1/Step4/Q2_R1__Guideline.pdf

Ikram, M., Gilhotra, N., & Gilhotra, R. M. (2015). Formulation and optimization of mucoadhesive buccal patches of losartan potassium by using response surface methodology. *Advanced Biomedical Research*, *4*(239).

http://doi.org/10.4103/2277-9175.168606

Jagtap, R. N., & Ambre, A. H. (2006). Overview literature on atomic force microscopy (AFM): Basics and its important applications for polymer characterization. *Indian Journal of Engineering & Materials Sciences*, *13*, 368–384. Retrieved from https://pdfs.semanticscholar.org/7ae2/d9392806ce08749ef60cc230b1ae2a1750f2.pdf

Jain, N., Gulati, N., Kumar, D., & Nagaich, U. (2012). Microspheres: Mucoadhesion Based Controlled Drug Delivery System. *RGUHS J Pharm Sci*, *2*(3), 28–40. Retrieved from www.rjps.in

Jhaveri, A. M., & Torchilin, V. P. (2014). Multifunctional polymeric micelles for delivery of drugs and siRNA. *Frontiers in Pharmacology*, *5*(77). http://doi.org/10.3389/fphar.2014.00077

Jin, B.-Z., Dong, X.-Q., Xu, X., & Zhang, F.-H. (2018). Development and in vitro evaluation of mucoadhesive patches of methotrexate for targeted delivery in oral cancer. *Oncology Letters*, *15*(2), 2541–2549. http://doi.org/10.3892/ol.2017.7613

Jones, M., & Leroux, J. (1999). Polymeric micelles - a new generation of colloidal drug carriers. *European Journal of Pharmaceutics and Biopharmaceutics : Official Journal of Arbeitsgemeinschaft Fur Pharmazeutische Verfahrenstechnik e.V*, *48*(2), 101–11. Retrieved from http://www.ncbi.nlm.nih.gov/pubmed/10469928

Karaman, S., Yilmaz, M. T., & Kayacier, A. (2011). Simplex lattice mixture design approach on the rheological behavior of glucomannan based salep-honey drink mixtures: An optimization study based on the sensory properties. *Food Hydrocolloids*, *25*(5), 1319–1326. http://doi.org/10.1016/j.foodhyd.2010.12.007

Karimi, P., Abdollahi, H., Aslan, N., Noaparast, M., & Shafaei, S. Z. (2010). Application of Response Surface Method and Central Composite Design for Modeling and Optimization of Gold and Silver Recovery in Cyanidation Process. *Mineral Processing and Extractive Metallurgy Review*, *32*(1), 1–16. http://doi.org/10.1080/08827508.2010.508828

Karki, S., Kim, H., Na, S.-J., Shin, D., Jo, K., & Lee, J. (2016). Thin films as an

emerging platform for drug delivery. *Asian Journal of Pharmaceutical Sciences*, *11*(5), 559–574. http://doi.org/10.1016/J.AJPS.2016.05.004

Kaszuba, M., Corbett, J., Watson, F. M., & Jones, A. (2010). High-concentration zeta potential measurements using light-scattering techniques. *Philosophical Transactions. Series A, Mathematical, Physical, and Engineering Sciences*, *368*(1927), 4439–51. http://doi.org/10.1098/rsta.2010.0175

Katzung, B.G., Masters, S.B., & Trevor, A.J. (2012). *Basic and Clinical Pharmacology (12*th ed.). New York: The McGraw-Hill Companies

Kaur, A., & Kaur, G. (2012). Mucoadhesive buccal patches based on interpolymer complexes of chitosan-pectin for delivery of carvedilol. *Saudi Pharmaceutical Journal* , *20*(1), 21–7. http://doi.org/10.1016/j.jsps.2011.04.005

Kedar, U., Phutane, P., Shidhaye, S., & Kadam, V. (2010). Advances in polymeric micelles for drug delivery and tumor targeting. *Nanomedicine: Nanotechnology, Biology and Medicine*, *6*(6), 714–729. http://doi.org/10.1016/j.nano.2010.05.005

Ku, M. S. (2008). Use of the Biopharmaceutical Classification System in early drug development. *The AAPS Journal*, *10*(1), 208–12. http://doi.org/10.1208/s12248-008-9020-0

Kulthe, S. S., Choudhari, Y. M., Inamdar, N. N., & Mourya, V. (2012). Polymeric micelles: authoritative aspects for drug delivery. *Designed Monomers and Polymers*, *15*(5), 465–521. http://doi.org/10.1080/1385772X.2012.688328

Li, H., & Chen, F. (2017). Preparation and quality evaluation of coenzyme Q10 long-circulating liposomes. *Saudi Journal of Biological Sciences*, *24*(4), 797–802. http://doi.org/10.1016/j.sjbs.2015.10.025

Lu, Y., & Park, K. (2013). Polymeric micelles and alternative nanonized delivery vehicles for poorly soluble drugs. *International Journal of Pharmaceutics*, *453*(1), 198–214. http://doi.org/10.1016/j.ijpharm.2012.08.042

Lyu, X., Zhao, C., Hua, H., & Yan, Z. (2016). Efficacy of nystatin for the treatment of oral candidiasis: a systematic review and meta-analysis. *Drug Design,*

Development and Therapy, *10*, 1161–71. http://doi.org/10.2147/DDDT.S100795

Ma, H., Shieh, K.-J., & Qiao, T. X. (2006). Marsland Company, Michigan, The United States Nature and Science. *Nature and Science*, *4*(3), 14–22. Retrieved from http://www.sciencepub.orgeditor@sciencepub.net

Mahajan, P., Kaur, A., Aggarwal, G., & Harikumar, S. L. (2012). International journal of drug development and research. *International Journal of Drug Development and Research*, *5*(1), 11–20. Retrieved from http://www.ijddr.in/drug-development/mucoadhesive-drug-delivery-system-a-review.php?aid=5005

Mai, W. (2017). Fundamental Theory of Atomic Force Microscopy. Retrieved September 2, 2018, from http://www.nanoscience.gatech.edu/zlwang/research/afm.html

Malvern Panalytical. (2017). The Zetasizer Nano range for DLS, ELS, SLS and microrheology. Retrieved September 2, 2018, from https://www.malvernpanalytical.com/en/products/product-range/zetasizer-range/zetasizer-nano-range?gclid=Cj0KCQjwlK7cBRCnARIsAJiE3MjUHQUKnXleyu6RUwhrRPyKXb0Yl6J2uHCHRtwaVhLDURYcZZov4JEaAuHHEALw_wcB

Mansuri, S., Kesharwani, P., Jain, K., Tekade, R. K., & Jain, N. K. (2016). Mucoadhesion: A promising approach in drug delivery system. *Reactive and Functional Polymers*, *100*, 151–172. http://doi.org/10.1016/J.REACTFUNCTPOLYM.2016.01.011

Masarudin, M. J., Cutts, S. M., Evison, B. J., Phillips, D. R., & Pigram, P. J. (2015). Factors determining the stability, size distribution, and cellular accumulation of small, monodisperse chitosan nanoparticles as candidate vectors for anticancer drug delivery: application to the passive encapsulation of [14C]-doxorubicin. *Nanotechnology, Science and Applications*, *8*, 67–80. http://doi.org/10.2147/NSA.S91785

Mazu, T. K., Bricker, B. A., Flores-Rozas, H., & Ablordeppey, S. Y. (2016). The Mechanistic Targets of Antifungal Agents: An Overview. *Mini Reviews in*

Medicinal Chemistry, *16*(7), 555–78. Retrieved from http://www.ncbi.nlm.nih.gov/pubmed/26776224

McCarron, P. A., Woolfson, A. D., & Keating, S. M. (1999). Response surface methodology as a predictive tool for determining the effects of preparation conditions on the physicochemical properties of poly(isobutylcyanoacrylate) nanoparticles. *International Journal of Pharmaceutics*, *193*(1), 37–47. http://doi.org/10.1016/S0378-5173(99)00311-7

Milne, C.P., Malins, A., & Joshi, N. (2012). *The Biopharmaceutics Classification System: Canary in the Coal Mine for Regulatory Science.* Retrieved from http://www.pharmoutsourcing.com/Featured-Articles/132305-The-Biopharmaceutics-Classification-System-Canary-in-the-Coal-Mine-for-Regulatory-Science/ Accessed on 19 December 2017

Morales, J. O., & McConville, J. T. (2011). Manufacture and characterization of mucoadhesive buccal films. *European Journal of Pharmaceutics and Biopharmaceutics*, *77*(2), 187–199. http://doi.org/10.1016/j.ejpb.2010.11.023

Mourabet, M., El Rhilassi, A., El Boujaady, H., Bennani-Ziatni, M., & Taitai, A. (2017). Use of response surface methodology for optimization of fluoride adsorption in an aqueous solution by Brushite. *Arabian Journal of Chemistry*, *10*(2), S3292–S3302. http://doi.org/10.1016/J.ARABJC.2013.12.028

Mourya, V. ., Inamdar, N., Nawale, R. ., & Kulthe, S. . (2010). Polymeric Micelles: General Considerations and their Applications. *Indian Journal of Pharmaceutical Education and Research*, *45*(2), 128–138. Retrieved from http://www.ijper.org/sites/default/files/IJPER_45_2_4.pdf

Mudshinge, S. R., Deore, A. B., Patil, S., & Bhalgat, C. M. (2011). Nanoparticles: Emerging carriers for drug delivery. *Saudi Pharmaceutical Journal* , *19*(3), 129–41. http://doi.org/10.1016/j.jsps.2011.04.001

Muzib, Y. I., & Kumari, K. S. (2011). Mucoadhesive buccal films of glibenclamide: Development and evaluation. *International Journal of Pharmaceutical Investigation*, *1*(1), 42–7. http://doi.org/10.4103/2230-973X.76728

National Nanotechnology Initiative. (2017). What is Nanotechnology? Retrieved August 31, 2018, from https://www.nano.gov/nanotech-101/what/definition

Nehoff, H., Parayath, N. N., Domanovitch, L., Taurin, S., & Greish, K. (2014). Nanomedicine for drug targeting: strategies beyond the enhanced permeability and retention effect. *International Journal of Nanomedicine*, *9*, 2539–55. http://doi.org/10.2147/IJN.S47129

Oerlemans, C., Bult, W., Bos, M., Storm, G., Nijsen, J. F. W., & Hennink, W. E. (2010). Polymeric Micelles in Anticancer Therapy: Targeting, Imaging and Triggered Release. *Pharmaceutical Research*, *27*(12), 2569–2589. http://doi.org/10.1007/s11095-010-0233-4

Oprime, P. C., Maria, V., Pureza, M., & Conceição De Oliveira, S. (2015). Systematic sequencing of factorial experiments as an alternative to the random order Sequenciamento sistemático de experimentos fatoriais como alternativa à ordem aleatória. *Gest. Prod*. http://doi.org/10.1590/0104-530X1266-16

Paithankar, H.V (2013) 'HPLC method validation for pharmaceuticals: A Review'. *International Journal of Universal Pharmacy and Bio Sciences*, 2(4), 229-240

Pankhurst, C. L. (2009). Candidiasis (oropharyngeal). *BMJ Clinical Evidence*, *2009*. Retrieved from http://www.ncbi.nlm.nih.gov/pubmed/19445752

Park, K. (2007). Nanotechnology: What it can do for drug delivery. *Journal of Controlled Release : Official Journal of the Controlled Release Society*, *120*(1–2), 1–3. http://doi.org/10.1016/j.jconrel.2007.05.003

Patil, S., Rao, R. S., Majumdar, B., & Anil, S. (2015). Clinical Appearance of Oral Candida Infection and Therapeutic Strategies. *Frontiers in Microbiology*, *6*, 1391. http://doi.org/10.3389/fmicb.2015.01391

PennState Eberly College of Science. (2018). 11.2.1 - Central Composite Designs. Retrieved September 2, 2018, from https://onlinecourses.science.psu.edu/stat503/node/59/

PermeGear. (2017). Franz Cells - PermeGear. Retrieved September 2, 2018, from http://permegear.com/franz-cells/

Phanindra, B., Moorthy, K. B., & Muthukumaran, M. (2013). Recent Advances in Mucoadhesive/Bioadhesive Drug Delivery System: A Review - Volume 2, No. 1, January 2013 - IJPMBS. *International Journal of Pharma Medicine and Biological Sciences*, *2*(1). Retrieved from http://www.ijpmbs.com/index.php?m=content&c=index&a=show&catid=115&id=46

Pietrzak, A., Grywalska, E., Socha, M., Roliński, J., Franciszkiewicz-Pietrzak, K., Rudnicka, L., … Krasowska, D. (2018). Prevalence and Possible Role of Candida Species in Patients with Psoriasis: A Systematic Review and Meta-Analysis. *Mediators of Inflammation*, *2018*, 1–7. http://doi.org/10.1155/2018/9602362

Rangasamy, M., & Parthiban, K. G. (2010). Recent Advances In Novel Drug Delivery Systems. *International Journal of Research in Ayurveda & Pharmacy*, *1*(2), 316–326. Retrieved from www.ijrap.net

Ravindran Chandrasekaran, A., Yoke Jia, C., Sheau Theng, C., Muniandy, T., Muralidharan, S., & Arumugam Dhanaraj, S. (2011). Invitro studies and evaluation of metformin marketed tablets-Malaysia. *Journal of Applied Pharmaceutical Science*, *1*(05), 214–217. Retrieved from https://pdfs.semanticscholar.org/b126/fdd661c80a2e5c7c5fcf81fb9cd52d789cae.pdf

Reliability Engineering Resources. (2018). Weibull.com. Retrieved September 1, 2018, from https://www.weibull.com/hotwire/issue180/hottopics180.htm

Rossiter D (ed). (2014). *South African Medicines Formulary* (11th ed.). Cape Town, RSA.

Ruozi, B., Tosi, G., Forni, F., Fresta, M., & Vandelli, M. A. (2005). Atomic force microscopy and photon correlation spectroscopy: Two techniques for rapid characterization of liposomes. *European Journal of Pharmaceutical Sciences*, *25*(1), 81–89. http://doi.org/10.1016/j.ejps.2005.01.020

Saadat, E., Amini, M., Khoshayand, M. R., Dinarvand, R., & Dorkoosh, F. A. (2014). Synthesis and optimization of a novel polymeric micelle based on hyaluronic acid

and phospholipids for delivery of paclitaxel, in vitro and in-vivo evaluation. *International Journal of Pharmaceutics*, *475*(1–2), 163–173. http://doi.org/10.1016/j.ijpharm.2014.08.030

Sabry, S. A. (2018). Sodium Cromoglycate Mucoadhesive Buccal Patches: Design, Fabrication, In Vitro and In Vivo Characterization. *International Journal of Applied Pharmaceutics*, *10*(2), 76. http://doi.org/10.22159/ijap.2018v10i2.24333

Safari, J., & Zarnegar, Z. (2014). Advanced drug delivery systems: Nanotechnology of health design A review. *Journal of Saudi Chemical Society*, *18*(2), 85–99. http://doi.org/10.1016/J.JSCS.2012.12.009

Sahu, A., Kasoju, N., Goswami, P., & Bora, U. (2011). Encapsulation of Curcumin in Pluronic Block Copolymer Micelles for Drug Delivery Applications. *Journal of Biomaterials Applications*, *25*(6), 619–639. http://doi.org/10.1177/0885328209357110

Saraswathi, B., Balaji, A., & Umashankar, M. S. (2013). Polymers In Mucoadhesive Drug Delivery System-Latest Updates. *Int J Pharm Sci*, *5*(3), 423–430. Retrieved from https://innovareacademics.in/journal/ijpps/Vol5Suppl3/7359.pdf

Satishbabu, B. K., & Srinivasan, B. P. (2008). Preparation and evaluation of buccoadhesive films of atenolol. *Indian Journal of Pharmaceutical Sciences*, *70*(2), 175–9. http://doi.org/10.4103/0250-474X.41451

Saxena, A., Tewari, G., & Saraf, S. A. (2011). Formulation and evaluation of mucoadhesive buccal patch of acyclovir utilizing inclusion phenomenon. *Brazilian Journal of Pharmaceutical Sciences*, *47*(4), 887–897. http://doi.org/10.1590/S1984-82502011000400026

Semalty, A., Semalty, M., & Nautiyal, U. (2010). Formulation and evaluation of mucoadhesive buccal films of enalapril maleate. *Indian Journal of Pharmaceutical Sciences*, *72*(5), 571–5. http://doi.org/10.4103/0250-474X.78522

Semalty, M., Semalty, A., & Kumar, G. (2008). Formulation and characterization of mucoadhesive buccal films of glipizide. *Indian Journal of Pharmaceutical Sciences*, *70*(1), 43–8. http://doi.org/10.4103/0250-474X.40330

Siddiqui, M. R., AlOthman, Z. A., & Rahman, N. (2017). Analytical techniques in pharmaceutical analysis: A review. *Arabian Journal of Chemistry*, *10*, S1409–S1421. http://doi.org/10.1016/J.ARABJC.2013.04.016

Singh, R., & Lillard, J. W. (2009). Nanoparticle-based targeted drug delivery. *Experimental and Molecular Pathology*, *86*(3), 215–223. http://doi.org/10.1016/j.yexmp.2008.12.004

South African Department of Health. (2012). *Standard Treatment Guidelines and Essential Medicines List For South Africa HOSPITAL Level Adults 2012 Edition*. Pretoria. Retrieved from www.doh.gov.za

State-Ease, I. (2018). Diagnostics Plots — Design-Expert 11.1.0 documentation. Retrieved September 2, 2018, from https://www.statease.com/docs/v11/contents/analysis/diagnostics/diagnostics-plots.html

Statistics South Africa. (2015). *Statistical release Mid-year population estimates 2015*. Pretoria. Retrieved from https://www.statssa.gov.za/publications/P0302/P03022015.pdf

Stetefeld, J., McKenna, S. A., & Patel, T. R. (2016). Dynamic light scattering: a practical guide and applications in biomedical sciences. *Biophysical Reviews*, *8*(4), 409–427. http://doi.org/10.1007/s12551-016-0218-6

Sunoqrot, S., Alsadi, A., Tarawneh, O., & Hamed, R. (2017). Polymer type and molecular weight dictate the encapsulation efficiency and release of Quercetin from polymeric micelles. *Colloid and Polymer Science*, *295*(10), 2051–2059. http://doi.org/10.1007/s00396-017-4183-9

Suri, S., Fenniri, H., & Singh, B. (2007). Nanotechnology-based drug delivery systems. *Journal of Occupational Medicine and Toxicology*, *2*(1), 16. http://doi.org/10.1186/1745-6673-2-16

Taillefer, J., Jones, M. -C., Brasseur, N., van Lier, J. E., & Leroux, J. -C. (2000). Preparation and Characterization of pH-Responsive Polymeric Micelles for the Delivery of Photosensitizing Anticancer Drugs. *Journal of Pharmaceutical*

Sciences, *89*(1), 52–62. http://doi.org/10.1002/(SICI)1520-6017(200001)89:1<52::AID-JPS6>3.0.CO;2-D

Thammana, M. (2016). A Review on High Performance Liquid Chromatography (HPLC). *Research & Reviews: Journal of Pharmaceutical Analysis*, *5*(2), 1–7. Retrieved from http://www.rroij.com/open-access/a-review-on-high-performance-liquid-chromatography-hplc-.php?aid=80688

The department of Health of South Africa (2013). *Essential treatment guidelines and essential medicines list for South Africa* (3rd ed.). RSA: The department of Health of South Africa

Thompson, G. R., Patel, P. K., Kirkpatrick, W. R., Westbrook, S. D., Berg, D., Erlandsen, J., … Patterson, T. F. (2010). Oropharyngeal candidiasis in the era of antiretroviral therapy. *Oral Surgery, Oral Medicine, Oral Pathology, Oral Radiology, and Endodontology*, *109*(4), 488–495. http://doi.org/10.1016/j.tripleo.2009.11.026

Tiwari, B. P., Bhushan, R., Nayan, G., & Sunil, P. (2013). An Overview: Sustained Release Drug Delivery Technologies With Polymeric System. *Pharma Science Monitor*, *4*(1). Retrieved from www.pharmasm.com

Trivedi, R., & Kompella, U. B. (2010). Nanomicellar formulations for sustained drug delivery: strategies and underlying principles. *Nanomedicine*, *5*(3), 485–505. http://doi.org/10.2217/nnm.10.10

Tucker, I. M., Corbett, J. C. W., Fatkin, J., Jack, R. O., Kaszuba, M., MacCreath, B., & McNeil-Watson, F. (2015). Laser Doppler Electrophoresis applied to colloids and surfaces. *Current Opinion in Colloid & Interface Science*, *20*(4), 215–226. http://doi.org/10.1016/J.COCIS.2015.07.001

Vahabi, S., Nazemi Salman, B., & Javanmard, A. (2013). Atomic force microscopy application in biological research: a review study. *Iranian Journal of Medical Sciences*, *38*(2), 76–83. Retrieved from http://www.ncbi.nlm.nih.gov/pubmed/23825885

Varanda, C., Portugal, I., Ribeiro, J., Silva, A. M. S., & Silva, C. M. (2017). Optimization

of bitumen formulations using mixture design of experiments (MDOE). *Construction and Building Materials*, *156*, 611–620. http://doi.org/10.1016/J.CONBUILDMAT.2017.08.146

Vaux, D. L., Fidler, F., & Cumming, G. (2012). Replicates and repeats-what is the difference and is it significant? A brief discussion of statistics and experimental design. *EMBO Reports*, *13*(4), 291–6. http://doi.org/10.1038/embor.2012.36

Vincent, J.L. (2001). *Surgical Treatment: Evidence-Based and Problem-Oriented, Candida infections in surgical intensive care unit patients.* Munich: Zuckschwerdt

Wang, J., Mongayt, D., & Torchilin, V. P. (2005). Polymeric micelles for delivery of poorly soluble drugs: Preparation and anticancer activity in vitro of paclitaxel incorporated into mixed micelles based on poly(ethylene glycol)-lipid conjugate and positively charged lipids. *Journal of Drug Targeting*, *13*(1), 73–80. http://doi.org/10.1080/10611860400011935

Weisstein, E. W. (2013). Ternary Diagram. Retrieved September 1, 2018, from http://mathworld.wolfram.com/TernaryDiagram.html

Wilczewska, A. Z., Niemirowicz, K., Markiewicz, K. H., & Car, H. (2012). Nanoparticles as drug delivery systems. *Pharmacological Reports* , *64*(5), 1020–37. Retrieved from http://www.ncbi.nlm.nih.gov/pubmed/23238461

Williams, D., & Lewis, M. (2011). Pathogenesis and treatment of oral candidosis. *Journal of Oral Microbiology*, *3*. http://doi.org/10.3402/jom.v3i0.5771

Williams, O. W., Sharafkhaneh, A., Kim, V., Dickey, B. F., & Evans, C. M. (2006). Airway Mucus: From production to secretion. *American Journal of Respiratory Cell and Molecular Biology*, *34*(5), 527–536. http://doi.org/10.1165/rcmb.2005-0436SF

Wilson, P., Stewart, A., Flournoy, V., William, S., & Vancura, A. (2001). Liquid Chromatographic Determination of Nystatin in Pharmaceutical Preparations. *Journal of AOAC International*, *84*(4), 1050–56. Retrieved from http://lib3.dss.go.th/fulltext/Journal/J.AOAC 1999-2003/J.AOAC2001/v84n4(jul-aug)/v84n4p1050.pdf

World Health Organisation. (2014). *Guidelines on the Treatment of Skin and Oral HIV-Associated Conditions in Children and Adults*. *Guidelines on the Treatment of Skin and Oral HIV-Associated Conditions in Children and Adults*. World Health Organization. Retrieved from http://www.ncbi.nlm.nih.gov/pubmed/26203484

World Health Organization (2015). *The International Pharmacopoeia (5th ed.).* [CD]

Xu, W., Ling, P., & Zhang, T. (2013). Polymeric Micelles, a Promising Drug Delivery System to Enhance Bioavailability of Poorly Water-Soluble Drugs. *Journal of Drug Delivery*, *2013*, 1–15. http://doi.org/10.1155/2013/340315

Zhou, W., Li, C., Wang, Z., Zhang, W., & Liu, J. (2016). Factors affecting the stability of drug-loaded polymeric micelles and strategies for improvement. *Journal of Nanoparticle Research*, *18*(9), 275. http://doi.org/10.1007/s11051-016-3583-y